Institute of Veterinary Physiology
of the Vetsuisse Faculty University of Zurich

Director: Prof. Dr. med. vet. Max Gassmann

Work under the academic supervision of
Dr. Markus Thiersch

Anemia of cancer in a spontaneously breast cancer developing mouse model

Inaugural Thesis

to obtain the title of Doctor from the
Vetsuisse Faculty University of Zurich

submitted by

Núria Fàbregas Bregolat

Veterinarian
of Barcelona, Spain

Approved at the request of:

Prof. Dr. med vet. Max Gassmann, supervisor
Prof. Dr. Ben Wielockx, co-supervisor

2019

Table of contents

1. Summary

Anemia of cancer (AC) has a high prevalence and capital clinical impact in cancer patients but is underdiagnosed and undertreated, due to the lack of effective and safe therapies. For a better treatment, it is essential to understand this pathological condition and to test potential strategies in preclinical models. However, few animal models to study AC have been established so far and none of them represents a spontaneously tumor-developing model. We characterized anemia in a spontaneously mammary tumor forming $Trp53^{flox}$WapCre mouse model to evaluate its usability as a model for AC. We observed that tumor-bearing mice develop inhibition of medullar erythropoiesis and prominent stress hematopoiesis in spleen, insensitivity to erythropoietin, a marked activation of the immune system and hypoferremia. Hypoferremia was treated by different protocols of single intravenous iron injections (Ferinject®), but iron supplementation was not sufficient to prevent AC, indicating that iron was not the limiting factor in our model. Impaired medullary erythropoiesis was accompanied by a marked induction of the myelopoiesis in bone marrow and spleen which might be a cancer-associated immunosuppressive strategy caused by several factors secreted by the tumor. Our model reflects a large variety of AC-related pathological changes that may complicate studies and drug tests but that might also reflect the human patient situation much closer than simplified cancer cell transplantation models.

2. Zusammenfassung

Anämie kommt in Krebspatienten häufig vor und beeinträchtigt die Lebensqualität und Prognose. Da sichere und effektive Behandlungsoptionen fehlen, ist die Krebsanämie unterdiagnostiziert und unterbehandelt. Für bessere Behandlungen müssen Pathologie und Behandlungsoptionen besser untersucht werden. Es gibt jedoch nur vereinfachte Tiermodelle, aber keines mit spontaner Tumorentwicklung. Wir haben die Pathologie von anämischen $Trp53^{flox}$WapCre Mäusen mit Brustkarzinom charakterisiert, um deren Verwendung als präklinisches Model zu testen. $Trp53^{flox}$WapCre Mäuse entwickeln Anämie durch Inhibition der Erythropoese im Knochenmark, begleitet durch eine Stress-Erythropoese in der Milz. Das Immunsystem wird deutlich aktiviert und es kommt zu einer Hypoferrämie, welche wir durch Eisensupplementation (Ferinject®) korrigieren wollten. Jedoch gelang es uns nicht die Anämie zu unterbinden, d.h. Eisenverfügbarkeit stellt nicht der limitierende Faktor in unserem Modell das. Die beeinträchtigte Erythropoese im Knochenmark haben wir auf eine starke Myelopoese zurückgeführt.

Unser Model spiegelt die Variabilität der Pathologie von Krebsanämien wider, und somit eventuell auch die klinische Situation von Patienten besser, als es vereinfachte Modelle mit Tumorzellimplantation könnten. Insbesondere die Unempfindlichkeit gegenüber Epo macht dieses Model einzigartig, um diesen Typ der Krebsanämie sowie Behandlungsoptionen der Zytokin-abhängigen Suppression der Erythropoese zu untersuchen.

3. Introduction

3.1 Anemia of cancer

Anemia in cancer patients is very frequent and exhibits a profound impact on the quality of life and on disease prognosis of cancer patients. 39% of them are anemic before starting any treatment[1] and it rises up to 90% in patients going under chemotherapy.[2] The incidence is influenced by the type of cancer,[3,4] sex and age of the patient[5,6] as well as on the stage of the disease,[7,3,4] being more severe in patients at advanced stages. The main consequence of anemia is the reduced capacity of oxygen transport within the organism and therefore affecting the function and metabolism of all organs and tissues. The most common symptoms are fatigue, weakness and reduced cognitive and physical capacity,[8] which result mainly from the response to hypoxia in the circulatory and renal systems[9] as well as in the tissues.

Anemia is one of the main reasons for cancer-related fatigue.[10] This fatigue can negatively influence the patient's tolerance and motivation to undergo antineoplastic treatment, thus not allowing patients to receive adequate and complete treatments and potentially impairing the therapeutic response.[11] Moreover, anemia is an independent risk factor for survival regardless of tumor type[7] and it seems to impair the tumor responsiveness to chemo- and radiotherapy.[12,3,13,14,15,16,17] Furthermore, anemia and the subsequent reduced oxygen transport might increase tumor hypoxia and thus, tumor malignancy, favoring tumor progression and metastasis formation through different mechanisms. These mechanisms include tissue acidosis, production of reactive oxidative species (ROS), immunodepression and alterations in tumor cells apoptosis.[18] Therefore, anemia in cancer is not only important for its role in deteriorating the quality of life and reducing the treatment options of the patients, but also because it increases tumor progression and spreading.

Despite its vast importance and major presence among cancer patients, this condition is still nowadays left untreated due to its complex pathogenesis and the potential risks of the current therapeutic approaches[19] such as infections after blood transfusion[20] or promoting tumor growth after Epo treatment.[21]

3.2 Pathophysiology of AC

In oncologic patients, anemia can be caused by multiple factors like the direct invasion of the bone marrow by the neoplastic cells, nutritional deficiencies, hemorrhage, hemolysis, kidney disease, liver insufficiencies, or the direct myelosuppressive effect of radio- or chemotherapy among others.[22] However, it is important to note that the term Anemia of Cancer (AC) specifically refers to a type of anemia, that is caused by chronic inflammation associated with advanced stages of cancer and the synthesis of proinflammatory cytokines by immune and cancer cells.[23]

The main mechanisms by which inflammation and released proinflammatory cytokines can cause anemia are: alterations in iron metabolism that lead to an iron restricted erythropoiesis; shortened erythrocyte life-span and increased erythrocyte destruction; direct suppression of erythropoiesis in bone marrow; and inhibition of the production of erythropoietin (Epo) in kidney[24] **(Fig. 1)**. In some patients the immune response to the tumor leads to the formation of antibodies that destroy the red blood cells (RBC) (autoimmune hemolytic anemia) or suppress the erythrocyte production (pure red-cell aplasia). In other AC types, the damage of the vascular endothelium by tumor emboli or activation of the coagulation by the tumor can physically injure erythrocytes and accelerate their destruction (microangiopathic hemolytic anemia).[25] In some cases, the tumor evokes an immune response characterized by massive phagocytosis of marrow cells.[26]

Figure 1

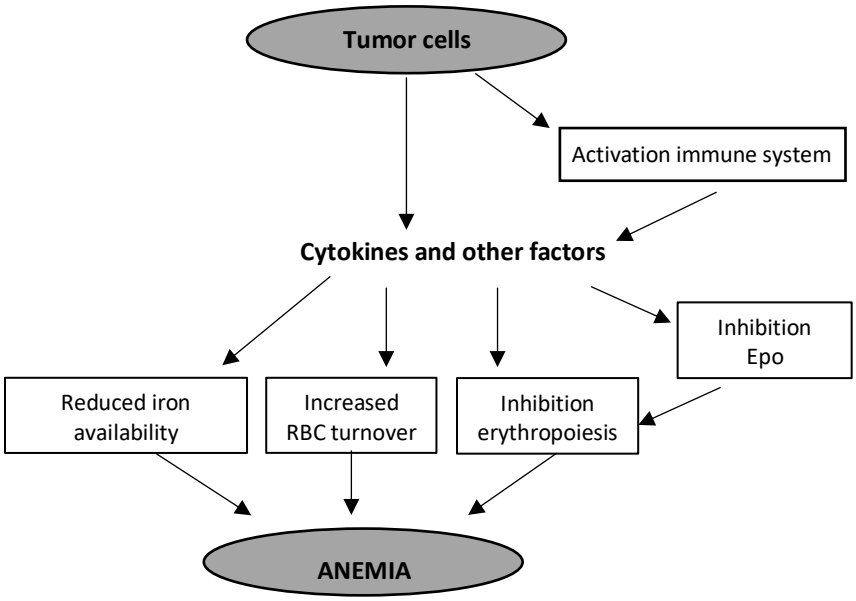

Fig. 1: Main pathogenic mechanisms of AC. Tumor cells produce and release cytokines and/or activate the immune system. The latter secreting more cytokines and factors causing anemia. These factors and cytokines can reduce iron availability for erythropoiesis, increase the turnover of the circulating erythrocytes or inhibit erythropoiesis either directly or by suppressing Epo production in the kidney.

Alterations in iron metabolism

Iron is involved in many vital functions of the body, including erythropoiesis, where it is necessary for the synthesis of hemoglobin. Conversely, excess of iron in the organism can be harmful due to its oxidizing potential and its capacity to generate reactive oxygen species (ROS), which damages tissues and organs.[27,28] For this reason, iron metabolism is tightly regulated under physiologic conditions in order to maintain systemic and cellular iron homeostasis.[29]

The iron balance in the body can be disrupted by AC or other systemic inflammatory conditions, leading to reduced iron availability in plasma (hypoferremia) and hence iron restricted anemia.[30] Hypoferremia is mainly caused by tumor-induced activation of immune cells that release cytokines like IL-6 and IL-1β which alter iron trafficking by increasing iron retention inside the macrophages and reducing duodenal iron absorption.[31] The iron metabolism in inflammatory conditions is mainly altered by interleukin-6 (IL-6),[32] which induces, through JAK2 and STAT2 signaling,[33] the synthesis of the liver peptidic hormone hepcidin. Hepcidin is the master regulator of the systemic iron metabolism and exerts its function by binding to ferroportin **(Fig. 2)**, the only known iron exporter, and it causes its internalization and degradation.[34] Besides inflammatory stimuli, hepatocytic hepcidin production is induced when iron levels are high, and reduced by erythroid activity in bone marrow through the production of different factors, especially erythroferrone (Erfe).[33] Hepcidin blocks iron absorption in the duodenum and iron release from cells, especially hepatocytes and macrophages. Macrophages recycle iron from the senescent erythrocytes, which is the main source of iron for the erythropoiesis.[35] Inflammation-induced levels of hepcidin cause an iron entrapment inside the cells, which reduces the iron concentration in plasma and thus, limits the iron available for the synthesis of hemoglobin ultimately causing iron restricted erythropoiesis.

In situations of anemia and stimulated erythropoiesis by Epo action, some erythroid precursors, specially proerythroblasts and erythroblasts, secrete Erfe, an hormone that inhibits hepcidin production in order to have more bioavailable iron for the boosted erythropoiesis.[36]

Figure 2

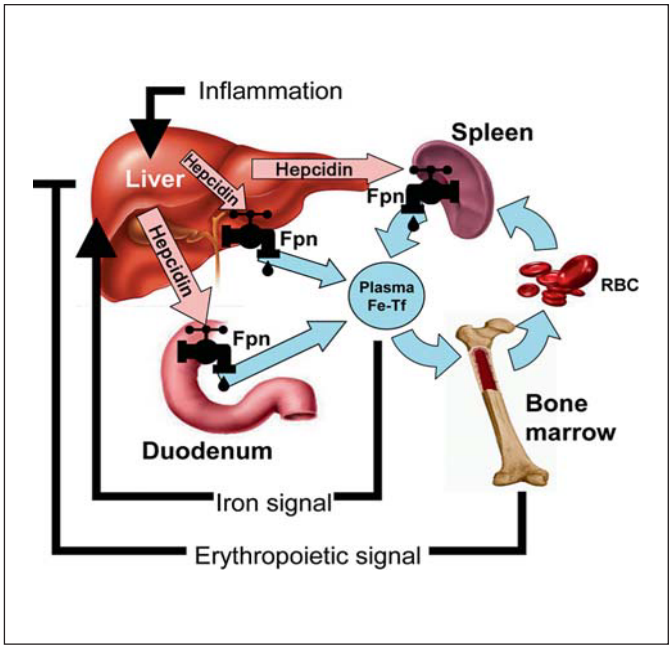

Fig. 2: Systemic iron metabolism regulation by hepcidin. Hepcidin-ferroportin (Fpn) interaction determines the flow of iron into the plasma. Hepcidin causes internalization and degradation of ferroportin. The gene expression of hepcidin is induced by iron as well as inflammation and suppressed by erythropoietic signaling. (Image taken from *Nemeth, E. & Ganz, T. The Role of Hepcidin in Iron Metabolism.* Acta Haematol. 122, 78 (2009)).

Although the hepcidin-ferroportin pathway is the main regulator of iron levels in plasma,[34,35,37] and therefore responsible of the iron-restricted erythropoiesis and the characteristic hypoferremia and hyperferritinemia observed in anemia of inflammation, other mechanisms are also involved in inflammation-induced changes in iron homeostasis. For example, tumor necrosis factor-alpha (TNF-α) reduces duodenal iron absorption through an hepcidin-independent, mechanism.[38] IL-1, IL-6, IL-10, or TNF-α promote iron acquisition into macrophages via transferrin receptor–mediated endocytosis, via divalent metal transporter 1 (DMT-1), or possibly also via increased iron acquisition by lactoferrin and lipocalin-2.[39] Additionally, bacterial lipopolysaccharides and interferon-γ (IFN-γ) block the transcription of ferroportin, thereby reducing cellular iron export.[40,41] Other factors impacting on iron metabolism are the reduced synthesis of transferrin, the iron-transport protein in plasma and the stimulation of ferritin production facilitating the intracellular storage of iron.[42]

Alterations in the erythropoiesis

The human body generates 2 million new RBC per second via erythropoiesis.[43] Erythropoiesis is a dynamic, complex, multistep process occurring in the bone marrow, where multipotent hematopoietic stem cell (HSC) differentiate into new RBC **(Fig. 3)**.[44] How RBC differentiate from hematopoietic pluripotent cells to mature red blood cells is a matter of debate[45] and several models have been proposed to describe hematopoiesis **(Fig. 4).** Immature hematopoietic progenitors are capable of giving rise to multilineage colonies. They undergo a differentiation process where they gradually diminish their proliferative and lineage potential. HSC differentiate to the common myeloid progenitor (CMP) which can further differentiate into the erythroid or the granulocytic lineage. Along the erythroid development path CMP develop into megakaryocytic-erythroid progenitor (MEP) and finally into the burst-forming unit-erythroid (BFU-E), which is the first progenitor committed solely to the erythroid lineage.[46] BFU-Es further differentiate into the colony forming unit-erythroid (CFU-E), which enter the terminal differentiation and RBC maturation.[43] Late erythroid maturation involves the differentiation of proerythroblasts into erythrocytes undergoing through different stages characterized by the gradual accumulation of hemoglobin, progressive decrease in cell size and nuclear condensation.[47] Finally, the enucleation results in the reticulocytes, which are released to the blood stream where they mature to red blood cells **(Fig. 3).**

Figure 3

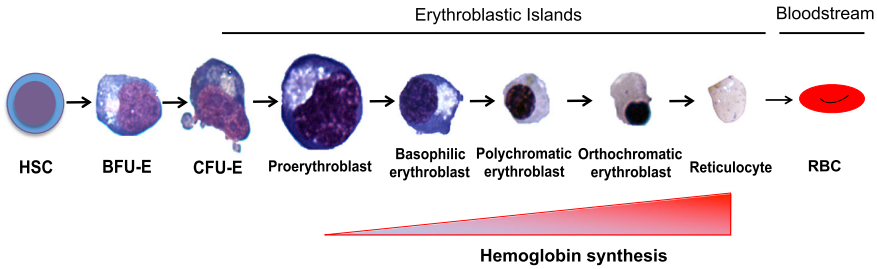

Fig. 3: Overview of the erythropoiesis. Hematopoietic stem cell (HSC) differentiate to burst-forming unit-erythroid (BFU-E), first progenitor cells committed solely to the erythroid lineage which further differentiate into the colony forming unit-erythroid (CFU-E) and proerythroblasts. Late erythroid maturation which occurs in the erythroblastic islands involves the differentiation of proerythroblasts into erythrocytes undergoing through different stages characterized by the gradual accumulation of hemoglobin, progressive decrease in cell size and nuclear condensation. Finally, the enucleation results in the reticulocytes, which are released to the blood stream where they mature to red blood cells. (Image taken from *Zivot, A., Lipton J. M., Narla, A. & Blanc, L. Erythropoiesis: insights into pathophysiology and treatments in 2017.* Molecular medicine (Cambridge, Mass.) **24,** 11 (2018)).

Figure 4

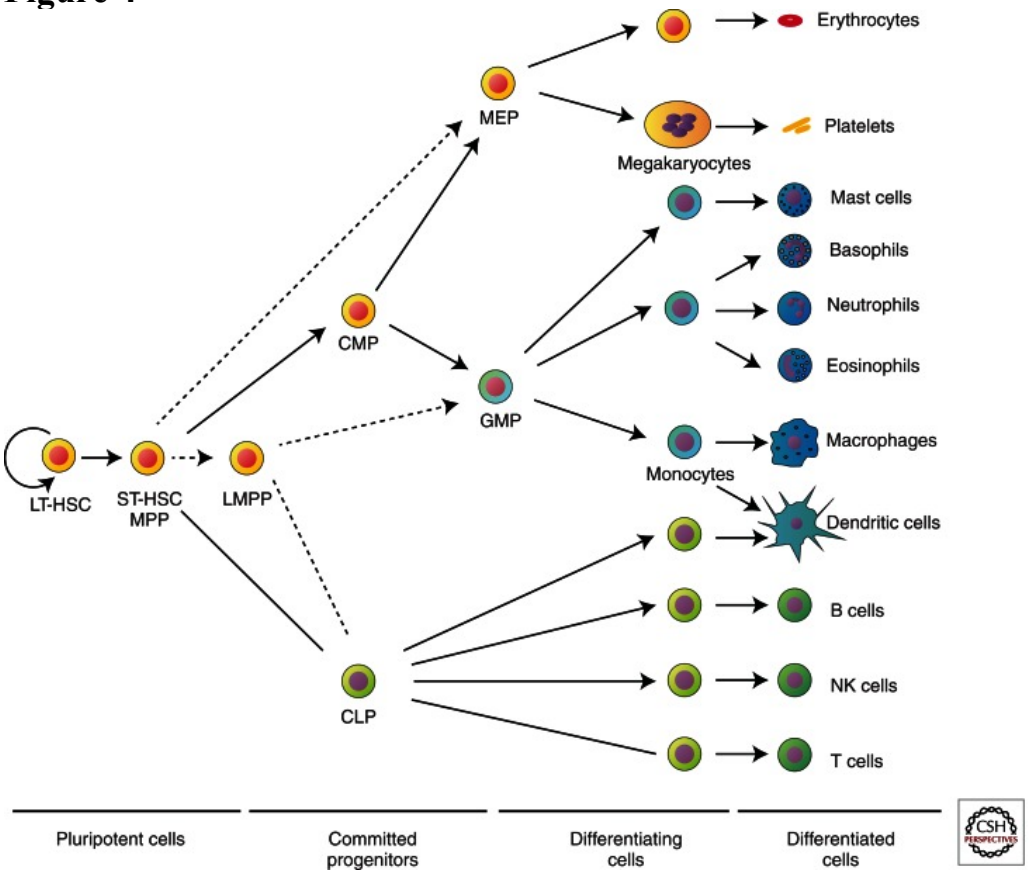

Figure 4: Different models proposed for the hematopoietic hierarchy. In the model proposed by the Weissman group[48,49,50] (solid arrows), multipotential progenitors (MPPs or short-term HSCs [ST-HSCs] give rise to either a common lymphocyte progenitor (CLP) or a common myeloid progenitor (CMP), which, in turn, gives rise to either a granulocyte-macrophage progenitor (GMP, equivalent to CFU-GM) or a megakaryocyte-erythroid progenitor (MEP). The alternate model suggested by the Jacobson group[51] (dotted arrows) involves the generation of MEPs directly from the MPPs/ST-HSCs, whereas a lymphoid-primed multipotential progenitor (LMPP) has the potential to generate both CLPs and GMPs. LT-HSC, Long-term hematopoietic stem cell; NK cell, natural killer cell. (Image taken from *Dzierzak, E. & Philipsen, S. Erythropoiesis: development and differentiation*. Cold Spring Harb. Perspect. Med. **3,** 1–16 (2013)).

These steps of hematopoiesis (including erythropoiesis), i.e. the production of the different cellular types which constitute the blood, are governed by multiple cytokines that promote survival, proliferation an differentiation of HSC and progenitor cells.[52] Among the cytokines, Epo and stem cell factor (SCF) are key regulators of erythropoiesis. Impaired erythropoiesis because of cancer inflammation can be caused by distinct mechanisms: e.g. reduced expression of Epo in the kidney, inhibition of Epo the biological activity,[53] or to inhibition of SCF production.[25]

Epo is a glycoprotein hormone synthesized in response to tissue hypoxia principally in interstitial fibroblasts and the proximal tubular cells of the kidney but also in minor extend in the liver in mice.[54] Its synthesis and release in plasma is regulated by tissue oxygen tension through hypoxia-inducible factor 2 (HIF-2) activity, and its main function is to stimulate RBC

production in order to compensate the hypoxia.[55] Epo binds to its receptor (EpoR) on the cellular membrane of the erythroid precursors in the bone marrow. The binding of Epo to its receptor promotes the proliferation and differentiation of the erythroid cells and inhibits their apoptosis mainly through the activation of the JAK-STAT signal transduction pathways.[56] EpoR is also expressed in other tissues and cells such as endothelial cells, neurons and myocardial cells where EpoR promotes cell repair an inhibits apoptosis.[57,58] Some studies in anemia of chronic disease showed lower Epo levels than expected for the severity of the anemia in most of the subjects.[23] Some cytokines, mainly IL-1 and TNF-α are known to inhibit Epo production by interfering with mediated GATA-2 or HNF4 transcription or by causing radical-mediated damage of Epo-producing kidney epithelial cells.[59,60] Additionally, proinflammatory cytokines, especially IL-6 and IL-1 also inhibit Epo function by impairing EpoR downstream signaling.[61] Furthermore, some cytokines like INF-γ, interleukin-10 (IL-10), granulocyte-colony stimulating factor (G-CSF) and IL-6 stimulates the production of the suppressor of cytokine signaling-3 (SOCS-3) which binds to JAK kinase and to EpoR resulting in the inhibition of the STAT3 activation.[62] Moreover, INF-γ, TNF-α and IL-1 can also target directly erythroid progenitors inducing apoptosis, inhibiting differentiation and proliferation of erythroid progenitor cells[63,25] and promoting differentiation of myeloid cells progenitors.[64,65]

Stem cell factor (SCF) also has a main role in the control of hematopoiesis.[66] In the bone marrow, it is produced by endothelial cells[67] and fibroblasts and binds to its receptor, c-kit.[68,69] SCF is essential for the maintenance of normal basal hematopoiesis and is also required for acute erythroid expansion during the recovery from anemia in adult mice.[70] It acts in conjunction with other cytokines and especially in coordination with Epo promoting the survival and expansion of stem cells as of as the expansion, survival and differentiation of different progenitors.[71] Other important hematopoietic regulators are interleukin-3 (IL-3) or common colony stimulating factor (CSF), granulocyte colony stimulating factor (G-CSF) and granulocyte-macrophage colony-stimulating factor (GM-SCF) which stimulates proliferation and differentiation of multiple progenitors specially granulocytes.[52]

Despite the direct inhibition of erythropoiesis, iron supply in bone marrow also act as a regulator of the hematopoiesis, being necessary for the differentiation of the later stages of erythropoiesis through the synthesis of heme group and regulating the transcription of hemoglobin genes.[72]

Alterations on the nutritional and metabolic state

Some of the immune system alterations associated to the tumor disease in cancer patients have effects in multiple organs and cause multiple symptoms as anorexia, vomits, loss of body weight and cachexia of cancer, reduction of muscle mass, increase in the resting energy expenditure with alterations in glucose, lipid and protein metabolism, fatigue and immunosuppression.[24] The severity of the immune alterations is proportional to the cancer stage and to the amount of inflammatory cytokines.[73,74] It has been shown that IL-6 levels are inversely correlated with albumin levels and cachexia in patients with lymphoma[75] and it has been related with the severity of weight loss in cancer patients.[24] Moreover, other proinflammatory cytokines as TNF-α, IL-1 and INF-γ have been related with weight loss and metabolic alterations in cancer patients,[76] by increasing the metabolic rate through activation of thermogenesis, inhibiting adipocyte and skeletal myocyte differentiation and reducing the food intake.[77] These alterations on the nutritional and the metabolic status of the cancer patients might affect the levels of iron, glucose, vitamins and other micronutrients useful for the erythropoiesis and therefore contribute on the pathogenesis of the AC.[24] Hence, it is important to take them in consideration for the diagnostic and treatment plan of the cancer related anemia.

3.3. Therapeutic approach of AC

Despite the high prevalence of AC and its important clinical significance, AC is currently undertreated and no specific aimed treatments for this kind of anemia have been yet approved.[24] Due to its multifactorial nature, it should be efficiently treated using multitargeted therapies. Before starting the treatment in a particular patient, an exhaustive evaluation of all the potential contributors to the anemia should be performed in order to target every treatable cause. Currently, the National Comprehensive Cancer Network (NCCN) provided a guideline for cancer- and chemotherapy induced anemia diagnosis and management.[78] It is important to keep in mind though, that anemia reflects the severity of the neoplastic disease, and the cure of cancer is so far the only way to cure anemia. A curative treatment of the cancer is not always possible and therefore, an individualized therapeutic strategy might be required to palliate the anemia and its multiple consequences in human cancer patients.[79] The drugs and therapeutic procedures most commonly used for the treatment of AC are: blood transfusions, erythropoiesis-stimulating agents (ESA), iron supplementation, nutritional supplementation and anti-inflammatory therapies.[23] Other agents that could be useful in the future include

hepcidin antagonists, iron-chelators therapy and use of cytokines and hormones that could modulate the erythropoiesis under inflammatory conditions.[24]

Blood transfusions

Red blood cells transfusions are a fast and effective method to increase hemoglobin levels, palliate anemia associated symptoms and improve quality of life in cancer patients. However, this treatment has some limitations like the limited availability of the blood products or the fact that some patients are unable to receive blood transfusions due to the presence of multiple alloantibodies or to their specific religious beliefs.[78] Moreover, blood transfusions have some associated risks, including fever, transfusion related allergic reactions, transmission of infectious diseases, alloimmunization, iron overload and immunosuopression.[20,80] Additionally they have been associated with multiorgan failure and increased mortality in patients under critical care.[81] Whether blood transfusions modulate the immune system, causing clinically relevant adverse effects, remains still undetermined.[82] Therefore, blood transfusions should be used only in patients with symptomatic or severe anemia who need a fast increase in the oxygen transport capacity.[78]

Erythropoiesis-stimulating agents (ESA)

Recombinant human erythropoietin (huEPO) is approved for treating anemia in patients with chronic kidney disease and anemia in cancer patients due to the chemotherapy. Despite not being specifically approved for the treatment of AC, the capacity of huEPO treatment in cancer patients to increase hemoglobin levels, reduce the need for blood transfusions and improve their quality of life has been demonstrated in several studies.[83,84,85] In general, ESA alone have a responsiveness rate among cancer patients presenting anemia of 55-65%[83] and increases to 70-90% when it is used in combination with iron supplementation.[86,87,88,89] Additionally, ESAs, due to its action in other organs, may have other systemic actions which might be beneficial, like a neuroprotective and anti-inflammatory effect as of as vascular and metabolic actions.[90,23] Currently, there are several forms available (epoetin alfa, epoetin beta, and darbepoetin alfa) with similar efficacy but different half-life after administration.[91,92]

However, concerns about huEPO safety have been raised because some studies showed that ESAs treatment in cancer patients is associated with an inferior survival and worse cancer outcomes.[93,94] However, these results are controversial since other analysis failed to confirm

these data.[95] Systematic reviews demonstrated a significantly higher risk of thromboembolic events in patients receiving ESAs for AC,[96,97,83,98] but again, some others pointed that this increased mortality could be related to the design of the studies, setting excessively high baseline hemoglobin levels before starting the treatment [99,100] and too high target hemoglobin levels.[101,102] Other adverse side effects of ESA treatment as hypertension, thrombocytopenia, hemorrhage and seizures have been also reported.[83] Additionally, due to the fact that EpoR is found in multiple cancer cell types,[103,21,104] it was hypothesized that the increased mortality could be due to the ability of Epo to stimulate tumor growth.[105,106] Indeed, some *in vitro* studies have shown that Epo is able to increase cell proliferation,[107] induce resistance to apoptosis[108] and promote cell migration.[109] In addition, some *in vivo* studies investigating the effect of ESA in tumor progression showed that ESAs were associated with increased tumor growth,[21,110] and it was hypothesized that it might be due to induction of neoangiogenesis, since Epo increases inflammation and ischemia-induced neovascularization by enhancing the mobilization of endothelial progenitor cells.[111] Due to all the aforementioned concerns about the safety of ESA treatment in cancer patients, these drugs should be used with caution.

Iron supplementation

Iron deficiency is a common comorbidity in cancer patients, affecting 29%-60% of this kind of patients.[112] Determination of the iron status is recommended before starting the treatment with ESA because erythropoiesis requires bioavailable iron, and lack of iron can lead to a fail of the treatment.[88] Patients might be classified as: iron replete, having absolute iron deficiency (ferritin <30 ng/dL, transferrin saturation <15%), or having functional iron deficiency (ferritin 30–800 ng/dL and transferrin saturation <20%).[113,114] Patients with absolute iron deficiency may be treated with iron supplementation only, while those with functional iron deficiency should receive ESAs along with parenteral iron.[114] Despite oral and parenteral iron forms are available in the market to treat iron deficiency, several studies have shown than parenteral iron is more effective for patients with cancer and functional iron deficiency.[115,116,117] Some studies showed that the addition of iron supplementation to the anemia treatment with ESA had greater increments in hemoglobin levels and the need for transfusion was reduced,[116,87,86] but still limited data about iron efficacy as monotherapy are available.[118] It is important to note though, that another study demonstrated a lack of benefit of adding intravenous iron to ESAs in anemic cancer patients with signs of functional

iron deficiency.[119] However, for patients with functional iron deficiency with high levels of ferritin (low circulating iron in plasma but replete iron stores), iron supplementation is not recommended since iron overload can cause ROS induction and aggravate the oxidative stress status leading to subsequent endothelial damage and increased risk of cardiovascular complications.[24] It is also important to mention that there are some safety concerns regarding iron supplementation in cancer patients. Besides the common adverse effects of parenteral iron administration as flushing, nausea, vomiting, diarrhea[120] and increased risk of infections,[121] it has been shown that iron has a role in all aspects of cancer development, including tumor initiation, growth and on the tumor microenvironment and metastasis.[122] It has been demonstrated in several animal studies that, in different types of cancer, excessive iron supplementation could lead to increased cancer cell proliferation.[123] Therefore, with the current data available, the iron status of patients with AC should be evaluated and supplemented when needed, especially those who does not respond to ESAs therapy alone.[24]

3.4 Mouse models of AC

Although AC is highly present in patients who suffer from cancer with a major clinical relevance for disease prognosis and treatment, this condition is still currently undertreated due in a great extent to the lack of safe treatment options.[124] Therefore there is a growing interest in characterizing new contributing factors to AC and finding new targets for its treatment. Preclinical models should contribute to the better understanding of the complex pathophysiology of this kind of anemia and facilitate the development of safer and more effective treatment strategies.[125] However, very few animal models for AC have been developed, all of them being injected tumor models (orthotopic models). Two of them are murine xenograft models were the alteration of the iron metabolism due to upregulation of hepcidin by IL-6 was studied and the efficacy of an IL-6 antibody (MR16-1) to mitigate the anemia was evaluated.[126,127] In another study, four synergic murine models, in which different tumor cells lines were injected into C57BL/6 mice, were characterized and the role of the inflammation and hepcidin on the AC was studied, getting different degrees of hepcidin involvement for each model, illustrating the great variability of the importance of the different etiological factors in the pathogenesis of AC.[125] Additionally, in another murine tumor model with 4T1 injected cancer cells, they showed that tumor was blocking medullar erythropoiesis through the production of granulocyte colony-stimulating factor (G-CSF). Additionally, they

showed the involvement of macrophages in the splenic erythropoiesis promoted by the tumor stress, which in turns, also have a role in promoting the tumor grrowth.[128]

To our knowledge, no genetically engineered animal models with spontaneous tumor development have been investigated. Our Trp53^{flox}WapCre mouse model is selectively deficient of the p53 tumor suppressor gene in luminal cells of the mammary tissue.[129] The deletion of this gene causes the spontaneous development of mammary tumors and AC. Alterations in the p53 gene are very common in human breast cancer.[130] Therefore, we tested if our transgenic Trp53^{flox}WapCre mouse model, might be a new model to investigate AC and if it might help to the better characterization and understanding a of this multifactorial and complicated condition helping to develop and evaluate safer and more effective therapeutic approaches.

3.5 Rational and objectives

AC has a huge clinical impact on cancer patients, not only impairing their quality of life and limiting their antineoplastic treatment options but also contributing to the disease progression. Nowadays, effective and safe treatment approaches are still lacking, and this is one of the main reasons why it is still in great extend left undertreated. Very few mice models of AC have been characterized and, to our knowledge, none of them being a model with spontaneous tumor development. The use of preclinical models can contribute to better understand this multifactorial and complex condition and help to design safer and more effective treatments. We characterized AC in Trp53^{flox}WapCre mice and analyzed if this model reflects the pathology of impaired erythropoiesis in AC of human patients and if it is useful to test multiple treatment approaches. We therefore focused on:

I) Defining the inflammatory response and the alterations in the iron metabolism
II) Testing the efficacy of iron supplementation
III) Analyzing the impact of cancer in hematopoiesis and erythropoiesis

4. Material and methods

4.1 Animal Experiments

Housing conditions

Mice were housed at 22±5 °C in a 12 h light/dark cycle and fed either with a standard rodent chow (250 mg/kg iron) (Kliba Nafag, #3436) or with an iron sufficient diet (50 mg/kg iron) (Kliba Nafag, #2222 modified) and water ad libitum. The experiments were performed in accordance with the Swiss animal law and with the approval of the ethical committee of the respective local authorities (Kanton Zurich).

Mouse models

Spontaneously tumor-developing mouse model. In this study, we used transgenic $Trp53^{flox}$WapCre mice[129] bred in our animal facilities in which the tumor suppressor gene p53 was deleted specifically from the mammary tissue using Cre/lox system. The genetic background of the mice used for the genetic modification was FVB wildtype.

FVB wild type. FVB wildtype mice were purchased from Envigo (Netherlands) at the age of 12 weeks. They were housed in our animal facility in the same conditions than $Trp53^{flox}$WapCre mice. At the age of 26-27 weeks plasma and organs were collected in order to compare iron parameters in plasma and tissue with $Trp53^{flox}$WapCre mice to discard aberrant iron metabolism modifications in our transgenic strain.

Allotransplanted tumor mouse model. Immunocompromised $Foxn1^{nu}$ mice of 8-9 weeks of age were purchased form Envigo (Netherlands) and housed in our facilities. Between 11-14 weeks of age they were anesthetized with isoflurane, and to 5 mice a fresh piece of approximately 3 mm^3 of a mammary tumor (>1cm^3) from a $Trp53^{flox}$WapCre previously euthanized using CO_2 was placed subcutaneously for allographic tumor transplantation. The skin was closed using 4/0 polypropylene surgical suture. 5 animals were sham operated in order to use as a control. All the tumors grew, but 3 out of 5 animals developed ulcers on the tumor site before reaching termination criteria and therefore they had to be euthanized before reaching the maximal tumor size.

Procedures

Tumor detection and measurement. Mice were monitored by visual observation and palpation every other day from 18 weeks of age or from tumor implantation until a tumor was found. After tumor detection, tumor length (L) and width (W) were measured every other day using a caliper and tumor volume (V) was calculated as [$V = (L \times W2)/2$].[131] Bodyweight was also measured every other day in tumor-bearing mice.

Epo treatment. Mice were manually restrained and subcutaneously injected with 1000 U/kg of Epo (Recormon, Roche) or saline 3 times a week beginning the first day of tumor detection with a 30 G BD micro-fine insulin syringe. Animals were euthanized when the tumor reached the maximal permitted tumor size of 2 cm^3 (single tumor) or 3 cm^3 (total volume of multiple tumors).

Iron treatment experiment. In the first experiment, mice were injected intravenously (i.v.) with either saline or 13,8 mg/kg of ferric carboxymaltose (Ferinject®) the same day than the tumor was detected. The dose of ferric carboxymaltose was calculated using the Ganzoni formula:[132]

Total iron deficit [mg] = BW [kg] x (target Hb - actual Hb) [g/dl] x 2.4) + storage iron [mg]

BW was the body weight of mice at the moment of the tumor diagnosis, target Hb refers to the upper 75% percentile of hemoglobin values in the tumor free control group and the actual Hb was the 25% percentile of hemoglobin vales of tumor-bearing mice when they reached maximal permitted tumor size of 2 cm^3 (single tumor) or 3 cm^3 (total volume of multiple tumors). Ferric carboxymaltose volume was diluted in 0.9% NaCl up to 100 µl of total volume solution. Mice were restrained in a self-made restrainer and the tail was placed into a warm water bath (30 - 35 °C) for around 3 minutes to dilate the tail veins. One of the lateral veins was injected using a 30 G BD micro-fine insulin syringe. Mice were euthanized when the tumor reached maximal permitted size of 2 cm^3 (single tumor) or 3 cm^3 (total volume of multiple tumors).

Alternatively, in subsequent experiments, mice were i.v. injected with 20 mg/kg instead of 13.8 mg/kg of ferric carboxymaltose (Ferinject®) or saline and either directly after tumor detection or when tumor size reached 1.5 cm^3. The experiment was terminated exactly 15 days after the i.v. injection in mice that received the injection after tumor development or 48 h after injection in mice that received the injection when the tumor reached a size of 1.5 cm^3.

Perfusion and sample collection. Tumor-bearing mice were euthanized by carbon dioxide (CO_2) at different stages of the disease: the same day of the tumor diagnosis (day 0), 7 days (7d) and 15 days (15d) after tumor diagnosis, or at end stage (ES): when they reached experimental termination criteria by maximal tumor permitted size (tumor volume of 2 cm^3 for single tumor or 3 cm^3 for multiple tumors). Tumor free age-matched animals were also euthanized and used as control. Immediately after euthanasia, the chest cavity of the mice was opened to expose the heart and 0.5-1 ml blood was collected by cardiac puncture into the right ventricle with a 1 ml syringe coated with heparin. The mice were then transcardially perfused with 20 ml ice-cold PBS by introducing a needle into the left ventricle of the heart after perforating the right atrium.

The organs listed in **Table 1** were immediately collected, weighed, cut and appropriate stored either in 4% paraformaldehyde (PFA) at room temperature for fixation and future histology use, or snap frozen in liquid nitrogen and stored at -80 °C for future quantificational analysis. Tissues incubated for 24-48 h in 4% PFA were then washed twice in 1x PBS and placed in 70% EtOH for longer storage at 4 °C.

Bone marrow from both femurs and tibias were collected by flushing the bone marrow cavity using a 1 ml syringe attached to a 24 G needle either with RPMI medium supplemented with 2.5% heat-inactivated FBS for the flow cytometry experiments, or with the LBA-TG buffer from the ReliaPrep® RNA Tissue Miniprep System and snap frozen for the subsequent RNA isolation.

Table 1: Overview of collected samples

Samples	4% PFA	Snap Frozen (80°)
Plasma		entire
Tumor (1st tumor detected)	1/2	1/4
Spleen	1/2	1/2
Liver	left lateral lobe	rest
Kidney	right	left
Lungs	entire	
Bone marrow (2 femurs and 2 tibias)		entire
Sternum	entire	

4.2 Analyzing mRNA expression by real time PCR

RNA extraction. RNA of harvested tissue, namely liver, spleen, kidney, tumor, healthy mammary tissue and bone marrow, was extracted using the ReliaPrep® RNA Tissue Miniprep System (Promega) following the supplier instructions. RNA concentration and purity (260/280 nm) was measured on the NanoDrop 2000 Spectrophotometer and RNA samples were stored at -80 °C or directly transcribed into cDNA.

Complementary DNA synthesis. 500 ng RNA was diluted in 10.5 µl sterile H_2O and 2 µl of Oligo-dT (10 µM) was added, gently mixed, centrifuged, incubated at 65 °C for 5 min and then put on ice immediately. 7.5 µl of the master containing 4 µl of 5x Reaction Buffer (Thermo Fisher), 0.5µl Thermo Scientific™ RiboLock RNase inhibitor (20 U), 2 µl dNTP Mix 10 mM (Thermo Scientific) and 1 µl RevertAid Reverse Transcriptase 200 U (Thermo Scientific) was added to each sample and incubated for 60 min at 42 °C. To heat-inactivate the RNase, the reaction was terminated by incubating the samples at 70 °C for 10 min. To obtain a cDNA concentration of 5 ng/µl, 80 µl of H2O was added and the cDNA was stored at -20 °C.

Primer Design. Primers were designed with Primer3 software as described by Rozen et al.[133] and purchased at Microsynth (Switzerland). Used primers are shown in **Table 2.**

Real time PCR. Master mix was prepared on ice containing 5 µl LightCycler 480 SYBR Green I Master (Roche Applied Science, Cat. 04707516001), 1 µl Primer forward (10 µM), 1 µl Primer reverse (10 µM) and 1 µl H_2O per sample. Samples were run in duplicates and 2 µl cDNA (5 ng/µl) was added to 8 µl master mix per well, in a MicroAmp Fast Optical 96-Well Reaction Plate (Applied Biosystems by life technologies) on ice. Plate was sealed with Optical Adhesive Covers (Applied Biosystems by Life Technologies), and centrifuged for 2-3 minutes at 2500 x g, before being placed in Thermocycler ABI7500 Fast (Applied Biosystems) to run Real-time PCR. The program for cDNA amplification was set to: 50° C for 2 min; 95° C for 10 min; 40 cycles at 95° C a 30 sec and 60° C for 40 sec, followed by melt curve analysis. Fold changes were determined by delta-delta Ct method[134] with beta-Actin or Gypa (Glycophorin A), for some genes measured in bone marrow and spleen, as reference gene.

Table 2. Primer sequences for genes analyzed with Real-time PCR (SYBR green method)

Target Gene	Primer Pair
β *-actin* Reference gene	Fwd: 5'CAACGGCTCCGGCATGTGC3' Rev: 5' CTCTTGCTCTGGGCCTCG 3'
Epo Erythropoietin	Fwd: 5' AGACAAAGCCATCAGTGGTC 3' Rev: 5' TGTGAGTGTTCGGAGTGGAG 3'
IL-6 Interleukin-6	Fwd: 5'CTCTGGGAAATCGTGGAAAT3' Rev: 5' CCAGTTTGGTAGCATCCATC 3'
SAA-1 Serum amyloid A1	Fwd: 5' GGGGAACTATGATGCTGCT 3' Rev: 5' ATTGGGGTCTTTGCCACT 3'
*IL-1**β*** Interleukin-1**β**	Fwd: 5' CCTGTGTAATGAAAGGCA 3' Rev: 5' CTGCTTGTGAGGTGCTGATG 3'
TNFα Tumor necrosis factor α	Fwd: 5' ATCAAGGACTCAAATGGGCTT 3' Rev: 5' GCAACCTGACCACTCTCCCT 3'
Hamp-1 Hepcidin-1	Fwd: 5' TTCCCAGTGTGGTATCTGTTG 3' Rev: 5' GGGAGGGCAGGAATAAATAAT 3'
Fpn Ferroportin	Fwd: 5' ACC CAT CCC CAT AGT CTC TGT 3' Rev: 5' CCG TCA AAT CAA AGG ACC AA 3'
Fth1 Heavy chain ferritin	Fwd: 5' GCCAGAACTACCACCAGGAC 3' Rev: 5' TTCAGAGCCACATCATCTCG 3'
Trf Transferrin	Fwd: 5' CACACACACCGAGAGGATGA 3' Rev: 5' TTCTCGTGCTCTGACACTGC 3'
BMP-6 Bone morphogenic protein-6	Fwd: 5' TGTGATGGAGAGTGTTCC 3' Rev: 5' GGCATTCAGTTTGGTTGG 3'
Hfe2 Hemojuvelin	Fwd: 5'TTGCTAGATAACGACTTCCTCTTTG3' Rev: 5'AGCCTGGTAGACTTTCTGGT3'
Hfe Homeostatic iron regulator	Fwd: 5' TGCTACCTAACGGGGATGAG 3' Rev: 5' GACGGTGACTCCACTGATGA 3'
TfR-1 Transferrin recepror-1	Fwd: 5' GAGACTACTTCCGTGCTACT 3' Rev: 5' GGAGACTCT CTTGGAGATAC3'
TfR-2 Transferrin recepror-2	Fwd: 5' CTGCGGAAGGAGATTTACAG 3' Rev: 5' ACTGGGACAGGAAGTAGAAC 3'
Erfe Erythroferrone	Fwd: 5' AGCGAGCTCTTCACCATCTC 3' Rev: 5' TGTCCAAGAAGACAGAAGTGTAGTG 3'
Epo-R Erythropoietin receptor	Fwd: 5' GTCCTCATCTCGCTGTTGCT 3' Rev: 5' CAGGCCAGATCTTCTGCTG 3'
Hbα Hemoglobin α chain	Fwd: 5' TGAAGCCCTGGAAAGGATGTTTG 3' Rev: 5' CCTTCTTGCCGTGACCCTTG 3'
*Hb**β*** Hemoglobin **β** chain	Fwd: 5' CGATGAAGTTGGTGGTGAGG 3' Rev: 5' ATAGCAGAGGCAGAGGATAGG 3'
Gypa Glycophorin A	Fwd: 5' ATGGCAGGGATTATCGGAAC 3' Rev: 5' CACCCTCAGGAGATTGGATG 3'
SCF Stem cell factor	Fwd: 5' TGGGAAAATAGTGGATGACCTCGTGT 3' Rev: 5' CGGGACCTAATGTTGAAGAGAGCACA 3'
SOCS-3 Suppressor of cytokine signaling 3	Fwd: 5' TCACCCACAGCAAGTTTCCC 3' Rev: 5' GCTCCAGTAGAATCCGCTCTC 3'
G-CSF Granulocyte colony-stimulating factor	Fwd: 5' GCAGGCTCTATCGGGTATTT 3' Rev: 5' TGGAAGGCAGAAGTGAAGG 3
GM-CSF Granulocyte-macrophage colony-stimulating factor	Fwd: 5'CTCACCCATCACTGTCACCC 3' Rev: 5'GACGACTTCTACCTCTTCATTCAAC3'

4.3 Analyzing plasma Epo concentration

For the quantitative determination of Epo concentration in plasma, we used Quantikine® ELISA Mouse Erythropoietin Immunoassay (#MEP00B) from R&D Systems, Inc. The protocol provided by the manufacturer was thoroughly followed. The optical density was determined with BioTeck Epoch™ 2 Microplate Spectrophotometer at 450 nm. Absorbances were corrected by subtracting the values of 540 nm from the values if 450 nm. Results were calculated by extrapolation of the standard curve which was calculated by four-parameter logistic (4-PL) regression.

4.4 Hematology and Clinical biochemistry

Hemoglobin was measured from fresh hole blood collected by cardiac puncture by ABL800 (Radiometer RSCH GmbH). Hematocrit was determined with blood-filled capillaries by measuring the ratio of the volume occupied by red blood cells to the volume of whole blood after 5 min at 120 rpm in the microcentrifuge (HETTICH). The rest of the blood was used for plasma extraction by centrifuging the blood at 2000 rpm for 10 minutes. The clear supernatant was removed and filled into a new tube to be snap frozen.

Hematology was performed in fresh hole blood collected by cardiac puncture and stored in EDTA coated tubes at 4°C. Analysis were performed using the Sysmex XT-2000iV within 1 hour after collection.

For **clinical biochemistry**, hole blood was collected by cardiac puncture with a heparin coated needle and kept in 1.5 ml microcentrifuge tubes at 4°C. Plasma was extracted by centrifuging the blood at 2000 rpm for 10 minutes. Analysis were performed with Roche Integra 800 analyzer within 1 hour after collection and following parameters were measured: bilirubin, glucose, urea, creatinine, total protein, cholesterol, triglycerides, alkaline phosphatase, aspartate transaminase and alanine transaminase.

4.5 Histology

Tissue embedding. Tissues stored in 70% EtOH were placed in paraffin embedding cassettes and chemical fixed in the Microm spin tissue processor STP-120. After embedding the tissues in paraffin blocks, the paraffinized tissues were cut in 3-5 μm sections.

Hematoxylin and Eosin (H&E) staining. Slides were deparaffinized in xylene, rehydrated through graded alcohols of decreasing concentrations, stained with hematoxylin and eosin and dehydrated again using increasing alcohol concentrations. All steps were performed using the automated staining system Discovery from Ventana Medical Systems, Inc.

Perl's-DAB enhanced staining. This stain was performed to visualize iron. The tissue sections were deparaffinized and incubated for 2 minutes in a solution 1:1 of 2% potassium ferrocyanide and 2% HCl. Next, they were washed with demineralized water and later with TBS. Thereafter, the slides were incubated for 15 minutes with the H_2O_2 blocking solution and washed with TBS. After, the slides were incubated for 5 min with DAB and washed again with water. Further, the slides were incubated with hematoxylin for 3 minutes and washed with tap water until they got a blueish coloration. To finalize, the slides were dehydrated and covered.

Ki-67 staining. The staining procedure is used to visualize cell proliferation and it was performed using the automated staining system Discovery from Ventana Medical Systems, Inc. Slides were deparaffinized in xylene and rehydrated trough graded alcohols of decreasing concentrations. After antigen retrieval slides were incubated with the primary rabbit monoclonal antibody Ki-67 (30-9) 1:1 from Roche (# 790-4286) for 32 minutes. The secondary antibody used was biotinylated donkey anti-rabbit* IgG 1:100 for 8 minutes. Discovery DAB Map detection kit from Roche (#760-124) was used for the antigen detection and the cellular background was stained with hematoxylin (incubation time of 4 min). Slides where dehydrated again using increasing alcohol concentrations and covered.

Cellular quantification. Ki-67 positive cells in the whole tissue sections of liver as well as cellularity of H&E stained bone marrow sections were quantified using Viopharm sofware by dividing the number Ki-67 positive cell or cellular nucleous by the analyzed area.

4.6 Analyzing plasmatic interleukin-6 concentration

Interleukin-6 (IL-6) concentration in plasma was determined by ELISA assay using U-PLEX Mouse IL-6 Assay® (#K152TXK-1) from Meso Scale Discovery (MSD).

Frozen heparinized plasma was thawed and centrifuged at 1000 x g for 1 min to pellet debris and the assay was performed according to the manufacturer recommendations. Briefly, the plate was coated with the biotinylated IL-6 antibody by incubating it for 1 hour at room temperature on a shaker at 500-1000 rpm. The plate was washed 3 times by adding 150 µl PBS-T

(0.05%Tween-20) to each well. Serial dilutions of the calibrator were prepared in order to generate the standard curve and 25 µl of diluent plus either 25 µl of plasma or standard were added to the correspondent well. The plate was then sealed and incubated for 1 h on the shaker at room temperature. The plate was rinsed again 3 times with 150 µl PBS-T and 150 µl of the 2X read buffer were added to each well before reading the plate on the MESO QuickPlex SQ 120 instrument (Meso Scale Discovery) with the MSD Workbench 4.0 software.

4.7 Iron parameters in plasma

Serum iron concentration was measured using the colorimetric Iron (SFBC) Bathophenanthrolin assay from Biolabo (#80008). Frozen heparinized plasma was thawed and 50 µl were used for the assay, which was performed in a 96-well plate. The assay was performed according to the manufacturer recommendations, but volumes were proportionally reduced. Briefly, 50 µl of solution R1 were added to 50 ml of sample in microcentrifuge tubes and vortexed for 2 minutes. After 5 minutes of incubation, each tube was centrifuged for 10 minutes at 3000 rpm. 50 µl of the mixture was then transferred to a 96 well. To generate the blank 25 µl of deionized water plus 25 µl or solution R1 were added to some wells, and for the standard, 25 µl of solution R3 plus 25 µl of solution R1. 50 µl of solution R2 was added to all wells and the plate incubated for 5 minutes at room temperature. After incubation, the plate was read at 535 nm in BioTeck Epoch™ 2 Microplate Spectrophotometer. For the calculation of the results, the following formula was used:

Iron plasma concentration (µl g/dL) = [Abs (Assay) /Abs (Standard)] x Standard concentration.

Unsaturated iron binding capacity was measured by a colorimetric method (ferene direct method): U.I.B.C. Unsaturated Iron Binding Capacity from Biolabo (#97408). 20 µl of thawed heparinized plasma was used for the assay, which was performed in a 96-well plate. The instructions of the manufacturer were thoroughly followed, but volumes were proportionally reduced. Briefly, 100 µl of solution R1 were added to each well, 20 µl of solution R2 were added to every well except on the blank, were 40 µl of deionized water was added instead. To the standard 20 µl of deionized water was added and to the rest of the wells 20 µl of sample. Before the addition of 2 ml of ferene (chromogen), the plate was read at 600 nm against the reagent blank using BioTeck Epoch™ 2 Microplate Spectrophotometer (A1). 20 min after the

addition of ferene, the plate was read again at the same wavelength (A2). For the calculation of the results, the following formula was used:

UIBC (µl g/dL) = 500 - [500 x (A2 Assay - A1 Assay) / (A2 Standard - A1 Standard)]

Total iron binding capacity (TIBC) was calculated using the following formula:

TIBC (µl g/dL) = Plasma iron concentration (µl g/dL) + UIBC (µl g/dL)

Transferrin saturation (Tsat) was calculated using the following formula:

Tsat (%) = (Iron concentration in plasma / TIBC) x 100

4.8 Analyzing ferritin concentration in plasma

For the quantitative determination of ferritin in plasma, we used the Mouse Ferritin ELISA kit (#80636) from Crystal Chem, Inc. 5 µl of thawed heparinized plasma was diluted to 1:40 with the diluent provided by the kit and used for the assay. The manufacturer instructions were thoroughly followed, and the absorbance was measured using BioTeck Epoch™ 2 Microplate Spectrophotometer at 450 nm and values at 630 nm were subtracted. All the samples were measured in duplicates. The concentration of ferritin was calculated by extrapolation of the mean absorbance for each sample to the standard curve which was calculated by 4-parameter logistic regression using a computer software.

4.9. Non-heme iron measurement in tissue

To analyze the amount of iron in tissue, we used a protocol for non-heme iron determination in tissue kindly provided by Bruno Galy and Sandro Altamura from the University of Heidelberg, which is a modification of the method described by Torrence and Bothwell.[135]

We first dried the tissue at 45° for 3 days. Next, in order to achieve the non-heme iron solubilization, we weighted the dried tissue fragments and added tissue-specific volumes (**Table 3**) of freshly prepared TCA/HCL reagent (**Table 4)**. We incubated the tissue at 65° for 2 days on the thermomixer at 1000 rpm. After incubation, we centrifuged the samples at 5000 rpm for 5 minutes to pellet the insoluble tissue remains.

Table 3. Volumes of TCA/HCL r and iron solution for non-heme iron measurement in tissue

Tissue	TCA/HCL per 0.01g of tissue	TCA/HCL for assay	Volume for assay
Liver	100 µl	20 µl	2 µl
Spleen	900 µl	20 µl	1 µl
Tumor	50 µl	20 µl	4 µl
Kidney	100 µl	20 µl	2 µl

To prepare the standard curve we diluted the standard iron solution Iron Standard for AAS, 10.00 g/L Fe in nitric acid (#02583) from Sigma-Aldrich to 40 µg/ml in TCA/HCL reagent and different dilutions of the standard were prepared (**Table 5**). 20 µl of the blank (only HCL/TCA) and the standard dilutions were loaded in duplicates in a 96 wells plate. To measure the samples 20 µl of TCA/HCL reagent was added to each swell and tissue specific sample volumes (**Table 3)** were added in triplicates to the plate. To the blank, standard series and two of each of the triplicates 100 µl of the stain solution (**Table 4**) was added. To the third sample well, we added 100 µl of the control solution (**Table 4**). The plate was incubated for at least 15 minutes at room temperature and absorbance was read by BioTeck Epoch™ 2 Microplate Spectrophotometer at 535 nm against blank within 3 hours. Previously to the calculation of the results, the absorbance of the well containing sample plus the control solution was subtracted from the correspondent average of the absorbance of the wells containing the same sample and stain solution.

Table 4. Reagents recipes for non-heme iron measurement in tissue

Solutions	
TCA/HCL	25.2 ml H2O 10.8 ml 37% HCL 4 ml 100% TCA
Stain solution	40 µl 10% BDA (bathophenanthroline disulfoxid acid) 570.8 µl of 70% thioglycolate 39.4 ml of 3 M sodium acetate
Control solution	570.8 µl of 70% thioglycolate 39.4 ml of 3 M sodium acetate

Table 5. Iron standard curve preparation for non-heme iron measurement in tissue

	µl of 40 µg/mL solution	µl HCl/TCA	Iron concentration (ng/µl)	Iron (ng) in 20 µl
1	0	200	0	0
2	1	199	0.2	4
3	2	198	0.4	8
4	5	195	1	20
5	10	190	2	40
6	20	180	4	80
7	30	170	6	120
8	40	160	8	160
9	50	150	10	200
10	60	140	12	240
11	75	125	15	300
12	100	100	20	400

4.10 Bone marrow smears

Bone marrow smears from tumor-bearing Trp53^{flox}WapCre mice at end stage (maximal permitted tumor size) and tumor free control mice were obtained from the medullar cavity of femur using the paint brush technique.[136] Slides were air-dried and stained with a Giemsa staining. The cells were morphologically evaluated and a differential count of the hematologic precursors was performed by light microscopy at 100x.

4.11 Flow cytometry experiments

Late erythropoiesis analysis in bone marrow and spleen of tumor-bearing Trp53^{flox}WapCre mice.

Cells from bone marrow and spleen from iron or saline treated or non-treated Trp53^{flox}WapCre tumor-bearing mice at end stage and age-matched tumor free mice were harvested, stained and analyzed by flow cytometry following a protocol adopted from Chen et al.[137]

Bone marrow cells were flushed out from the medullar cavity of the two femurs and two tibias by using a 1 ml syringe attached to a 24 G needle with ice-cold RPMI cell culture medium enriched with 2.5 % FBS. Clumps were dispersed by gently pipetting with a 10 ml pipette.

In order to obtain a single cell suspension, the spleen was strained by pouring it through a 40 µm strainer using the barrel of a 2 ml syringe until only small portion of fibrous tissue remained on the strainer.

Bone marrow and spleen cells were resuspended in a defined volume of staining buffer (PBS supplemented with 0.5% BSA and 0.1% sodium azide) and the concentration was evaluated by using a Neubauer chamber. $3x10^6$ cells were diluted in 100 ml of staining buffer and Fc membrane receptors were blocked with 1 µl/10^6 cells of Purified anti-mouse CD16/32 Antibody (# 101302) from Biolegend for 15 minutes on ice. Cells were washed with 1 ml of staining buffer and centrifuged at 500 x g for 5 minutes at 4°C.

Cells were stained by resuspending the cell pellet with the labeled-antibodies cocktail in a total volume of 100 µl of PBS: 1 µl FITC anti-mouse TER-119/Erythroid Cells Antibody (#16205) from Biolegend, 0.625 µl of APC-Cy™7 Rat Anti-Mouse CD45 (#561037) from BD Pharmingen™, 0.3125 µl APC/Cyanine7 anti-mouse Ly-6G/Ly-6C (Gr-1) Antibody (#108423) from Biolegend, 0.625 µl APC Rat Anti-Mouse CD44 Clone IM7 (RUO) (#561862) from BD Pharmingen™ and 1 µl of Zombie Yellow™ Fixable Viability Kit (#423103) from Biolegend. Cells were incubated with the labeled-antibodies cocktail for 30 minutes on ice in the dark.

After incubation, cells were washed 3 times with 1 ml of staining buffer and centrifuged at 500 x g for 5 minutes at 4°. Then, cells were resuspended in 0.2 ml of staining buffer and filtered with a 40 µm strainer. Cell suspensions were kept at 4° in the dark and analyzed within the next 2 hours with Cytoflex S Flow Cytometer from Beckman Coulter Life Sciences.

Results were analyzed with FlowJo software (Tree Star, Ashland, OR, USA). The gating strategy showed in **Figure 5** was applied to all bone marrow and spleen samples. In detail, events considered debris were discarded **(Fig. 5A).** Events placed on the middle diagonal of the FSC-H versus FSC-A plot were considered single cells and therefore included in the analysis **(Fig. 5B).** For all dyes, the correspondent FMO (fluorescence minus one) control was used to define the gates. Zombie Yellow™ is an amine-reactive fluorescent dye that is non-permeant to live cells but permeant to the cells with compromised membranes; therefore, only unstained cells were selected **(Fig. 5C).** Ter119 is an erythroid-specific glycophorin expressed in late

erythroid precursors (from proerythroblasts to mature erythrocyte). All FITC-Ter119^{+} cells were considered as late erythroid precursors.

As described by Chen et al.,[138] with maturation, erythroid precursors show progressive decrease of CD44 surface expression with decreased cell size. Therefore all Ter119^{+} cells were displayed in a APC-CD44 versus FSC-A plot allowing to differentiate 5 different clusters corresponding to the different stages of the maturation **(Fig. 5E)**: proerythroblasts (I), basophilic erythroblasts (II), polychromatic erythroblasts (III), orthochromatic erythroblasts and reticulocytes (IV) and mature erythrocytes (V).[139] CD45/GR1+ cells where considered leukocyte precursors.

Figure 5

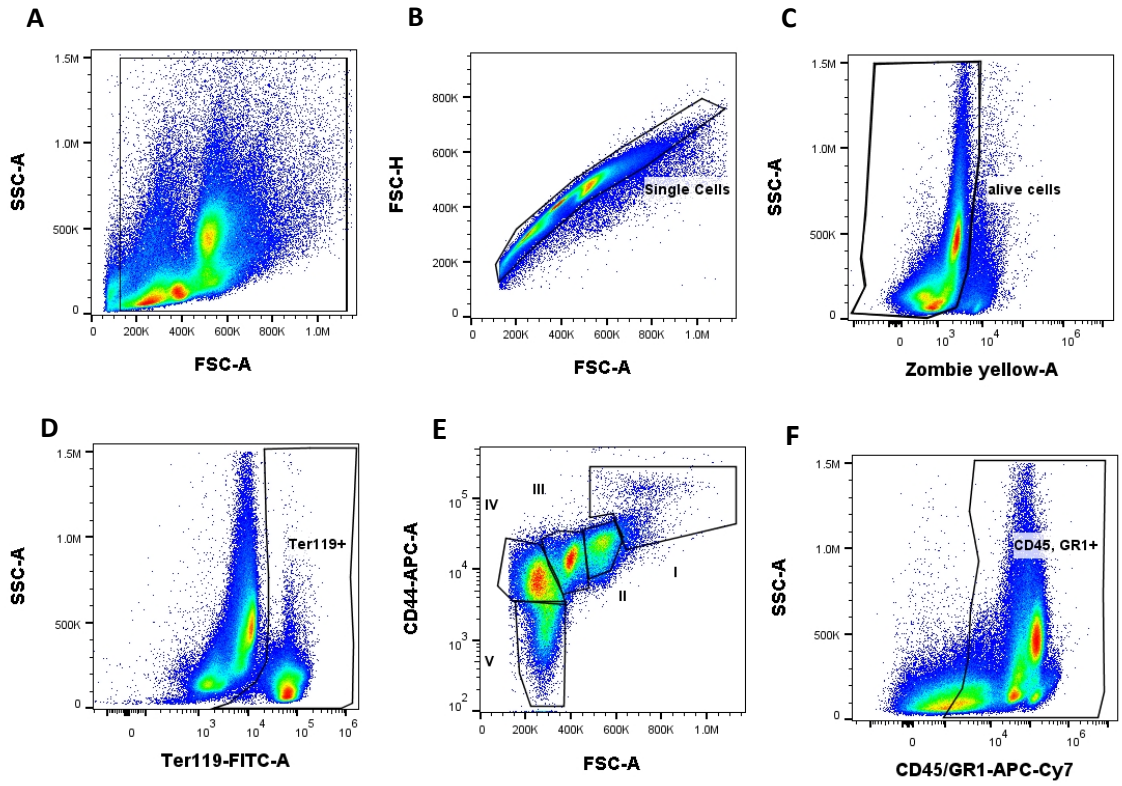

Fig 5: Flow cytometric analysis of late erythroid maturation in bone marrow and spleen in tumor-bearing Trp53^{flox}WapCre mice

Shown are representative images of the gated plots and the gating strategy used for the late erythroid maturation assessment in bone marrow and spleen of tumor free and tumor-bearing Trp53^{flox}WapCre mice. **(A)** Events considered cells were gated in a forward scatter (FSC-Area; cell size) vs. side-scatter (SSC-Area, cell complexity) plot, **(B)** single cell gating in FSC-Area vs. FSC-Height plot, **(C)** live cell gating by Zombie Yellow (stains dead cells) vs. SSC-Area plot, **(D)** Ter119^{+} (late erythroid precursors) gating on living cells in Ter119 vs SSC-Area plot, **(E)** different clusters were identified in FSC-Area vs. CD44 plot and based on the decreasing cell size and CD44 membrane concentration on the erythroid cells with maturation, the different stages of the late erythroid maturation were gated: proerythroblasts (I), basophilic erythroblasts (II), polychromatic erythroblasts (III), orthochromatic erythroblasts and reticulocytes (IV) and mature erythrocytes (V); **(F)** CD45/GR1^{+} cells (leukocyte precursors) gating in CD45/GR1 vs SSC-Area plot.

Early erythropoiesis analysis in bone marrow of tumor-bearing Trp53^{flox}WapCre mice.

Bone marrow cells from tumor-bearing Trp53^{flox}WapCre mice at end stage and age matched tumor free mice harvested, stained and analyzed by flow cytometry following the protocol defined by Pronk et al.[140]

Bone marrow cells were passed through 23 G needles to get single-cell suspensions. Two femurs per mouse were used for hematologic stem cells (HSC) analysis, and 2 femurs and 2 tibiae per mouse were used for sorting. For surface staining, cells were incubated with c-kit (A780, 2B8; eBioscience), Sca1 (PE-Cy5 or PE-Cy7 or PE-Cy5.5, D7; eBioscience), CD34 (FITC, RAM34; eBioscience), CD135 (PE or PE-Cy5, A2F10; eBioscience), CD48 (APC, HM48-1; eBioscience), CD150 (PE-Cy7, TC15-12F12.2; BioLegend), CD105 (PE, 12-1051-82, ThermoFisher) and CD41 (FITC, 11-0411-82; ThermoFisher) for 55 minutes. Lineage-positive cells were excluded using a cocktail of biotinylated antibodies and staining with streptavidin (SA; eF450; eBioscience). The lineage cocktail included CD3 (145-2C11; eBioscience), CD19 (eBio1D3; eBioscience), NK1.1 (PK136; eBioscience), Ter119 (Terr119; eBioscience), CD11b (M1/70; eBioscience), Gr1 (RB6-8C5; eBioscience), and B220 (RA3-6B2; eBioscience). A total of $3x10^6$ cells per mouse were acquired. Fluorescence-activated cell sorting (FACS) analysis was performed on LSRII (Becton Dickinson), and sorting was done on Aria II (Becton Dickinson). Cell numbers were counted on MACS quant. Data were analyzed with DIVA (Becton Dickinson), MACS quantify (Miltenyi), or FlowJo (Tree Star, Ashland, OR, USA). The used gating strategy was adopted from Pronk et al.[140] and is shown in **Figure 6.** In detail, cells not stained by the lineage cocktail where selected**.** C-kit$^+$/ SCA-1$^+$ cells were positively gated and from those, events CD48-/CD150+ were considered hematopoietic stem cells (HSC), whereas events CD48+/CD150$^-$ expression were considered multipotent progenitors (MPP).

Additionally, c-kit$^+$/SCA1$^-$ events were selected. CD150$^+$/CD41$^+$ cells were considered Mkp (megakaryocyte precursors) and CD41$^-$ events were selected and plotted again as CD16_32 versus CD150. All events CD16_32$^-$ were selected and plotted as CD105 vs CD150. In this plot the rest of early precursors populations were defined: CD105$^-$/ CD150$^-$ were considered as pre-granulocyte-monocyte lineage cells (Pre-GM), CD105$^-$/CD150$^+$ pre-megakaryocyte-erythrocyte progenitors (pre-MgE), CD105$^+$/ CD150$^+$ pre-colony forming units erythrocyte (pre-CFU) and CD150$^-$/ CD105$^+$ were considered colony forming units erythrocyte (CFUe).

Figure 6

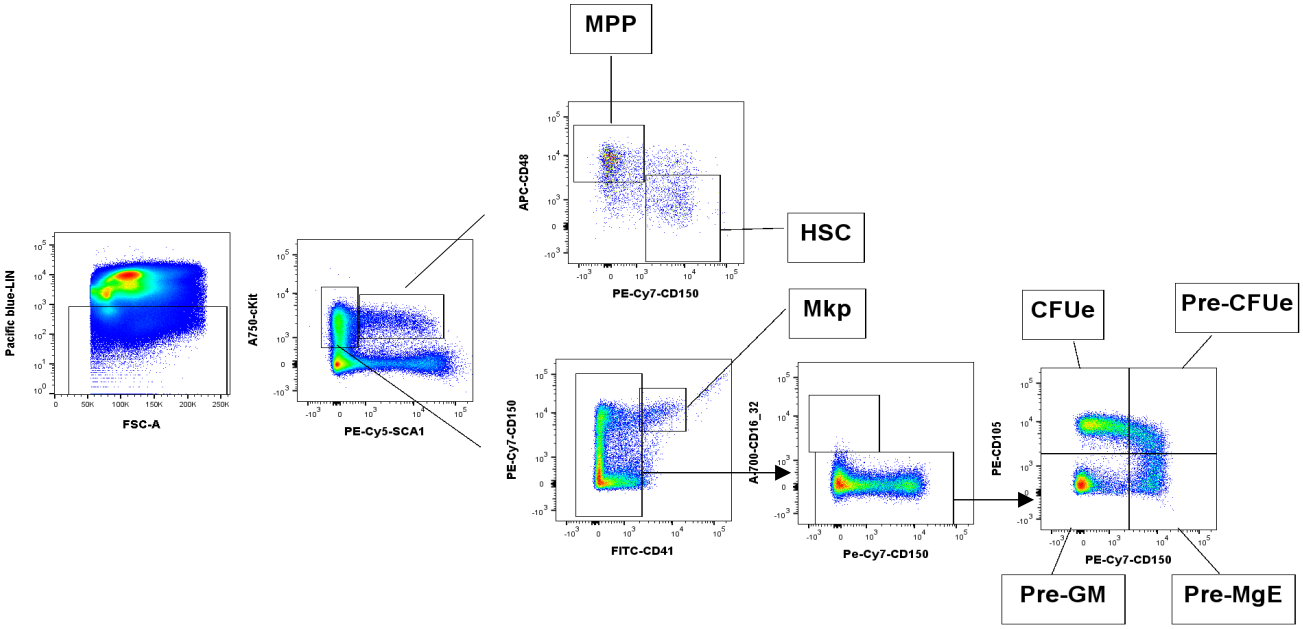

Fig. 6: Flow cytometric analysis of early erythropoiesis in bone marrow of tumor-bearing Trp53^{flox}WapCre mice
Shown are representative images of the gated plots and the gating strategy used for the early hematopoietic precursors assessment in bone marrow. Lin$^-$ cells were selected**.** C-kit$^+$/ SCA-1$^+$cells were selected and from those, events CD48$^-$/CD150$^+$ were considered hematopoietic stem cells (HSC), whereas events CD48+/CD150$^-$ expression were considered multipotent progenitors (MPP). From c-kit$^+$/SCA1$^-$ events, CD150$^+$/CD41$^+$ cells were considered Mkp (megakaryocyte precursors) and CD41$^-$ events were selected and plotted as CD16_32 versus CD150. Events CD16_32$^-$ were plotted as CD105 vs CD150. CD105$^-$/ CD150$^-$ were considered as pre-granulocyte-monocyte lineage cells (Pre-GM), CD105$^-$/CD150$^+$ pre-megakaryocyte-erythrocyte progenitors (pre-MgE), CD105$^+$/ CD150$^+$ pre-colony forming units erythrocyte (pre-CFU) and CD150$^-$/ CD105$^+$ were considered colony forming units erythrocyte (CFUe).

4.12 Statistics

All statistics were performed in GraphPad Prism6 (GraphPad Software, San Diego, US). Data distribution was analyzed with the Kolmogorov-Smirnov test.[141] To compare 2 independent groups, we used either an Unpaired Student t-test for parametric distributed data or a Man-Whitney test for non-parametric distributed data.[141] To compare three or more independent groups with just one independent variable, we used either One-way-ANOVA with a Dunnett's Multiple Comparison Test for parametric data or a Kruskal-Wallis test, with a Dunn's Multiple Comparison Test for non-parametric data. Correlation analyses were performed with linear regression analysis.[141] A p-value of ≤ 0.05 was considered significant.[142] The respective statistical tests are indicated in the figure legends.

5. Results

5.1 Trp53^{flox}WapCre mice develop breast cancer associated with Epo-resistant anemia

Trp53^{flox}WapCre mice developed subcutaneous mammary tumors between 20 and 36 weeks of age. Typically, the tumors were mammary carcinomas associated with large necrotic areas with diffuse and severe neutrophilic inflammation (**Fig. S1**). Between 18 to 43 days after the tumor onset, tumor-bearing mice reached experimental termination criteria (defined as end stage, ES), which were defined by a single tumor volume of 2 cm^3 or by a total volume of 3 cm^3 in mice with multiple tumors.

Tumor-bearing Trp53^{flox}WapCre mice developed AC. Hematocrit and hemoglobin levels were reduced from average 42.39% or 13.13 g/dl respectively in tumor free to 35.71% or 10.76 g/dl tumor-bearing Trp53^{flox}WapCre mice at end stage (p_{Hct}=0.0001 and p_{Hb}=0.0001) **(Fig. 7A, B)**. The treatment with subcutaneous injection of 1000 U/kg Epo three times per week from tumor onset was not able to palliate the anemia **(Fig. 7C)** but did also not increase tumor growth in our mouse model **(Fig. 7D).**

Figure 7

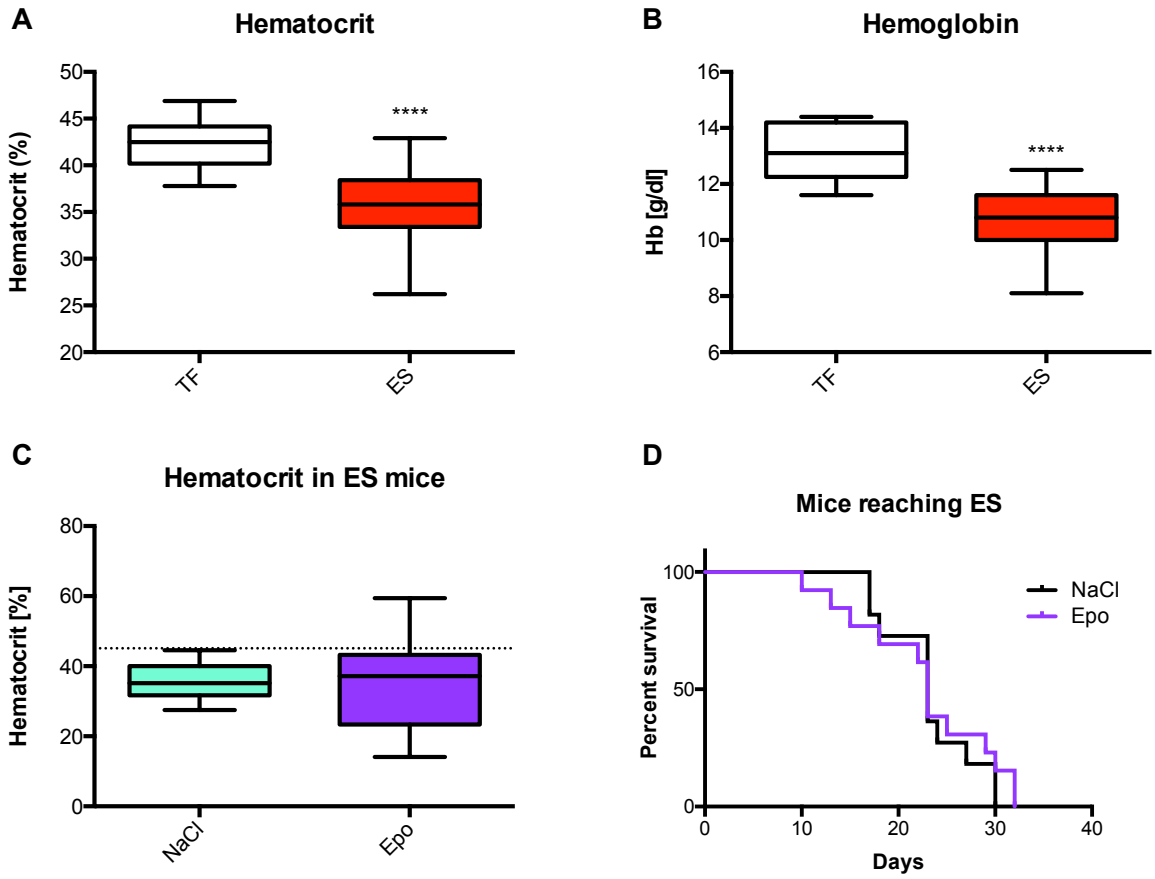

Fig.7 Epo resistant anemia in tumor-bearing Trp53^{flox}WapCre mice
Shown is **(A)** hematocrit and **(B)** hemoglobin of age-matched tumor free (TF, white box) and tumor-bearing Trp53^{flox}WapCre mice after reaching termination criteria (defined as end stage; ES, red box). **(C)** Shown is the hematocrit of tumor-bearing Trp53^{flox}WapCre mice at end stage subcutaneously injected with either with 1000 U/kg Epo (Epo, purple box) or saline (NaCl, green box) 3 times a week. The black dotted line indicates the median of the untreated tumor free Trp53^{flox}WapCre mice**. (D)** Kaplan-Meier survival curve of tumor-bearing Trp53^{flox}WapCre mice treated with 1000 U/kg Epo (purple line) or saline (NaCl, black line) 3 times per week (n=12-14). Of note, the survival curve does not indicate the time when the mice died from cancer but the time point the experiment was terminated because of reaching maximal permitted tumor size (of 2 cm^3 for single or a total of 3 cm^3 for multiple tumors) **A, B, C:** Data are shown as box plot with min to max whiskers and an Unpaired Student t-test was performed; ****p<0.0001 (n=9-30)**.**

5.2 Trp53^{flox}WapCre mice develop AC at advanced stages of tumorigenesis

To assess if AC in tumor-bearing Trp53^{flox}WapCre mice occurs early or late during tumor progression, we analyzed hematological parameters at different stages of the disease from day 0 (the day of tumor diagnosis) to day 7 and 15 after tumor diagnosis as well as at end stage (ES) **(Fig. 8 and Table 6**). We observed a trend of reduced hematocrit levels in tumor-bearing mice immediately after tumor onset (day 0), but statistical differences (p=0.0008) were only observed

between tumor free (41.67%) and tumor-bearing mice at end stage (34.83%) **(Fig. 8A).** Hemoglobin levels were neither reduced on day 0 nor in more than 50% of tumor-bearing mice on day 15. However, a few mice started to develop anemia especially mice that displayed already large tumors on day 15 **(Fig. 8 B)**. However, end stage tumor-bearing Trp53^{flox}WapCre mice showed clearly lower hemoglobin levels (10.85 g/dl) than tumor free mice (13.82 g/dl) (p=0.0088). The reduced hemoglobin levels in tumor-bearing mice correlated with a decreased erythrocyte number, an increased mean corpuscular volume (MCV) and a decreased mean corpuscular hemoglobin concentration (MCHC) **(Table 6).** The reticulocyte count was not changed in any of the tumor stages analyzed, indicating that tumor-bearing animals at advanced stages of the disease present a no-regenerative macrocytic anemia.

Figure 8

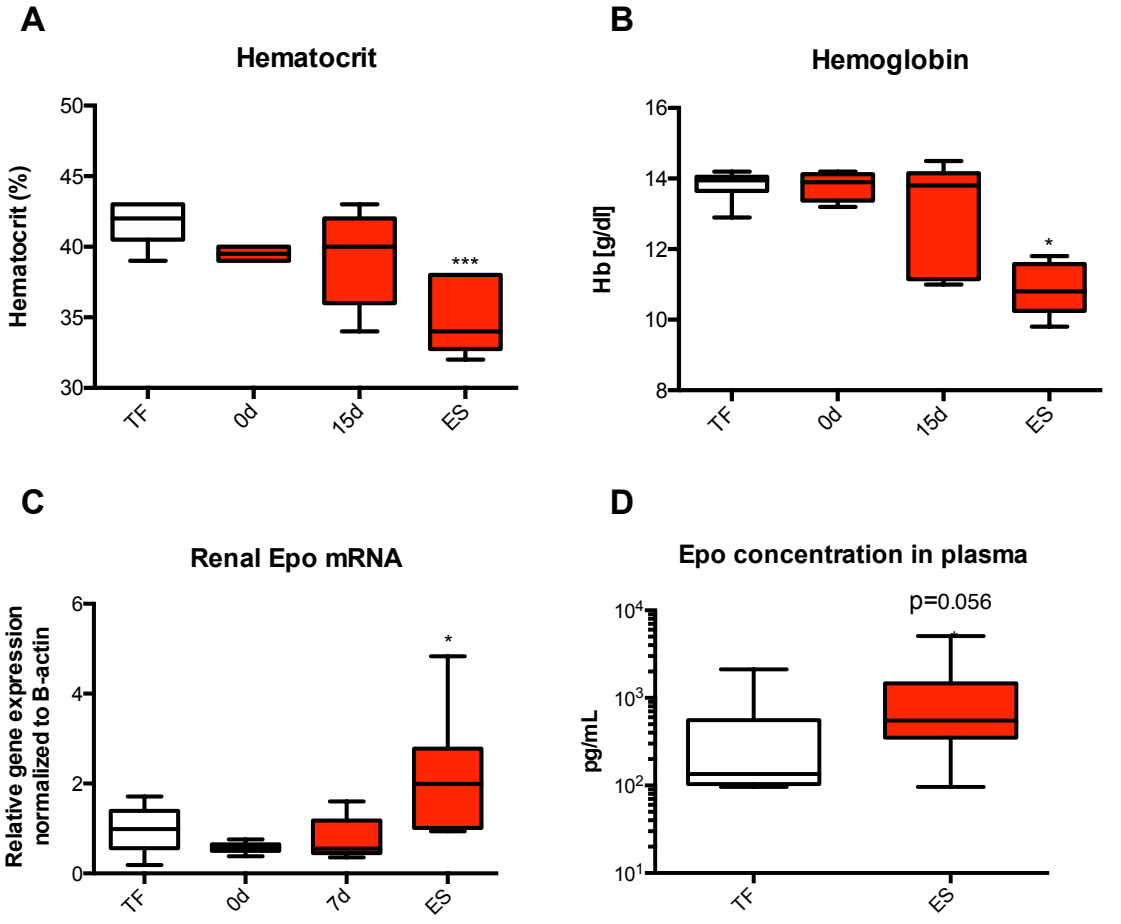

Fig.8 Time course of anemia of cancer in Trp53^{flox}WapCre mice.
Shown is **(A)** hematocrit, **(B)** hemoglobin and **(C)** renal *Epo* mRNA levels of tumor free (TF, white boxes) and tumor-bearing Trp53^{flox}WapCre mice (red boxes) at different stages of the disease: immediately after tumor diagnosis (0 d), 7 days (7 d) and 15 days after de diagnosis (15 d) or when mice reached experimental termination criteria by maximum permitted tumor size (end stage, ES). **(D)** Epo concentration in plasma of tumor free (TF, white box) and tumor-bearing Trp53^{flox}WapCre mice (red boxes) at end stage (ES) was measured by ELISA. Data are shown as box plot with min to max whiskers and One-way ANOVA (panel A and C) with a Dunnett's Multiple Comparison post hoc test., a Mann Whitney test (panel D) and a Kruskal-Wallis with a Dunn's Multiple Comparison post hoc test (panel B) was performed; (n=4-13); *p<0.05; ***p<0.001.

To analyze if the Epo production increased in response to AC, we measured Epo mRNA levels in the kidney **(Fig. 8C)** immediately after tumor diagnosis (day 0) and at early stages of tumor progression (day 7), but no differential Epo mRNA expression was observed in these time points. However, Epo mRNA levels in mice with large tumors, i.e. end stage (ES) were 2.02-fold higher than in tumor free mice. Additionally, Epo plasma levels increased in tumor-bearing mice 4.34-fold but did not reach significance (p-value 0.056) **(Fig. 8D).**

Table 6: Hematological parameters of tumor free and tumor-beating Trp53^{flox}WaypCre mice at different timepoints after tumor onset.

Parameter	TF	0d	15d	ES	Statistical test
Erythrocyte count (10^6/µl)	9.772 ± 0.32	9.495 ± 0.37	9.128 ± 0.81	7.697 ± 0.62****	1w ANOVA
RDW (%)	23.02 ± 0.74	23 ± 0.94	22.52 ± 0.36	22.08 ± 1.2	KW
MCV (fl)	42.67 ± 0.52	42 ± 1.15	43 ± 0.71	45.17 ± 1.17**	KW
MCH (pg)	14 ± 0.0	14.75 ± 0.50	14.2 ± 0.84	14 ± 0.63	KW
MCHC (g/dL)	33.17 ± 0.75	34.75 ± 0.50	32.8 ± 1.64	31.33 ± 1.03**	KW
Reticulocytes (%)	6.308 ± 2.00	8.24 ± 0.17	5.982 ± 1.78	9.065 ± 0.79	KW
Reticulocytes ($10E^6$/µl)	0.6178 ± 0.20	0.7608 ± 0.04	0.5358 ± 0.11	0.7114 ± 0.09	KW

Values are presented as mean ± standard deviation; RDW: red cell distribution width; MCV: mean corpuscular volume; MCH: mean corpuscular hemoglobin; MCHC: mean corpuscular hemoglobin concentration. TF: tumor free control mice; 0d: mice at day of tumor diagnosis; 15d: mice at 15 days after tumor diagnosis; ES: tumor-bearing mice at end stage (when they reach termination criteria, i.e. maximal permitted tumor size). 1w ANOVA: One-way ANOVA with Dunnett's Multiple Comparison Test; KW: Kruskal-Wallis test, Dunn's Multiple Comparison Test (n=4-6); ****p<0.0001, **p>0.01.

Spleen weight of tumor-bearing mice increased (splenomegaly) during disease progression and was 2.44-fold higher at end stage than in tumor free mice **(Fig. 9A).** This marked increase in the spleen size together with the histological spleen analyses of tumor-bearing mice at end stage (**Fig. 9C, D)** suggested that stress erythropoiesis occurred in the spleen.

Similar to spleen, the liver weight was larger (hepatomegaly) in tumor-bearing mice at late stages than in tumor free mice **(Fig. 9B),** but no alteration of the hepatocyte morphology, number of inflammatory cells or focus of extramedullary erythropoiesis could be histologically observed **(Fig. 9 E, F).** The increased liver weight might have been a result of increased cellular hepatocyte replication **(Fig. S2)** because tumor-bearing mice displayed more Ki67 positive cells in the liver than tumor free mice.

Figure 9

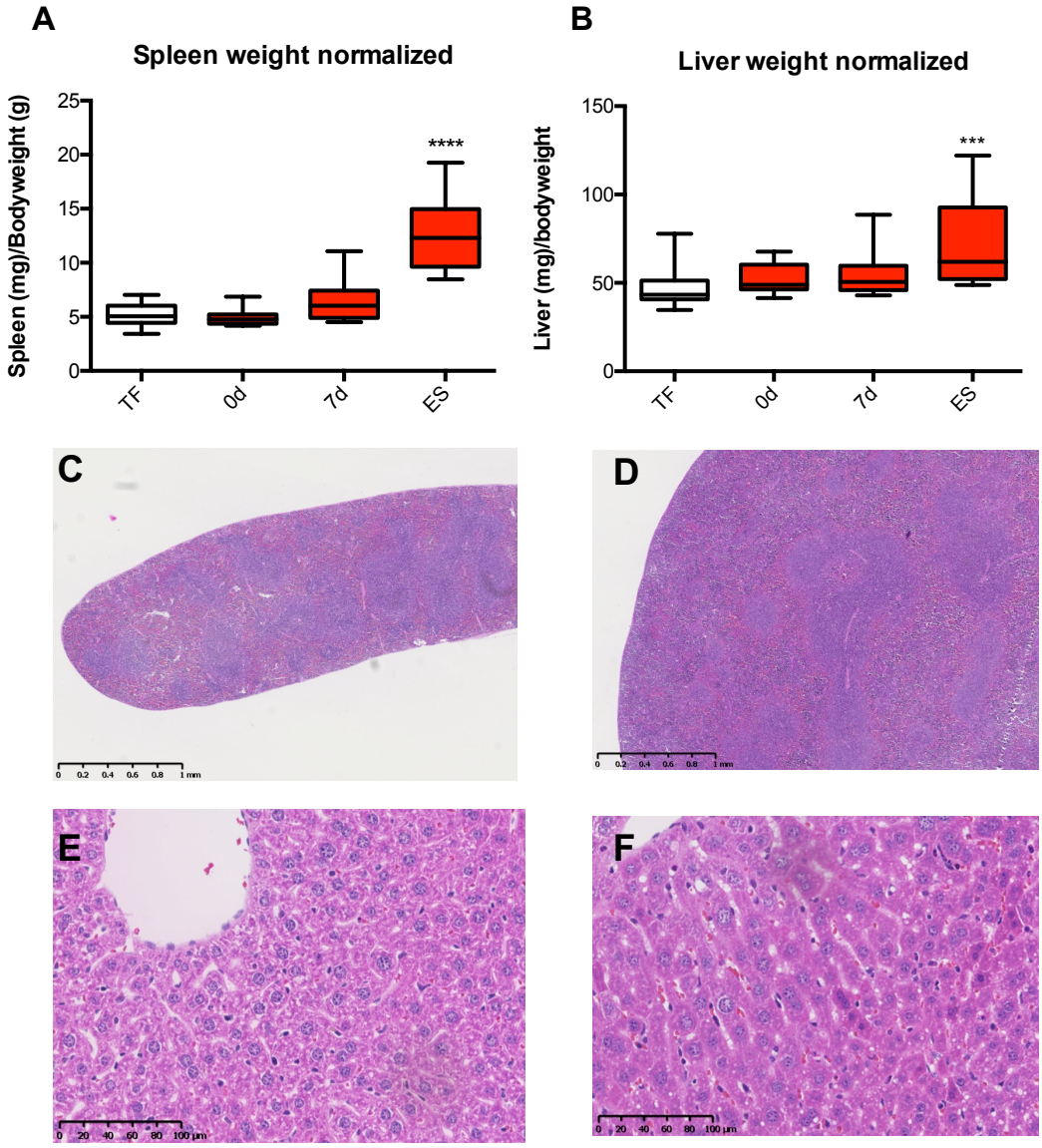

Fig.9 Organ weight and histological changes in spleen and liver of tumor-bearing Trp53^{flox}WapCre.
Shown are (**A**) spleen weight and **(B)** liver weight normalized to the body weight of tumor free (TF, white boxes) and tumor-bearing Trp53^{flox}WapCre mice (red boxes) at different stages of the disease: immediately after tumor diagnosis (0d), 7 days after tumor diagnosis (7d) or when mice reached experimental termination criteria by maximum permitted tumor size (end stage, ES)**.** Data are shown as box plot with min to max whiskers and One-way ANOVA (panel A) with a Dunnett's Multiple Comparison post hoc test. And a Kruskal-Wallis with a Dunn's Multiple Comparison post hoc test (panel B) was performed (n=10-13); ****p<0.00001; ***p<0.001; Representative H&E stained tissue sections of spleen from **(C)** tumor free mice and **(D)** tumor-bearing mice. Scale bar 1 mm. Representative sections of liver from **(E)** tumor free mice and **(F)** tumor-bearing mice**.** Scale bar 100 µm.

To analyze the general health status of the mice and verify that neither kidney nor liver pathologies contributed to the anemia pathogenesis in Trp53^{flox}WapCre mice, we analyzed clinical markers (specified in **Table 7**) in plasma of tumor free and tumor-bearing mice. We observed no differences in the creatinine and a slight decrease in the urea plasma concentration from 36.18 to 31.62 mg/dl (p=0.035) between tumor free and tumor-bearing (end stage) mice,

indicating that kidney function was not impaired. Hepatic aspartate (AST) and alanine transaminases (ALT) levels were decreased from 496.7 to 173.4 IU/L, however only significant at p=0.102, and from 39.57 to 21.57 IU/L (p=0.035), respectively. Additionally, alkaline phosphatase (AP) decreased from 89.0 in tumor free to 30.5 IU/L levels in tumor-bearing mice (p=0.0001) and total protein increased from 40.43 in tumor free to 50.00 g/l in tumor-bearing mice (p=0.0058). Glucose, bilirubin, cholesterol and triglyceride did not change in tumor-bearing mice, suggesting that both liver and kidney function were not altered.

Table 7: Plasma biochemistry of tumor free and tumor-bearing (end stage, ES) Trp53^{flox}WapCre mice.

Parameter	TF	ES	Statistical test
Creatinine (mg/dl)	<0.17 ± 0.0	<0.17 ± 0.0	
Urea (mg/dl)	36.18 ± 2.906	31.62 ± 4.155*	Unpaired t test
Aspartate transaminase (AST) IU/l	496.7 ± 473.4	173.4 ± 97.57	Unpaired t test
Alanine transaminase (ALT) IU/l	39.57 ± 18.86	21.57 ± 6.705*	Unpaired t test
Alkaline Phosphatase (AP) (IU/l)	89.00 ± 7.321	30.50 ± 11.61****	Unpaired t test
Total protein (g/l)	40.43 ± 1.718	50.00 ± 7.371**	Unpaired t test
Glucose (mg/dl)	186.2 ± 28.59	163.4 ± 30.84	Unpaired t test
Bilirubin (mg/dl)	<0.1843 ± 0.058	<0.24 ± 0.1261	Mann Whitney test
Cholesterol (mg/dl)	106.3 ± 8.025	116.6 ± 42.14	Mann Whitney test
Triglycerides (mg/dl)	191.9 ± 49.27	202.2 ± 182.7	Mann Whitney test

Values presented as mean ± standard deviation; TF: tumor free control mice; ES: tumor-bearing mice at end stage (when they reach termination criteria). (n=7) *p<0.05; **p<0.01; ****p<0,0001.

5.3 Trp53^{flox}WapCre mice develop a marked inflammatory response during tumor progression

Because AC is usually associated with inflammation, we investigated the number of inflammatory cells in peripheral blood of tumor free and tumor-bearing mice at different stages of the disease **(Fig. 10).** The overall leukocyte count was 2.29-fold increased (p<0.0001) in end stage (ES) tumor-bearing mice but not at earlier time points **(Fig. 10A)** and it is mainly a consequence of the approximately 10-fold higher numbers of neutrophils **(Fig. 10B)** and

monocytes **(Fig. 10C)**. In contrast, the number of lymphocytes **(Fig. 10D)** and eosinophils **(Fig. 10E)** did not differ between tumor free and tumor-bearing mice. Basophils were decreased at end stage in tumor-bearing mice (p=0.067) **(Fig. 10F)**. These results indicate a marked cellular inflammatory response in peripheral blood of tumor-bearing animals at end stage, which predominantly involved neutrophils and monocytes.

Besides the cellular response, we observed on molecular level that interleukin-6 (IL-6), an inflammatory cytokine with a principal role in anemia of inflammation pathogenesis, was increased. *IL-6* mRNA expression in tumor tissue of tumor-bearing mice at end stage was approximately 5 times higher than in normal mammary tissue of tumor-free $Trp53^{flox}$WpCre mice **(Fig. 11A)**. In addition to tumor *IL-6* mRNA levels, we measured IL-6 protein concentration in plasma of tumor free and tumor-bearing mice immediately and 15 days after tumor onset as well as at end stage **(Fig. 11B).** We observed increased IL-6 plasma levels already 15 days after tumor onset, but differences were only significant (p=0.0041) at the end stage when IL-6 levels were approximately 50 times higher than in tumor free mice. To confirm that tumor-bearing mice responded to the elevated IL-6 levels we analyzed the liver mRNA expression levels of serum amyloid-A1 (*SAA-1*), a liver marker of IL-6 activity. Correlating with the IL-6 serum levels, we observed an increased SAA-1 mRNA expression with disease progression, which already reached significance 7 days after the tumor diagnosis (p=0.05) and even became 158.48 times higher than tumor free mice at end stage (p<0.0001) **(Fig. 11C)**.

Figure 10

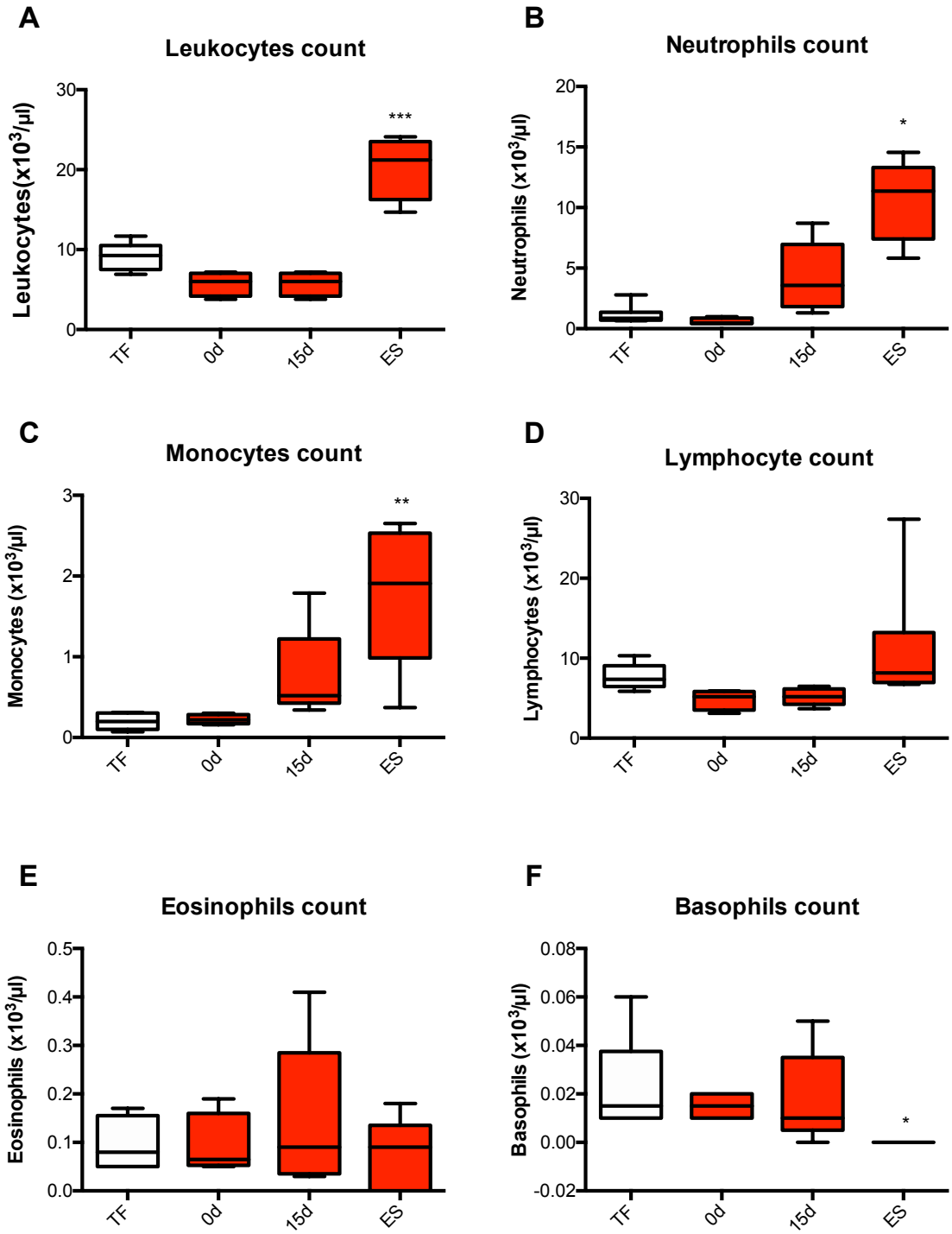

Fig. 10: Differential leukocyte count in peripheral blood of tumor free and tumor-bearing Trp53floxWapCre mice. Shown are leukocytes **(A),** neutrophils **(B),** monocytes **(C),** lymphocytes **(D),** eosinophils **(E)** and basophils **(F)** cell count in peripheral blood of tumor free mice (TF, white boxes) and tumor-bearing mice at different stages of the disease: immediately after tumor diagnosis (0 d), 15 days after tumor diagnosis (15 d) and at end stage (ES), when tumors reached the maximal permitted size and the experiment was terminated. Data are shown as box plot with min to max whiskers and a One-way ANOVA with a Dunnett's Multiple Comparison post hoc test (panel A, E and F) or Kruskal-Wallis with a Dunn's Multiple Comparison post hoc test (panel B, C and D) was performed; (n=4-6); *p<0.05, **p<0.01, ***p<0.001.

Moreover, we analyzed the expression in tumor tissue of some proinflammatory cytokines involved in the regulation of the erythropoiesis and compared them with healthy mammary tissue of tumor-free mice. We found that interleukine-1β (*IL-1*β) expression was 5.7-fold ($p<0.0001$) increased in tumor tissue **(Fig. 11D),** but conversely, the expression of tumor necrosis factor alpha (*TNF-α)* was reduced by 10.3-fold ($p=0.0002$) in tumor tissue **(Fig. 11E).** These results show that some proinflammatory cytokines that might be involved in the AC pathogenesis are secreted by the tumor or the inflammatory cells present in the tumor tissue.

Figure 11

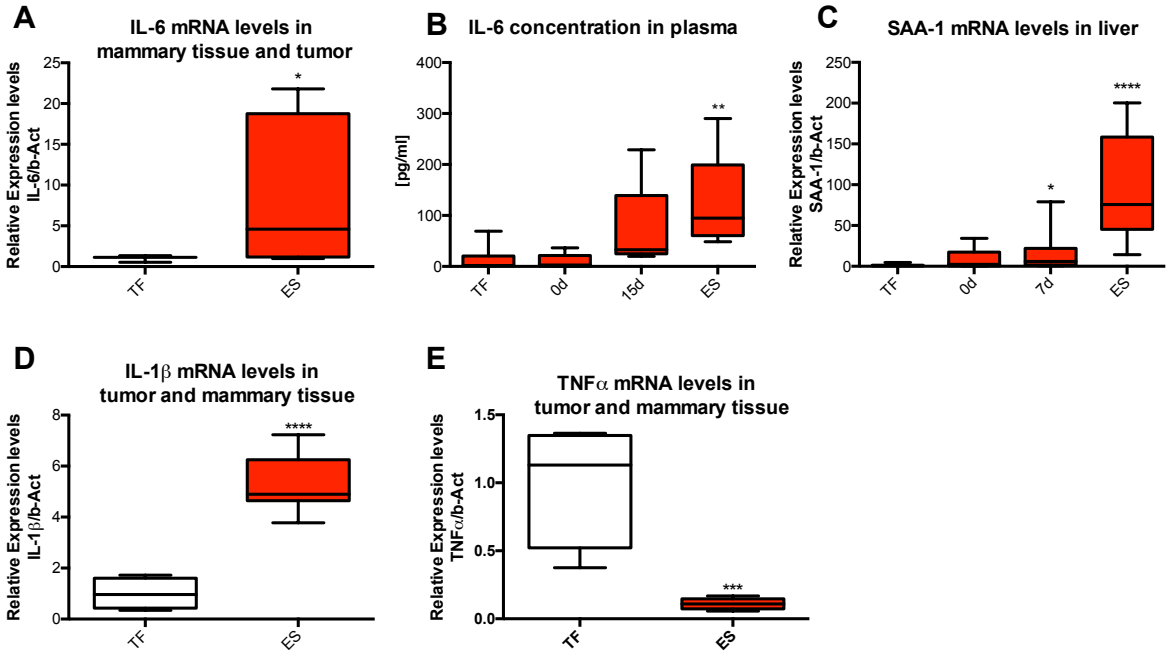

Fig. 11: Induced IL-6 levels and other cytokines expression in tumor-bearing Trp53^{flox}WapCre mice.
Shown is **(A)** interleukin-6 *(IL-6*) mRNA levels in normal mammary tissue of tumor free mice (TF) and in tumor tissue of tumor-bearing-mice at end stage (ES) and **(B)** interleukin-6 (IL-6) plasma levels as well as **(C)** liver serum amyloid-A (*SAA-1)* mRNA expression levels of tumor free (TF, white boxes) and tumor-bearing-mice (red boxes) at different stages of the disease: immediately after tumor diagnosis (0 d), 15 days after tumor diagnosis (15 d) and at end stage (ES), when tumors reached the maximal permitted size and the experiment was terminated. **(D)** Interleukin-1β (*IL-1β*) and tumor necrosis alpha (*TNFα*) relative mRNA expression in healthy mammary tissue of tumor free mice (TF, white boxes) and in tumor tissue of tumor-bearing mice at end stage (ES, red boxes). Data are shown as box plot with min to max whiskers and either an Unpaired Student t-test (panel A, D, E) or a Kruskal-Wallis with a Dunn's Multiple Comparison post hoc test (panel B and C) was performed (n=3-11). *p<0.05; **p<0.01; ****p<0.0001, ***p<0.001

5.4 Reduced iron availability in tumor-bearing Trp53^{flox}WapCre mice

Alteration of iron availability is one the most frequent cause of anemia of inflammation. Because the severe inflammation and Epo unresponsiveness in tumor-bearing Trp53^{flox}WapCre mice, we analyzed if iron status was altered. Both, iron concentration and transferrin saturation were decreased by 19.01% ($p=0,0049$) and 54.7% ($p<0.0001$), respectively, in the serum of

tumor-bearing mice when compared to tumor free mice **(Fig. 12A, B).** Together with the unsaturated iron binding capacity and the total iron binding capacity that increased by 174.89% ($p<0.0001$) and 70.24% ($p<0.0001$), respectively **(Fig. 12C, D**), these data suggested that tumor-bearing mice suffered reduced iron availability. Plasma ferritin concentration reflects the amount of stored iron in the body and was 2.25-fold ($p<0.0001$) lower in tumor-bearing $Trp53^{flox}$WapCre mice that reached maximal permitted tumor size (end stage ES) than in tumor free **(Fig. 12E)**. However, the ferritin plasma concentration was already 1.5-fold lower ($p<0.0001$) on the day of the tumor diagnosis (day 0) and 1.98-fold lower ($p=0.01$) 7 days after tumor diagnosis than in tumor free mice. Iron concentration in liver and spleen was 1.3-fold ($p=0.0104$) and 3.4-fold ($p<0.0001$) lower, respectively, in tumor-bearing than in tumor free mice **(Fig. 12F,G),** but the total amount of liver stored iron was 1.56-fold ($p<0.0001$) higher in tumor-bearing mice than in tumor free mice and it was no different in the spleen of because of the increased liver and spleen size (shown in **Fig. 9**) in tumor-bearing animals **(Fig. 12H, I).**

Figure 12

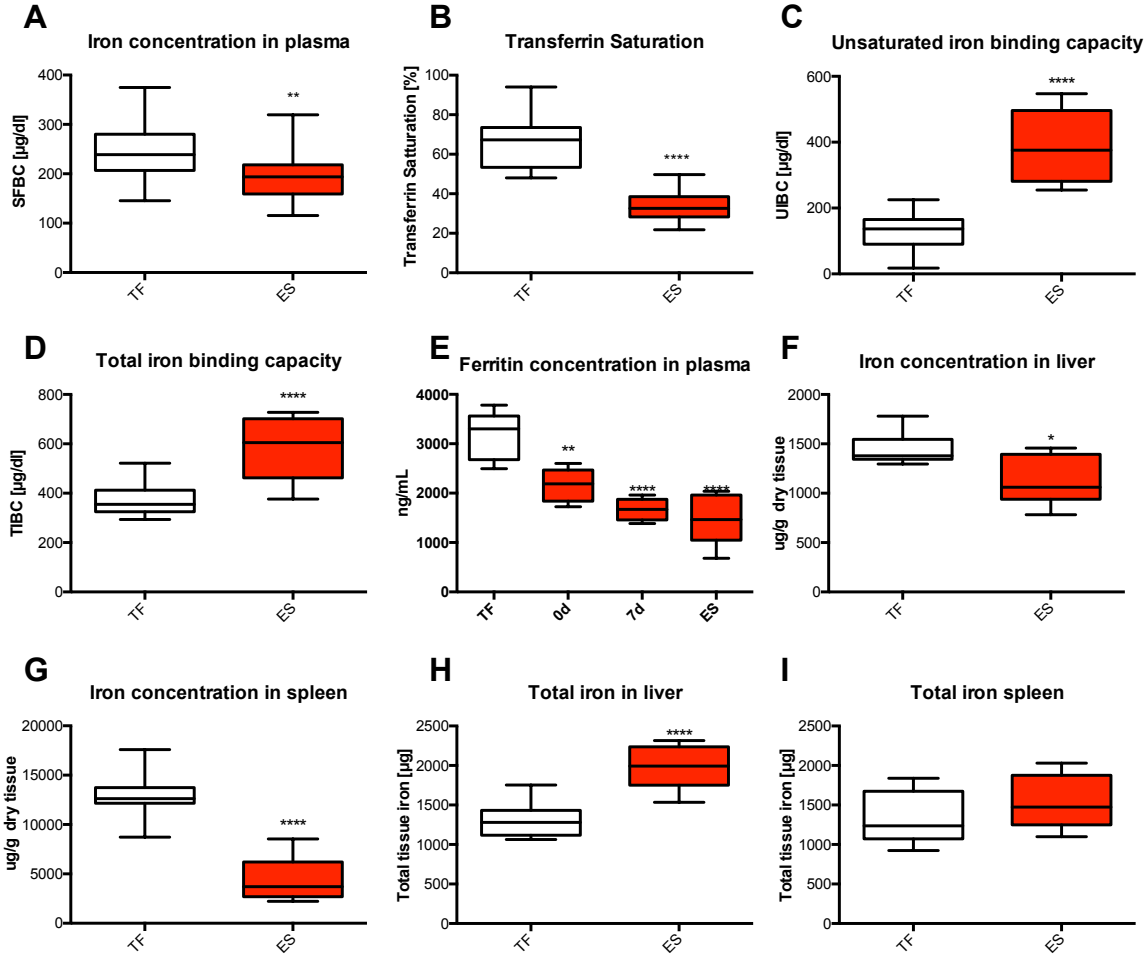

Fig. 12: Iron status in tumorbearing Trp53^{flox}WapCre mice
Shown are **(A)** iron concentration, **(B)** transferrin saturation, **(C)** unsaturated iron binding capacity and **(D)** total iron binding capacity in plasma of tumor-bearing Trp53^{flox}WapCre mice at end stage, i.e. reaching maximal permitted tumor size (ES, red boxes) and tumor free control mice (TF, white boxes). **(E)** The ferritin concentration was measured by ELISA in plasma of tumor free (TF, white boxes) and tumor bearing-mice (red boxes) at different stages of the disease: immediately after tumor diagnosis (0d), 7 days after tumor diagnosis (7d) and at end stage, when maximal tumor size was reached (ES). **(F)** The non-heme iron concentration in dried liver, **(G)** the non-heme iron concentration in dried spleen, **(H)** the total non-heme iron content in the liver and **(I)** the total non-heme iron content spleen. Data are shown as box plot with min to max whiskers and either an Unpaired Student t-test (panel A, C, D, F, G, H, I), a Mann Whitney test (panel B) or a One-way ANOVA with a Dunn's Multiple Comparison post hoc test was performed (n=6-22). *p<0.05; **p<0.01; ****p<0.0001.

A Perl's DAB enhanced stain for tissue iron distribution confirmed that iron in liver and spleen of tumor-bearing mice was decreased **(Fig. 13A, B, C, D)**. Spleen iron was mainly stored in the macrophages of the red pulp of tumor free (**Fig. 7A**) and tumor-bearing mice (**Fig. 13B**), however, to a lesser extent in tumor-bearing mice. Liver iron of tumor free mice was stored in the Kupffer cells, but also distributed in the cytoplasm of the hepatocytes. However, reduced iron staining in tumor-bearing mice was mainly observed in the hepatocytes but less in Kupffer cells **(Fig. 13C, D).** Likewise, reduced iron staining in the bone marrow of tumor-bearing animals was also observed **(Fig. 13E, F)**. Kidney iron was mainly detected at the proximal tubules **(Fig. 13G, H)** but tumor-bearing mice animals showed a less intense staining than tumor free mice, suggesting that tumor-bearing mice might filter less iron. Iron in tumor tissue was unequally distributed **(Fig. 13I)**. Only a few tumor areas showed a detectable iron accumulation, mainly inside the inflammatory cells, such as macrophages, but also in the cytoplasm of cancer cells

Figure 13

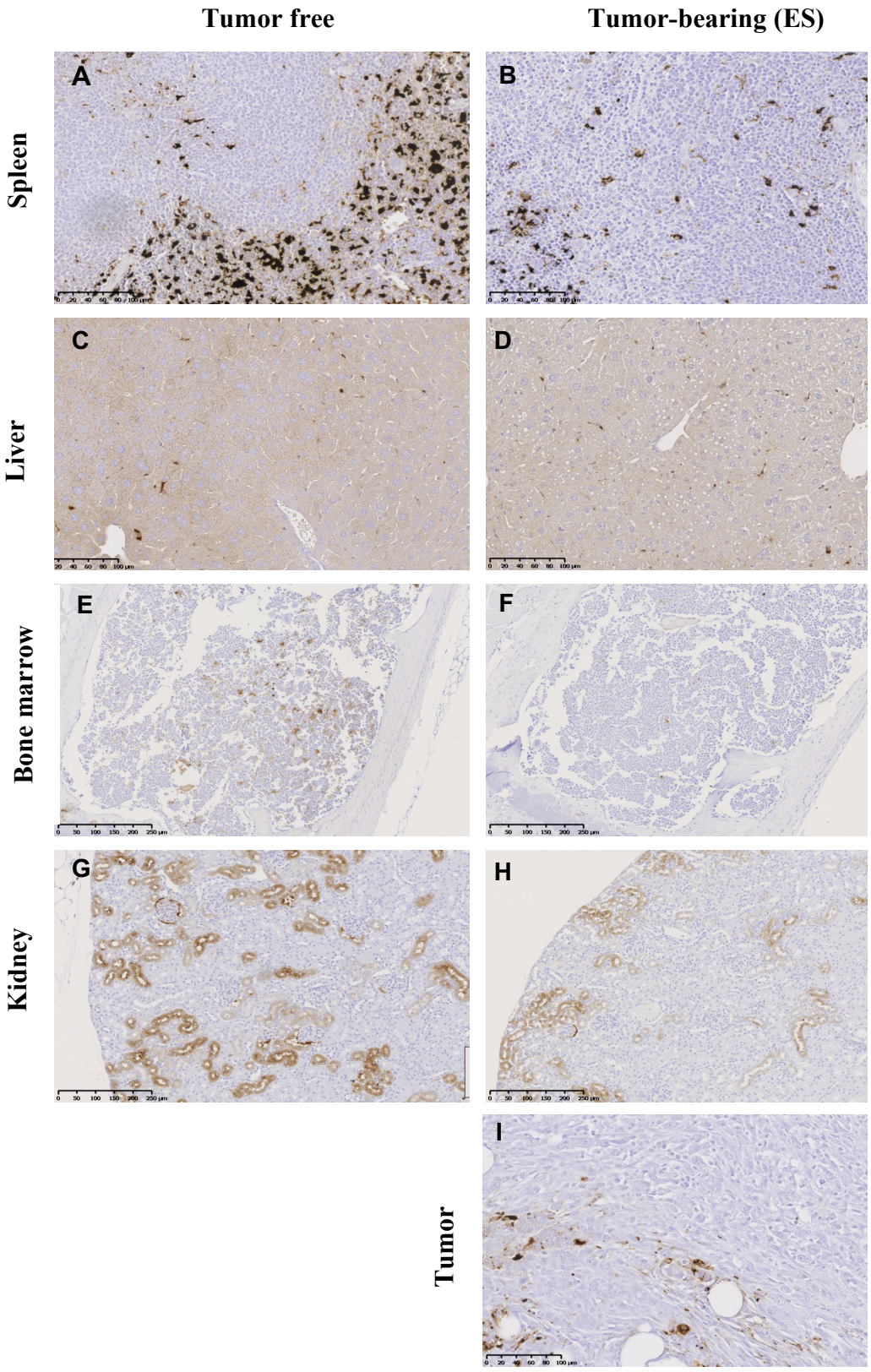

Fig 13. Iron accumulation and distribution in spleen, liver, bone marrow, kidney and tumor of Trp53^{flox}WapCre mice. Tissue sections were stained with DAB-enhanced Perls' to stain (**A, B)** spleen, **(C, D)** liver**, (E, F)** bone marrow, **(G, H)** kidney and **(I)** tumor tissue. Shown are representative images of tumor free control mice (left panels) and tumor-bearing Trp^{53}floxWapCre mice, at end stage, i.e. when they reached maximal permitted tumor size (right panels). Scale bar 100 or 250 µm.

5.5 Altered iron metabolism in tumor-bearing Trp53^{flox}WapCre mice

Because of the reduced iron availability in tumor-bearing mice we analyzed different genes related to iron metabolism in the liver in order to investigate the mechanisms leading to the decrease of iron in blood. We analyzed mRNA levels of hepcidin *(Hamp 1* and *Hamp 2)*, which is the IL-6 inducible major regulator of iron homeostasis. Despite the marked inflammatory response in tumor-bearing mice, *Hamp1* mRNA levels (**Fig. 14 A**) (and *Hamp2*; data not shown) did not increase but remained constant in early cancer progression phases of tumor-bearing mice and decreased 2.4-fold ($p<0.001$) at late tumor progression stages. Gene expression of ferroportin (*Fpn*)**,** the only known iron exporter, was not differentially regulated **(Fig. 14B)** but it might have been regulated post-transcriptionally and post-translationally in tumor-bearing Trp53^{flox}WapCe mice. *Fth1* encoding for the heavy subunit of ferritin, the iron storage protein, was decreased 1.32-fold ($p<0.01$) in tumor-bearing mice at end stage, but not early during the disease progression **(Fig. 8C)**. In contrast, mRNA expression of the serum iron carrier transferrin (*Trf*) increased 2.44-fold ($p<0.0001$) in late tumor progression stages but not in early stages **(Fig. 14D).** Bone morphogenic protein-6 (*BMP-6*) responds to varying iron storage levels and increases hepcidin expression through the BMP-SMAD pathway when iron levels in tissue are high[33]. However, *BMP-6* mRNA expression did not increase in tumor-bearing mice but was reduced 5.98-fold ($p<0,001$) in late stages of tumor progression **(Fig. 14E);** and gene expression of Hemojuvelin (*Hfe2*), a BMP-6 coreceptor, was not differentially regulated **(Fig. 14F).** Homeostatic iron regulator (*Hfe*) induces hepcidin expression when serum iron levels are high, but liver mRNA levels of *Hfe* **(Fig. 14G)** as well as both transferrin receptors 1 (*TfR1*) and 2 (*TfR2*) were not differentially regulated **(Fig 14H, I).** Taken together, we observed differential mRNA levels of genes involved in iron homeostasis, transport and storage, indicating that tumor inflammation impacts on iron metabolism.

Figure 14

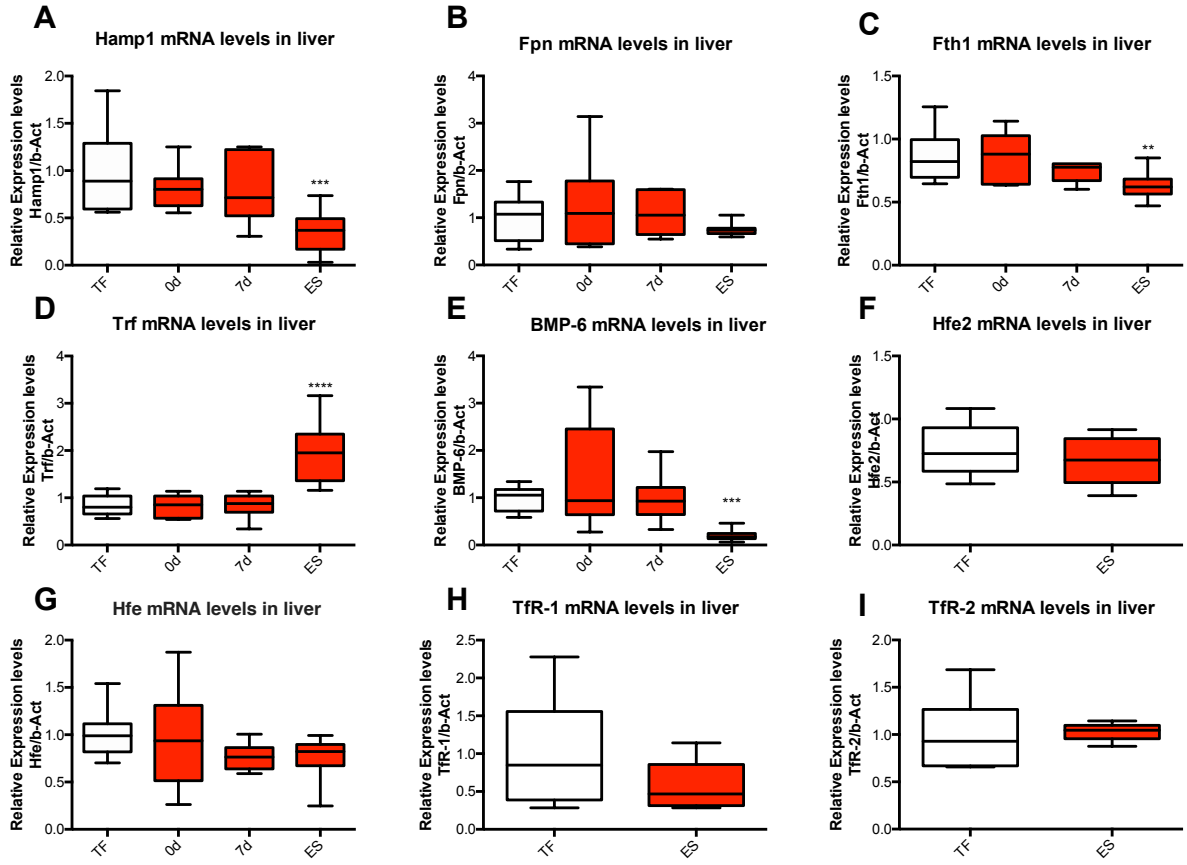

Fig. 14: Liver mRNA levels of genes involved in iron metabolism in tumor-bearing Trp53^{flox}WapCre mice.
Shown are **(A)** hepcidin-1 (*Hamp-1*), **(B)** ferroportin (*Fpn*)**, (C)** ferritin heavy chain (*Fth1*), **(D)** transferrin (*Trf*), **(E)** bone morphogenic protein 6 (*BMP-6*), **(F)** hemojuvelin (*Hfe2*), **(G)** homeostatic iron regulator (*Hfe*), **(H)** transferrin recepror-1 (*TfR-1*) and **(I)** transferrin receptor-2 (*TfR-2*) 2 relative mRNA levels in the liver of tumor free mice (TF, white boxes) and tumor-bearing (red boxes) Trp53^{flox}WapCre mice at different stages of tumor progression: immediately after tumor diagnosis (0d), 7 days after tumor diagnosis (7d) and at end stage (ES, when maximal permitted tumor size was reached). Data are shown as box plot with min to max whiskers and either a one-way ANOVA with Dunnett's Multiple Comparison post hoc test (panel A, B, C, D, G), a Kruskal-Wallis with a Dunn's pot hoc test (panel E) or an unpaired student`s t-test (panel F, H, I) was performed (n=5-11); ***p<0.001, **p<0.05; ****p<0.0001.

Additionally, we analyzed the mRNA levels of some genes related with iron metabolism in bone marrow and spleen. The genes expressed mainly on the erythroid precursors were normalized to glycophorin-1(*Gypa*), a marker for erythroid precursors.[143] Erythroferrone (*Erfe*) was opposite regulated in bone marrow than in spleen. In bone marrow the expression was increased 17.45-fold (p=0.0004) while in spleen was reduced 4.58-fold (p=0.0021) **(Fig. 15**A). We found no differences on the Epo receptor (*EpoR*) expression in bone marrow whereas in spleen the expression in tumor-bearing animals was reduced 1.78-fold (p=0.048) **(Fig. 15B).** Regarding hemoglobin alpha and beta chains, only a small reduction of 1.31-fold (p=0.0173) in bone marrow alpha chain expression level was found **(Fig. 15C, D).** Transferrin receptor 1 (*TfR1*) expression was increased in bone marrow 2.15-fold (p=0.0096) and spleen 1.33-fold

(p=0.0236) of tumor-bearing mice **(Fig. 15E),** while transferrin receptor-2 expression (*TfR2*) was not modified **(Fig. 15F).**

Figure 15

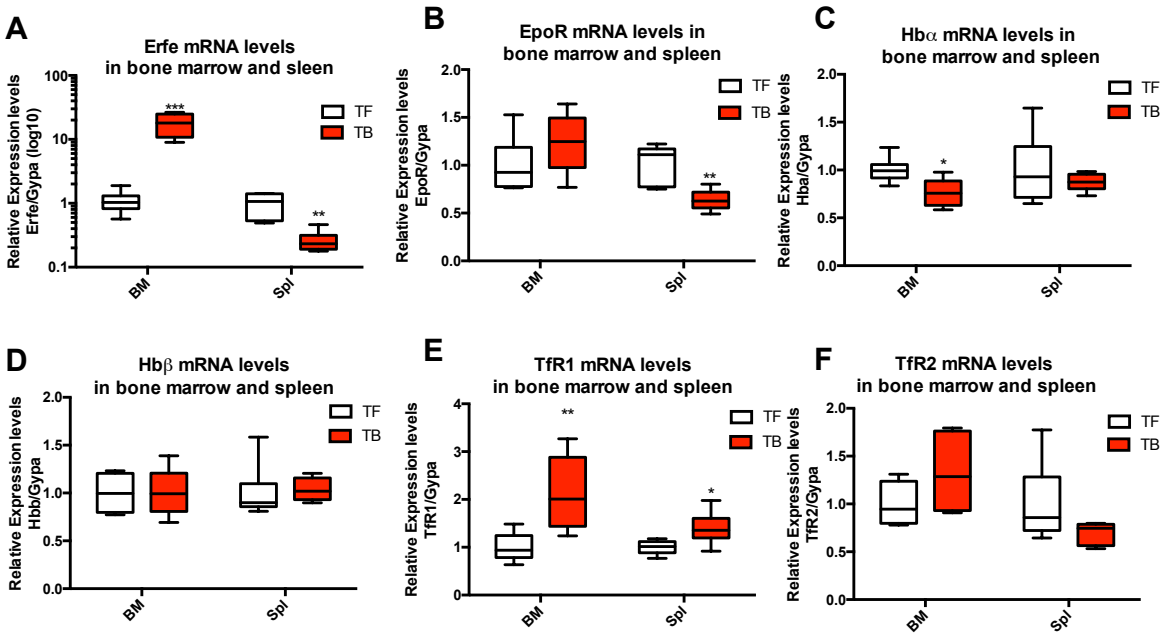

Fig. 15: Bone marrow and spleen mRNA levels of genes related with iron metabolism in tumor-bearing Trp53^{flox}WapCre mice.
Shown are **(A)** erythroferrone (*Erfe*); **(B)** Epo receptor (*EpoR*)**, (C)** hemoglobin alpha chain (*Hbα*); **(D)** hemoglobin beta chain (*Hbβ*); **(E)** transferrin recepror-1 (*TfR-1*); **(F)** transferrin receptor-2 (*TfR-2)* relative mRNA levels normalized to glycophorin-1 (*Gypa)* in bone marrow and spleen of tumor free mice (TF, white boxes) and tumor-bearing at end stage (ES, red boxes). Data are shown as box plot with min to max whiskers and either an Unpaired Student`s t-test (panel A, B, E, F) or a Mann Whitney test (panel C, D) was performed (n=4-6). *p<0.05; **p<0.01; ***p<0.001.

5.6 Tumors of Trp53^{flox}WapCre mice do not cause anemia when transplanted into immunocompromised Foxn1^{nu} mice

To further verify that inflammation is the driving force in AC in Trp53^{flox}WapCre mice, we implanted tumors harvested from Trp53^{flox}WapCre mice subcutaneously into immunocompromised Foxn1^{nu} mice. Similar to the Trp53^{flox}WapCre mouse model, a tumor size of 2 cm^3 was the experiment termination criteria, which was reached within 29 and 49 days. However, 3 out of 5 tumor-bearing nude mice started to develop skin ulceration at the tumor site and the experiment was prematurely terminated. We observed no clear differences in hematocrit and hemoglobin levels between tumor implanted and sham operated nude mice **(Fig. 16A, B).** Additionally, neither spleen nor liver weight differed between tumor-bearing and tumor free mice **(Fig. 16C, D)**, however a trend of increased spleen size in tumor-bearing mice was noted**.** Similarly, only a trend of reduced serum iron concentration and transferrin

saturation in tumor-bearing animals was observed **(Fig. 16E, F)** whereas unsaturated and total iron binding capacity did not differ **(Fig. 16G, H)**.

Figure 16

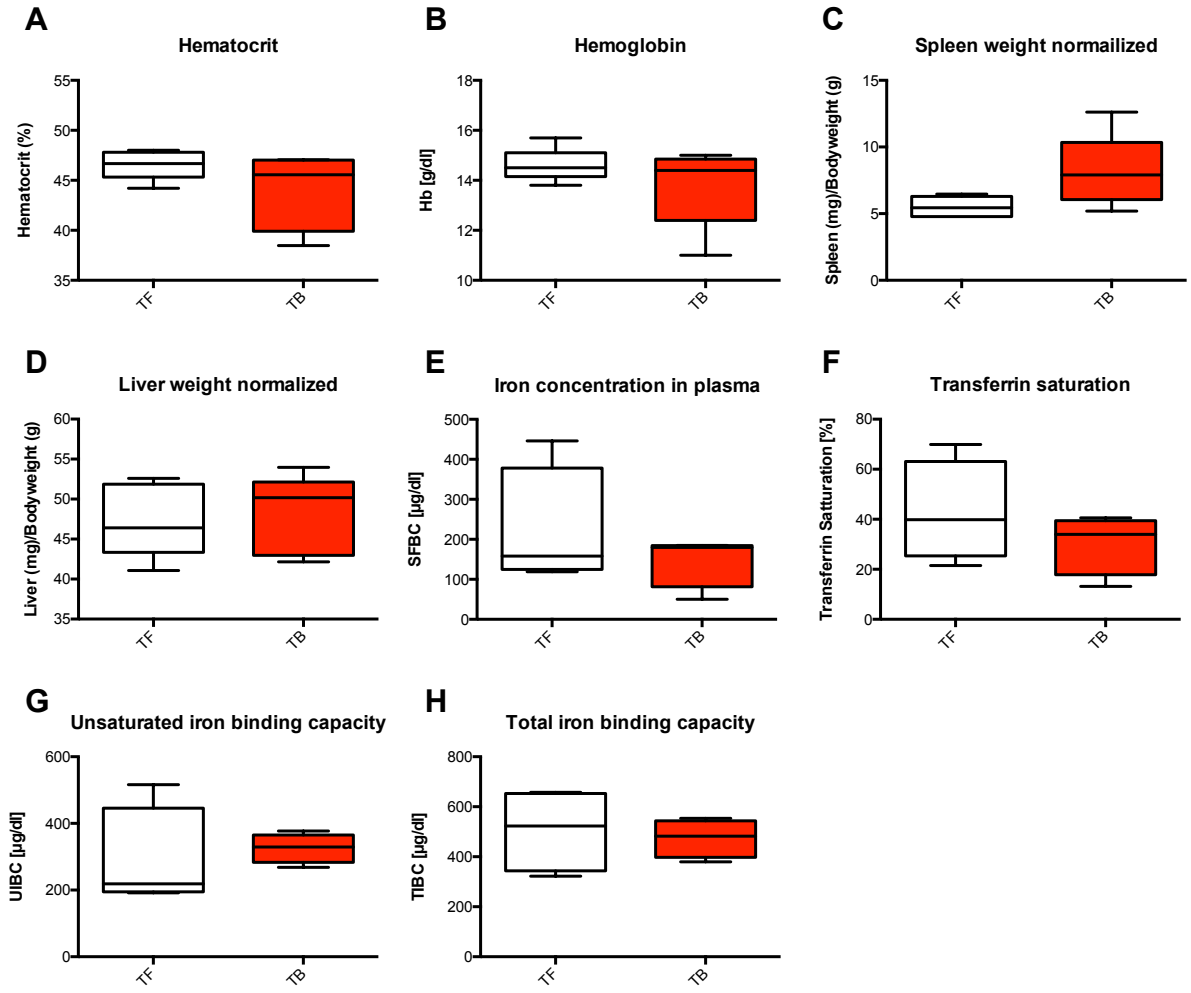

Fig 16: Hematology and iron parameters in immunocompromised Foxn1^{nu} mice after the transplantation of tumors of Trp53^{flox}WapCre mice
Shown is **(A)** hematocrit**, (B)** hemoglobin**, (C)** spleen weight as well as **(D)** liver weight normalized to body weight**, (E)** plasma iron concentration**, (F)** transferrin saturation, **(G)** unsaturated iron binding capacity and **(H)** total iron binding capacity of immunocompromised Foxn1^{nu} mice implanted with tumors of Trp53^{flox}WapCre mice (TB) or sham operated (TF). Data are shown as box plot with min to max whiskers and an Unpaired Student`s t-test for all panels (except panel B, Mann Whitney test) was performed (n=5).

5.7 Single intravenous injection of ferric carboxymaltose (Ferinject®) does not mitigate anemia in tumor-bearing Trp53^{flox}WapCre mice

Tumor-bearing Trp53^{flox}WapCre mice with anemia display features of iron deficiency, especially reduced serum and tissue iron concentration, reduced ferritin and elevated

transferrin. To analyze if iron supplementation restores normal blood levels in anemic, tumor-bearing Trp53^{flox}WapCre mice, we treated mice with a single intravenous injection of 13.3 mg/kg ferric carboxymaltose (Ferinject®) or saline on the day of tumor diagnosis. Iron supplementation did neither accelerate nor delay the time until mice reached the maximal tumor volume **(Fig. 17A)** and no differences in hematocrit, hemoglobin, iron parameters in serum or iron content in liver, spleen or tumor were found between iron treated or saline injected groups at end stage **(Fig. 17B-L).** We repeated the experiment with a higher dose of ferric carboxymaltose of 20 mg/kg and sampled plasma and tissue 15 days after the injection in all mice to exclude i) that the administrated iron dose was too low to compensate the reduced iron levels, or ii) that the time between iron administration (on the day of tumor diagnosis) and sampling plasma and tissues was too long. As described above, hematocrit and hemoglobin values were not restored **(Fig. 18A, B),** but plasma iron concentration increased slightly from 219.5 µg/dl in saline treated to 278 µg/dl (p=0.0286) in iron treated mice **(Fig. 18C)**. However, unsaturated and total iron binding capacity also slightly increased from 153.4 µg/dl in saline to 369.3 µg/dl in iron treated mice (p=0.0122) or from 372.9 µg/dl to 719.4 µg/dl (p=0.0012), respectively **(Fig. 18D, E)**. Neither transferrin saturation **(Fig. 18F)** nor tissue iron concentration in liver, spleen and tumors differed between saline and iron treated mice **(Fig. 18G, H, I)**, suggesting that reduced tissue iron levels could not be restored by iron supplementation. Additionally, the incapability to increase hemoglobin levels despite the slightly elevated plasma iron levels suggest that supplemented iron was either not available or sufficient for erythropoiesis or that iron availability was not rate limiting during erythropoiesis in tumor-bearing mice.

Figure 17

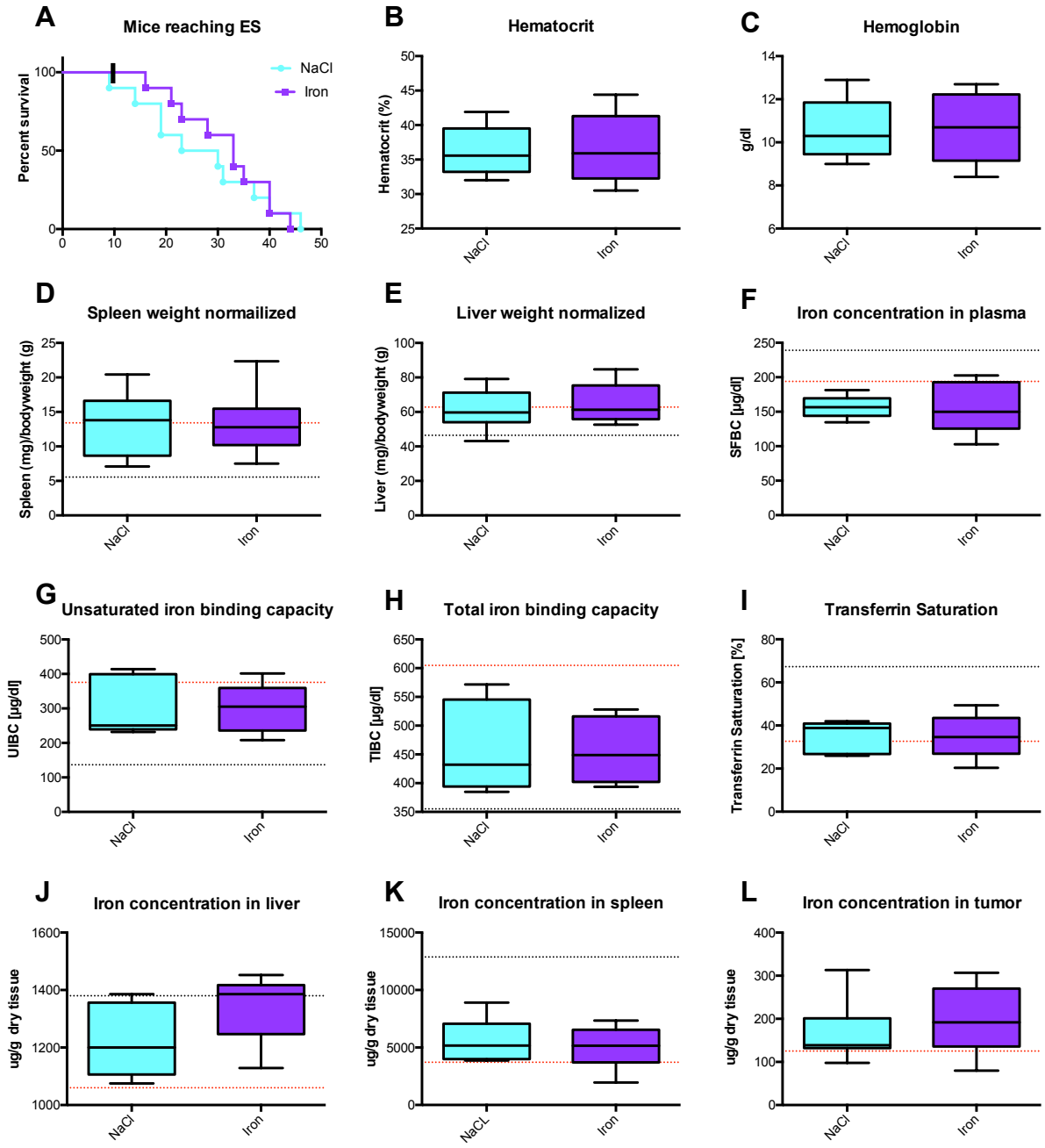

Fig. 17: Tumor progression, hematology and iron parameters in tumor-bearing Trp53^{flox}WapCre mice after a single administration of 13.28 mg/kg of ferric carboxymaltose.
Shown is **(A)** Kaplan-Meier survival curve, **(B)** hematocrit, **(C)** hemoglobin, **(D)** spleen weight normalized to the body weight, **(E)** liver weight normalized to the body weight, **(F)** plasma iron concentration, **(G)** unsaturated iron binding capacity, **(H)** total iron binding capacity, **(I)** transferrin saturation, **(J)** iron concentration in liver, **(K)** iron concentration in spleen and **(L)** iron concentration in tumor of tumor-bearing Trp53^{flox}WapCre mice receiving an intravenous single injection of 13,28 mg/kg ferric carboxymaltose (Ferinject®) (Iron, purple boxes and lines) or saline (NaCl, blue boxes and lines) the day of the tumor diagnosis. Mice were euthanized when tumor volume reached maximal permitted size and parameters measured post mortem. Black dotted line indicates the median of untreated tumor free mice and red dotted line indicates the median of tumor-bearing Trp53^{flox}WapCre mice when tumor volume reached maximal permitted size. Data are shown as (panel A) Kaplan-Meier Survival curve (n=10) and (panel B-L) as box plot with min to max whiskers. An Unpaired Student's t-test was performed for panels B-L (n=5-10).

Figure 18

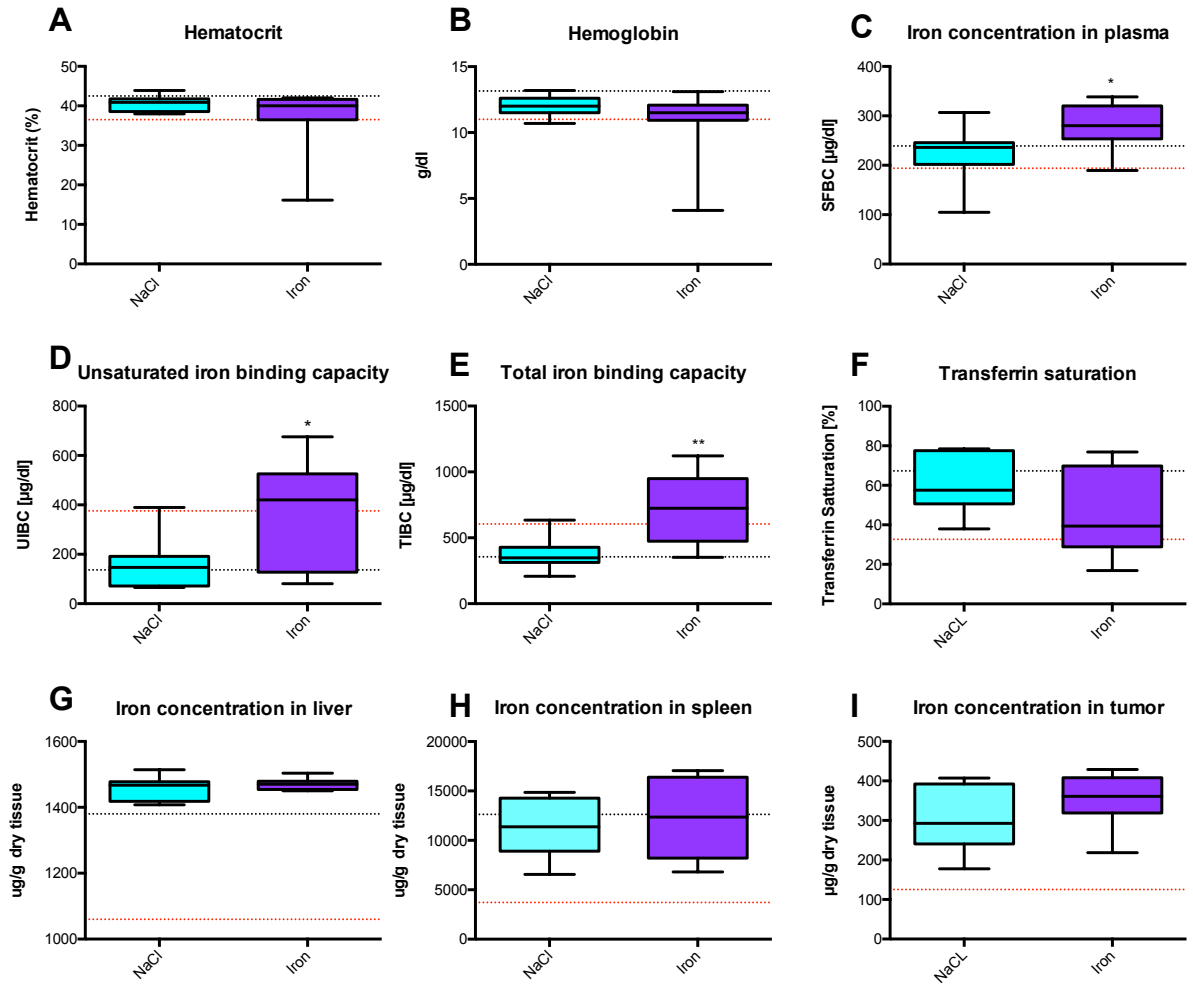

Fig. 18: Hematology and iron parameters in tumor-bearing Trp53^{flox}WapCre mice 15 days after a single intravenous injection of 20 mg/kg ferric carboxymaltose.
Shown is **(A)** hematocrit, **(B)** hemoglobin, **(C)** plasma iron concentration, **(D)** unsaturated iron binding capacity, **(E)** total iron binding capacity, **(F)** transferrin saturation, **(G)** iron concentration in liver, **(H)** iron concentration in spleen and **(I)** iron concentration in tumors of tumor-bearing Trp53^{flox}WapCre mice receiving a single intravenous injection of 20 mg/kg ferric carboxymaltose (Ferinject®) (Iron, purple boxes) or saline (NaCl, blue boxes) the day of the tumor diagnosis. Mice were euthanized 15 days after iron injection and parameters measured post mortem. Black dotted line indicated the median of untreated tumor free mice and red dotted line indicates the median of tumor-bearing Trp53^{flox}WapCre mice when tumor volume reached maximal permitted size. Data are shown as box plot with min to max whiskers. An Unpaired Student`s t-test was performed (n=6-11); *p<0.05, **<0.01

5.8 Iron treatment acutely stimulates erythropoiesis in spleen but not in bone marrow of Trp53^{flox}WapCre mice

To analyze if acute iron supplementation might stimulate erythropoiesis, tumor free and tumor-bearing Trp53^{flox}WapCre mice with tumors bigger than 1.5 cm received a single intravenous injection of 20 mg/kg of ferric Carboxymaltose (Ferinject®). Bone marrow and spleen were harvested 48 h post-injection and analyzed by flow cytometry. Iron supplementation did not change cellularity in bone marrow or spleen of tumor-bearing mice in comparison to untreated

tumor-bearing mice **(Fig. 19A, B).** While the proportion of Ter119^{+} (late erythroid precursors) and CD45/GR1^{+} (leukocyte precursors) cells in bone marrow did not change in iron treated mice, the proportion of Ter119 $^{+}$ in spleen was increased from 41.58 to 53.83% (p=0.0089) and the proportion of CD45/GR1^{+} cells was decreased from 68.03 to 57.05% (p=0.0299**) (Fig. 19C, D)**. No effect of the iron treatment was observed in the proportion of the different stages of the erythroid precursor's maturation in the bone marrow nor in the spleen **(Fig. 19E-I)**. These results might suggest that ferric carboxymaltose treatment could acutely impact on the stress erythropoiesis occurring in the spleen, boosting the production of erythroid cells.

Figure 19

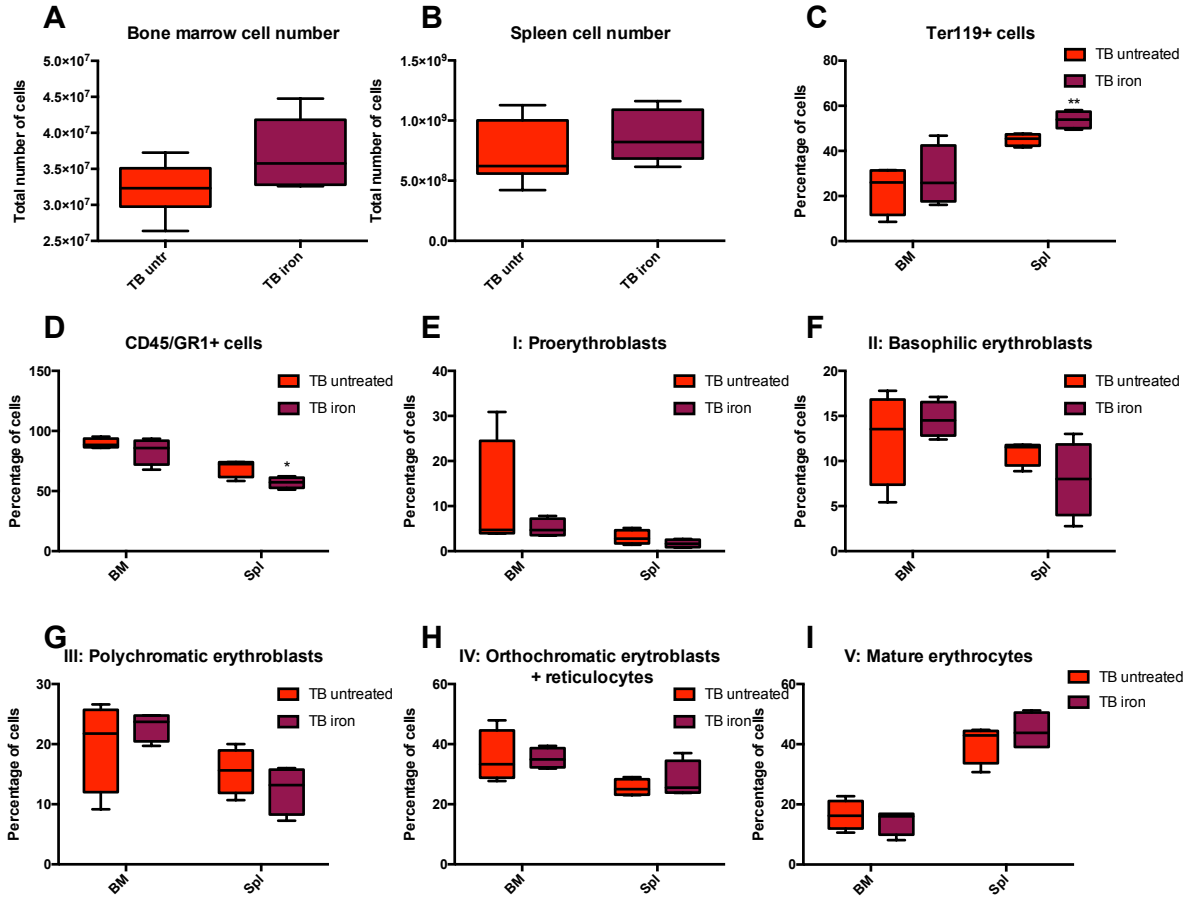

Fig 19: Flow cytometry analyses of late erythroid precursors in the bone marrow and spleen of tumor-bearing Trp53^{flox}WapCre mice treated 48h before euthanasia with a single i.v. injection of ferric carboxymaltose
Shown is **(A)** total cellular number in bone marrow; (B) total cell number in spleen; **(C)** percentage of ter119 positive cells in bone marrow and spleen **(D)** percentage of CD45, GR1 positive cells in bone marrow and spleen; **(E)** percentage of erythroblasts; **(F)** percentage of basophilic erythroblasts; **(G)** percentage of polychromatic erythroblasts; **(H)** percentage of orthochromatic erythroblasts and reticulocytes and **(I)** mature erythrocytes in bone marrow and spleen of tumor-bearing mice treated with a single i.v. injection of ferric carboxymaltose 48h before tissue sampling (TB iron, garnet boxes) and untreated tumor-bearing mice (TB untr, red boxes). Data are shown as box plot with min to max whiskers. An Unpaired Student`s t-test was performed (n=4); *p<0.05; **p<0.01.

5.9 Impaired bone marrow erythropoiesis in tumor-bearing Trp53^{flox}WapCre mice cannot be compensated by activated stress erythropoiesis in the spleen

To analyze erythropoiesis in Trp53^{flox}WapCre tumor-bearing mice we morphologically assessed bone marrow smears and quantified the differential cellular count in tumor-bearing and tumor free mice. Hematologic precursor cells of tumor-bearing mice were morphologically not different from tumor free mice and also no signs of iron deficiency were observed. However, the bone marrow smears revealed that the proportion of mature **(Fig. 20A)** and immature erythroid precursors **(Fig. 20B)** decreased from 40.83% and 1.25% in tumor free mice to 17.100% (p=0.0142) and 0.525% (p=0.0238) in tumor-bearing mice. In contrast, the proportion of late **(Fig. 20C)** and early myeloid precursor cells **(Fig. 20D)** increased from 41.18 to 70.08%(p=0.0076), and from 1.65 to 4.15% (p=0.002) in tumor-bearing mice. Lymphoid precursors **(Fig. 20F)** decreased from 12.35 to 6.025% (p=0.0341) in the tumor-bearing mice, and no changes between tumor free and tumor-bearing mice in the proportion of macrophages, plasma cells, basophils and eosinophils precursors was observed **(Fig. 20G-I)**. Histological analyses of H&E stained bone marrow sections **(Fig. 20J, K)** showed that cell density did not differe between tumor free and tumor-bearing mice **(Fig. 20L)**. However, the H&E bone marrow sections visually confirmed the increased number of myeloid precursors and the reduced number of erythroid precursors.

Figure 20

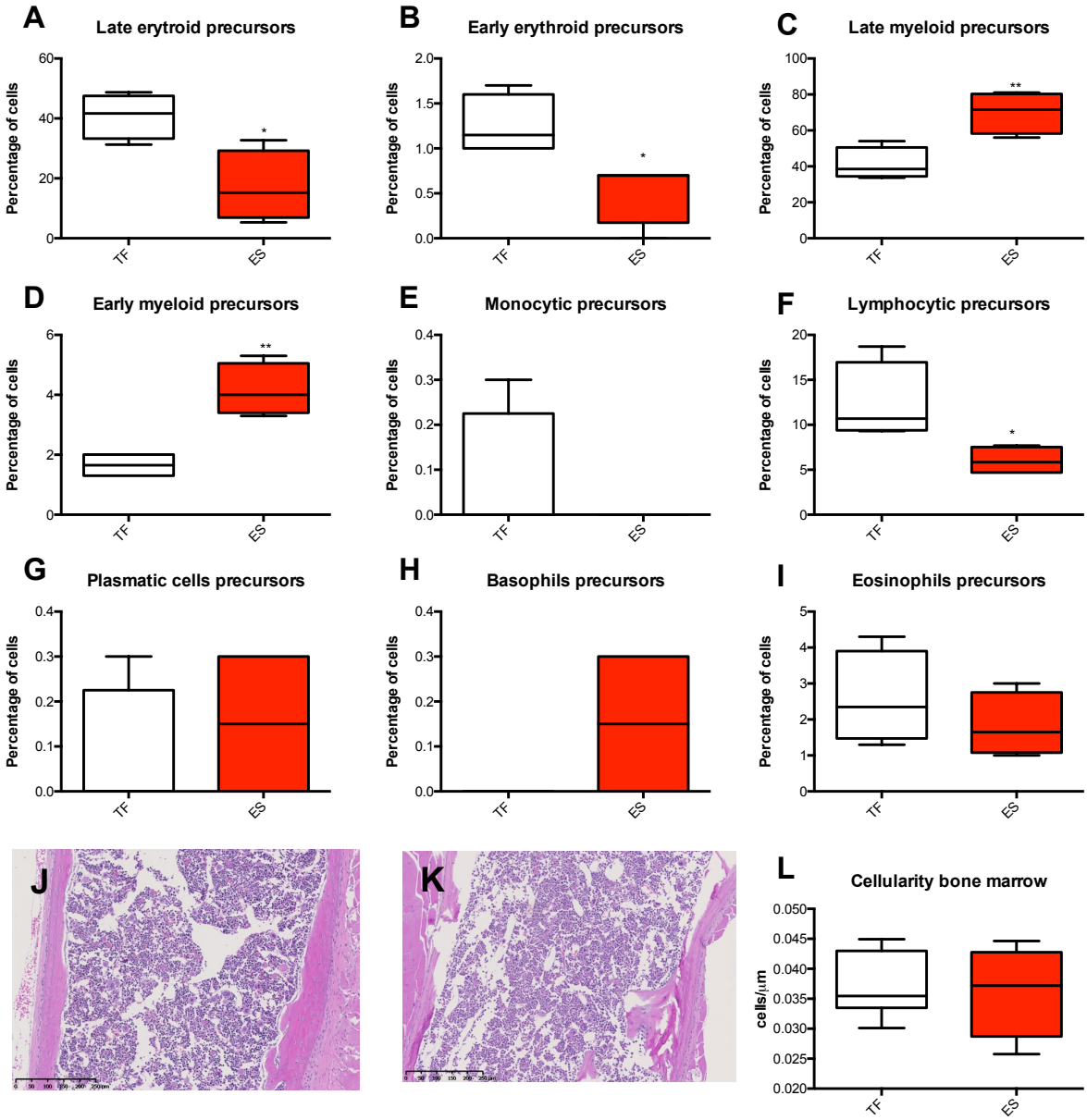

Fig. 20: Differential cellular count in bone marrow smears and bone marrow histology of tumor-bearing Trp53^{flox}WapCre mice

Shown is the percentage of **(A)** mature and **(B)** immature erythroid precursors, **(C)** mature and **(D)** immature myeloid precursors, **(E)** monocyte precursors, **(F)** lymphocytes precursors, **(G)** plasma cells precursors, **(H)** basophils precursors and **(I)** eosinophils precursors in bone marrow smears obtained of femurs of age-matched tumor free (TF, white boxes) and tumor-bearing Trp53^{flox}WapCre mice after reaching maximal permitted tumor size (end stage (ES), red boxes). Panel J and K show representative images of H&E stained bone marrow sections of tumor free **(J)** and tumor-bearing **(K)** Trp53^{flox}WapCre mice after reaching maximal permitted tumor size. Panel **(L)** shows the cellularity, quantified with Visopharm software, of age-matched tumor free (TF, white boxes) and tumor-bearing Trp53^{flox}WapCre mice after reaching maximal permitted tumor size (end stage (ES), red boxes). Data are shown as box plot with min to max whiskers. An Unpaired Student`s t-test was performed (n=4-6); *p<0.05; **p<0.01.

To investigate erythropoiesis in bone marrow and spleen of Trp53^{flox}WapCre mice in more detail, we used flow cytometry analysis to analyze both, the early and the late stages of the erythropoiesis.

To analyze the late erythroid precursors at different stages of their maturation, from proerytroblast to mature erythrocyte, we isolated bone marrow and spleen cells, labeled them with fluorescent CD45, GR-1, Ter119, CD44 antibodies and analyzed them by flow cytometry **(Fig. 21)**.

Figure 21

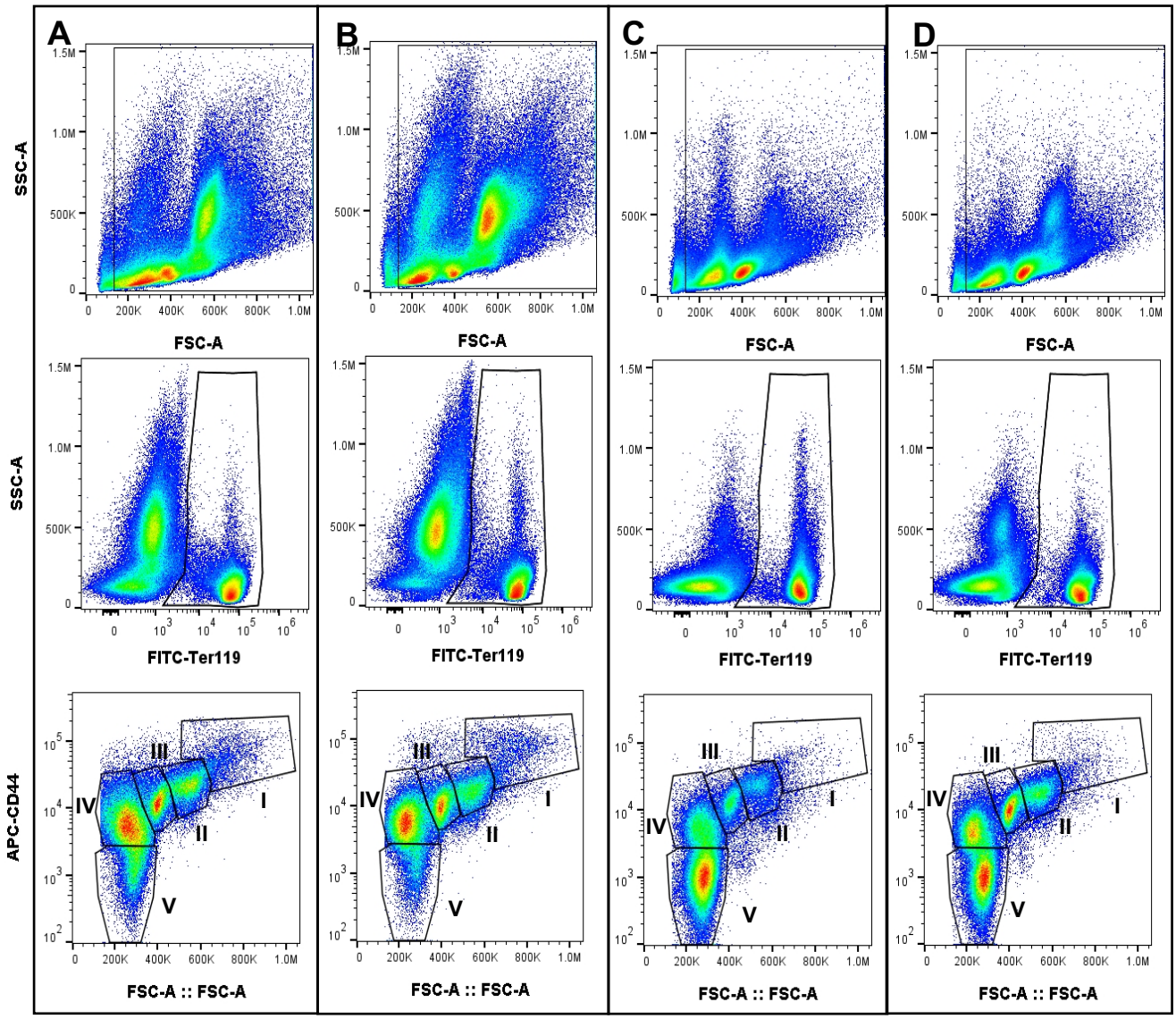

Fig 21: Flow cytometric analysis of late erythroid maturation in bone marrow and spleen in tumor-bearing Trp53^{flox}WapCre mice

Shown are representative images of the gated plots and the gating strategy used for the erythroid maturation assessment in bone marrow of tumor-free mice **(A),** bone marrow of tumor-bearing mice at end stage **(B),** spleen of tumor-free control mice **(C)** and spleen of tumor-bearing mice at end stage **(D).** The gates on the lower plots indicates the different stages of the late erythroid maturation: proerythroblasts (I), basophilic erythroblasts (II), polychromatic erythroblasts (III), orthochromatic erythroblasts and reticulocytes (IV) and mature erythrocytes (V).

The total cell number in bone marrow did not differ between tumor free and tumor-bearing Trp53^{flox}WapCre mice **(Fig. 22A),** confirming the histological bone marrow analyses **(Fig. 20L)**. The proportion of Ter119 positive erythroid precursors decreased from 45.8% in tumor free mice to 23.01% in tumor-bearing mice (p=0.0126) **(Fig. 22B)** but the proportion of CD45 and GR-1 positive granulocytes increased from 72.95% in tumor free mice to 89.53% in tumor-bearing mice (p=0.0183) **(Fig. 22C).** In contrast to the unchanged cellularity, the reduced erythropoiesis and the increased production of granulocytic precursors in bone marrow, the spleen cellularity increased in tumor-bearing mice from 2.369x10^8 to 7.2x10^8 total cell number (p=0.0018) **(Fig. 22D)**, that caused splenomegaly – the enlargement of the spleen **(Fig. 9A)**. Additionally, the proportion of erythroid and granulocytic precursors in the spleen, did not differ between tumor-bearing and tumor free control mice **(Fig. 22E, F).**

Figure 22

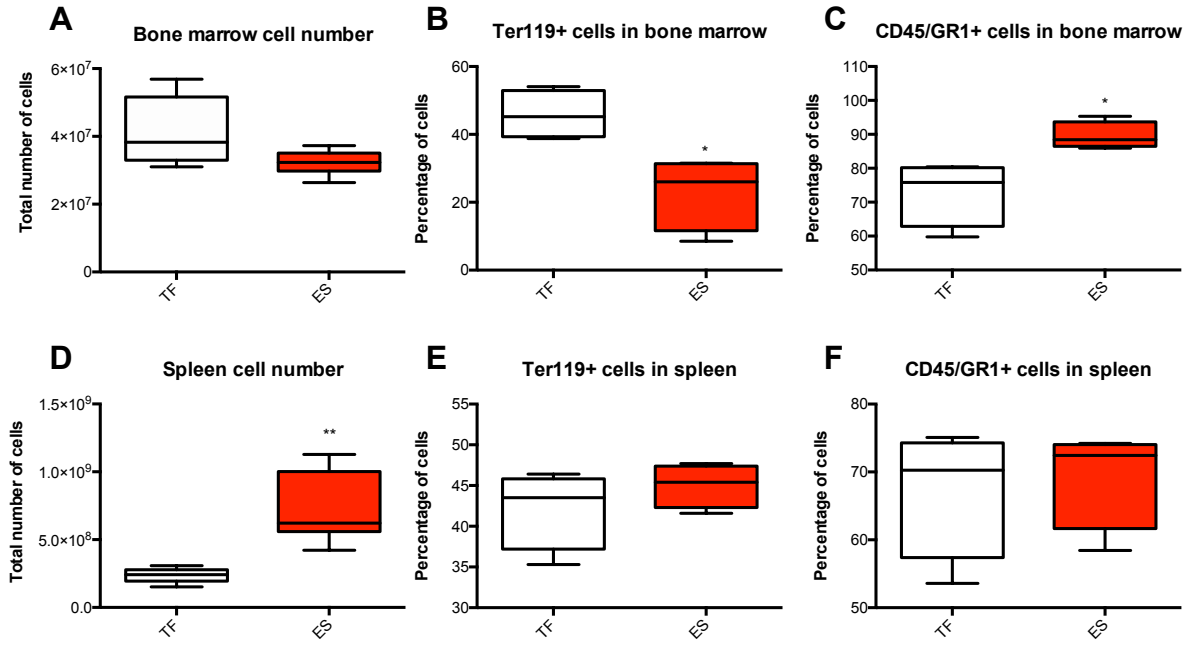

Fig 22: Flow cytometry analysis of late erythroid precursors and granulocyte precursors from bone marrow and spleen of tumor-bearing Trp53^{flox}WapCre mice
Shown is **(A)** total cellular number, **(B)** percentage of ter119 positive erythroid precursor cells and the percentage of **(C)** CD45 and GR1 positive granulocytes precursor cells in bone marrow as well as **(D)** the total cellular number, **(E)** percentage of ter119 positive erythroid precursor cells and the percentage of **(F)** CD45 and GR1 positive granulocytes precursor cells in spleen of tumor free (TF, white boxes) and tumor-bearing mice after they reached maximal permitted tumor size (end stage, ES, red boxes). Data are shown as box plot with min to max whiskers. An unpaired student`s t-test was performed (n=4); *p<0.05; **p<0.01.

Despite the reduced total amount of late erythroid progenitors in the bone marrow, the relative proportion of the different maturation stages from proerythroblast to mature red blood cell did not differ in bone marrow of tumor-bearing Trp53^{flox}WapCre mice (**Fig. 23)**. However, we

observed the opposite in the spleen: although we observed no difference in the total amount of total late erythroid progenitors between the spleens of tumor-bearing and tumor free mice **(Fig. 22E)**, the relative proportion of all the stages from proerythroblast to orthochromatic red blood cells and reticulocytes increased and the mature red blood cell fraction decreased in tumor-bearing mice. In detail, proerythroblasts increased from 0.7575 to 3.05% (p=0.0289) **(Fig. 23A)**, basophilic erythroblasts increased from 4.49 to 10.95% (p=0.0029) **(Fig. 23B)**, polychromatic erythroblasts increased from 6.9 to 15.5% (p=0.0084) **(Fig. 23C)** and orthochromatic erythroblasts as well as reticulocytes increased from 15.2 to 25.5% (p=0.0096) **(Fig. 23D).** In contrast, the proportion of mature red blood cells decreased from 68.7 to 40.33% (p=0.0022) in the spleen of tumor-bearing mice **(Fig. 23E)**. In conclusion, these results indicate that late erythropoiesis is not impaired in bone marrow but a reduced number of erythroid precursors occurs. In contrast, late erythropoiesis is boosted in the spleen.

Figure 23

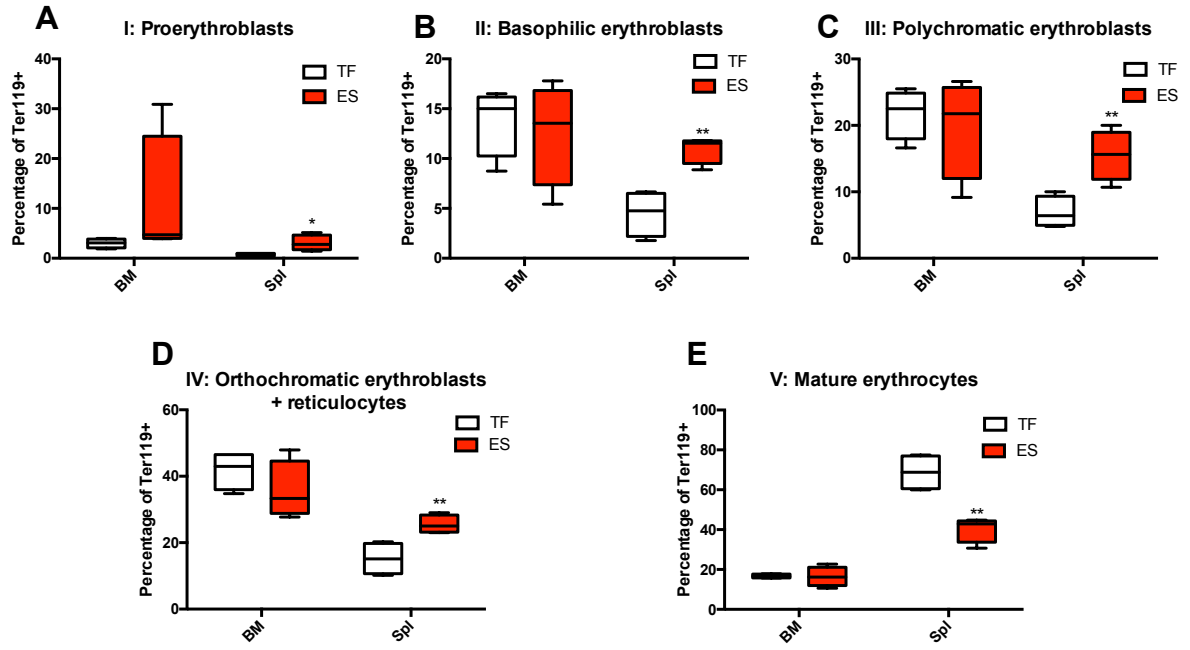

Fig.23: Flow cytometry analyses of different maturation stages of late erythroid precursors in the bone marrow and spleen of tumor-bearing Trp53^{flox}WapCre mice

Percentage of the different stages of the late erythroid maturation analyzed by flow cytometry: **(A)** proerythroblasts; **(B)** basophilic erythroblasts; **(C)** polychromatic erythroblasts; **(D)** orthochromatic erythroblasts and reticulocytes and **(E)** mature erythrocytes in bone marrow and spleen of tumor free (TF, white boxes) and tumor-bearing mice after they reached maximal permitted tumor size (end stage, ES, red boxes). Data are shown as box plot with min to max whiskers. An Unpaired Student`s t-test was performed (n=4); *p<0.05; **p<0.01.

As a reduction of the proportion of the late erythroid precursors was found in bone marrow, the earliest stages of erythropoiesis in this organ were analyzed[144] from hematopoietic stem cells (HSC) to colony forming units erythrocyte (CFUe). Bone marrow cells were stained with different fluorescently labeled antibodies: LIN-cocktail, CKit, SCA-1, CD105, CD150, CD48, CD41, CD16_CD32 and analyzed by flow cytometry.

Neither the proportion of hematopoietic stem cells (HSC) nor the downstream multipotent progenitor (MPP) differed in tumor-bearing mice **(Fig. 24A, B).** The percentage of pre-granulocyte-monocyte lineage cells (PreGM) was increased from 0.797 to 1.32% (p=0.0232) in tumor-bearing mice **(Fig. 24C)** whereas the bipotent pre-megakaryocyte-erythrocyte progenitors (Pre MgE) decreased from 0.25 to 0.156% (p=0.0561) **(Fig. 24D).** No change was observed in the erythroid committed restricted progenitors (Pre-CFUe) or in the megakaryocyte progenitors (MkP) **(Fig. 24E, G),** but a reduction on the colony forming units erythrocyte (CFUe) from 0.76 to 0.244% (p=0.0039) was observed in bone marrow of tumor-bearing mice at end stage **(Fig. 24F).**

These results suggest that early erythropoiesis is impaired in bone marrow, and that hematopoietic precursors in tumor-bearing mice seem to be more committed towards a granulocytic fate in detriment of the erythropoietic cell lineage, driving to a reduced number of CFUe and therefore less late erythroid progenitors.

Figure 24

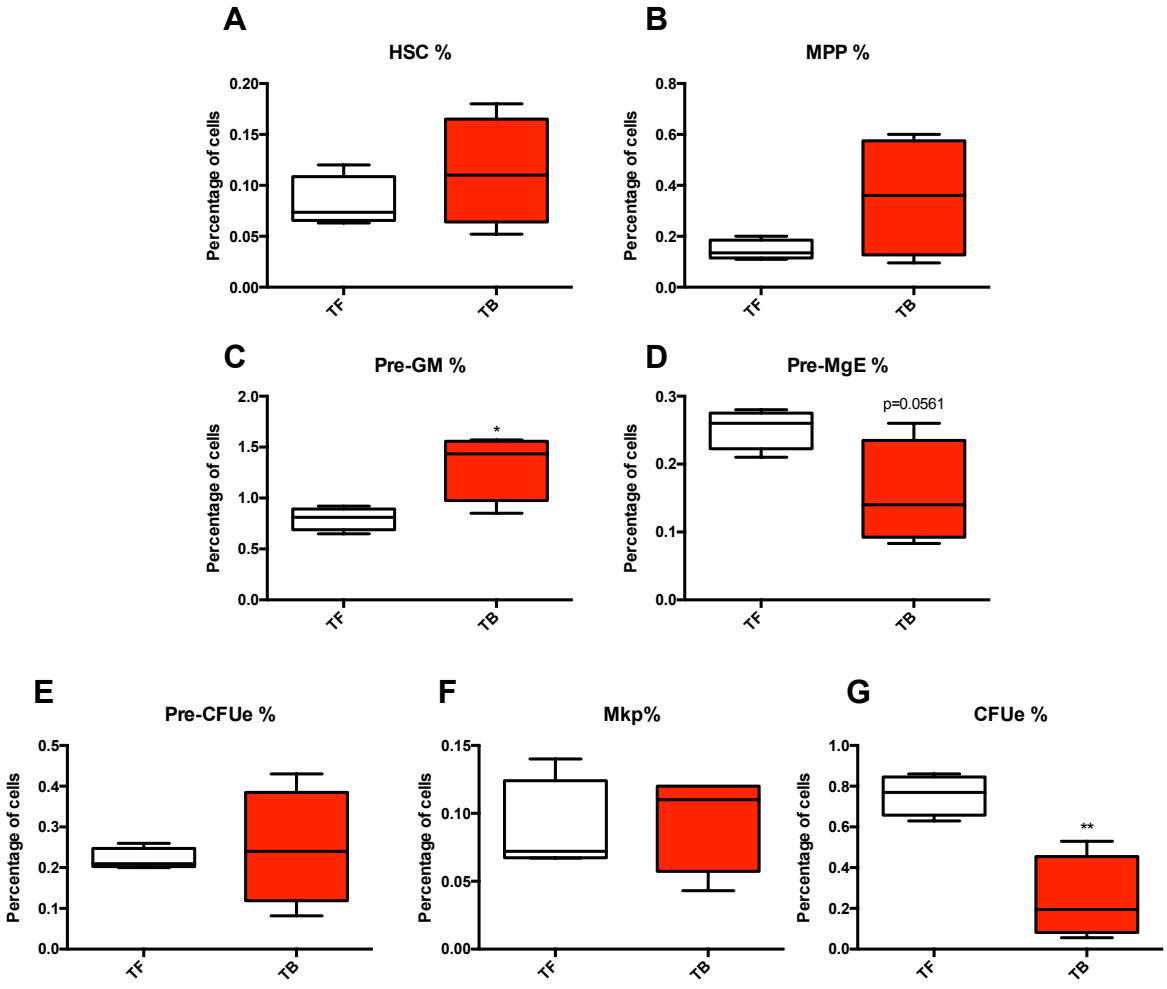

Fig. 24: Flow cytometry analyses of different maturation stages of early hematopoietic precursors in the bone marrow of tumor-bearing Trp53^{flox}WapCre mice

Percentage of the different early hematopoietic precursors analyzed by flow cytometry: **(A)** hematopoietic stem cells (HSC), **(B)** multipotent progenitor (MPP), **(C)** pre-granulocyte-monocyte lineage cells (PreGM), **(D)** pre-megakaryocyte-erythrocyte progenitors (Pre MgE), **(E)** pre-colony forming units erythrocyte (CFUe), **(F)** megakaryocyte progenitors, **(G)** colony forming units erythrocyte (CFUe) in bone marrow of tumor free (TF, white boxes) and tumor-bearing mice after they reached maximal permitted tumor size (end stage, ES, red boxes). Data are shown as box plot with min to max whiskers. An Unpaired Student`s t-test was performed (n=4); *p<0.05; **p<0.01.

5.10 Hematopoiesis in spleen and bone marrow of Trp53^{flox}WapCre mice is differently regulated

As we observed that erythropoiesis was impaired in bone marrow but not in the spleen, we analyzed the mRNA expression in spleen and bone marrow of some proteins related with the regulation of the erythropoiesis: stem cell factor (*SCF*) and suppressor of cytokine signaling 3 (*SOCS-3*) **(Fig. 25).** Interestingly, we observed that its expression in tumor-bearing animals is

altered in bone marrow but not in spleen. The expression of *SCF* was reduced 4.3-fold (p=0.0015) and *SOCS-3* was increased 2.41-fold (p=0.0225).

Figure 25

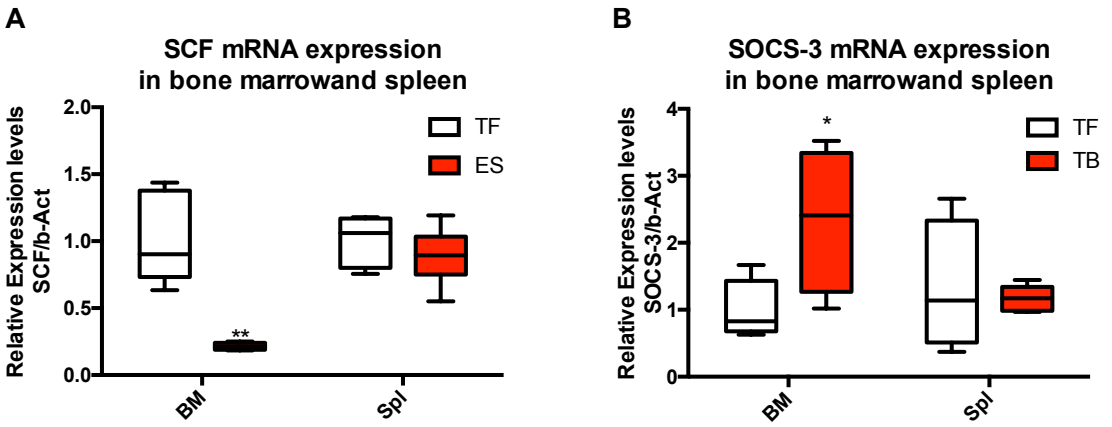

Fig. 25: Bone marrow and spleen mRNA expression of genes related with erythropoiesis in tumor-bearing Trp53floxWapCre mice.
Shown are **(A)** stem cell factor (*SCF*) and **(B)** suppressor of cytokine signaling 3 (*SOCS-3*) relative mRNA expression normalized to *b-actin* in bone marrow and spleen on of tumor free mice (TF, white boxes) and tumor-bearing at end stage (ES, red boxes). Data are shown as box plot with min to max whiskers and an Unpaired Student`s t-test was performed (n=4-6). *p<0.05; **p<0.01.

As an increase on the myeloid cells proportion was observed, we analyzed granulocyte colony-stimulating factor (G-CSF) and granulocyte-macrophage colony-stimulating factor (*GM-CSF*) expression in tumor tissue. These cytokines promote the differentiation of hematopoietic precursors towards a myelocytic fate. We detected mRNA expression for G-CSF (average CT value = 25.8) and for GM-CSF (average CT value = 29.7) in tumor tissue while in the healthy mammary tissue mRNA expression was not detected.

6. Discussion

AC impairs the quality of life of cancer patients and might have a deleterious effect on cancer disease progression, by promoting the tumor growth and reducing the efficacy of the antitumoral agents.[18,14] Anemia is also the most common comorbidity among cancer patients but despite its high prevalence and critical clinical impact on cancer, it is still nowadays underrecognized and undertreated, mainly due to the fact that its pathogenesis is multifactorial and the lack of safe and effective therapies.[79] To develop or improve treatment strategies, preclinical studies of AC are required to recapitulate human pathogenesis. However, only few animal models are available[125,127,128,145] and, until today, no spontaneous tumor developing animal model exists that recapitulates all stages of cancer disease including immunoediting and tumor incidence. Thus, we characterized AC in Trp53^{flox}WapCre mice with spontaneous tumor development and treated anemic mice with iron supplementation.

Our results showed that Trp53^{flox}WapCre mice display multifactorial epo-resistant cancer related anemia with a prominent inflammation, hypoferremia and inhibition of the medullar erythropoiesis. A single intravenous iron injection of ferric carboxymaltose was not effective to mitigate anemia in our model because hematopoiesis is altered at the level of early hematopoietic precursor cells and not at late stages of progenitors that are already committed to the erythroid fate. Thus, Trp53^{flox}WapCre mice mimic the pathology of impaired erythropoiesis (especially cytokine-dependent inhibition of erythropoiesis) in AC of human patients.

6.1 Trp53^{flox}WapCre mice develop Epo-resistant anemia.

Trp53^{flox}WapCre mice developed AC during tumor progression in the absence of chemo- or radiotherapy. We observed that hemoglobin and hematocrit values were reduced already early after tumor onset and continuously declined throughout tumor progression. Cancer associated anemia is multifactorial and especially liver and kidney pathologies are very frequent comorbidities that can contribute to anemia. However, we found little evidence for a hepatic and no evidence for a renal pathology: in the liver, we observed neither morphologic nor pathologic or inflammatory changes except a slightly increased cell proliferation. We assume that hepatocyte replication (hyperplasia) in anemic tumor-bearing Trp53^{flox}WapCre mice might be a consequence of a tumor-induced hepatic synthesis of inflammatory proteins, such of acute

phase proteins.[146] Epo mRNA levels in the kidney as well as Epo plasma levels were slightly increased in anemic tumor-bearing mice suggesting that i) kidney was able to produce Epo and ii) mice tried – at least partially – to restore normal blood values by increasing Epo expression. In fact, one of the main causes of AC is the reduced renal Epo synthesis.[24] Low Epo expression levels might be either caused by a kidney malfunction[147] or might be the consequence of proinflammatory cytokines that inhibit Epo production in the kidney.[59,60] Anyway, both pathologies result in an inadequate erythropoietic response, which cannot compensate the anemia.[23] If the slightly elevated Epo levels of 1109 pg/ml in anemic Trp53floxWapCre were too low to mitigate anemia in our mouse model is not clear because Epo levels in anemic mice strongly depend on mouse strain and the type of anemia.[148,126,128]

Epo treatment did not prevent anemia in our anemic tumor model. Because AC is most frequently treated with Epo in human patients,[78] we did so with our mice. The use of high (1000 U/kg) Epo dosages did not induce adverse events; neither increased tumor progression nor increased mortality, which is an important finding in the light of ongoing debate about ESA safety.[112] The safety has been questioned within the last decades because several independent studies reported on increased mortality among cancer patients due to a higher prevalence of thromboembolic events[96,97,99,101] or increased tumor growth in some cancer types of cancer.[21,110] Whether or not cancer patients show increased tumor progression after Epo treatment might depend on EpoR expression levels in cancer cells and it might be possible that EpoR expression levels in Trp53^{flox}WapCre mice are too low to impact on cancer growth. Besides tumor growth, Epo treatment in anemic tumor-bearing mice did also not restore the levels of red blood cells. To confirm that the Epo non-responsiveness resulted from tumor development and progression and not from inactive Epo, we also treated tumor-free Trp53^{flox}WapCre mice with Epo. Because tumor free mice responded with increased red blood cells production after Epo administration (data not shown), we concluded that only tumor-bearing anemic Trp53^{flox}WapCre mice were non-responsive to Epo. Such a non-responsiveness to the ESA treatment also occurs in 35-45% of human cancer patients[83] and is either caused by proinflammatory cytokines that inhibit Epo signaling[149] or by a reduced iron availability for erythropoiesis.[150,151]

In our model, mean corpuscular volume (MCV) increased and due to the fact that the mean corpuscular hemoglobin (MCH) was not modified, the resulting MCHC value decreased most likely due to the increased erythrocyte size (macrocytosis) only.[152] The non-regenerative macrocytic anemia that we found in anemic tumor-bearing Trp53^{flox}WapCre mice suggests that anemia might be caused by an impairment of erythropoiesis. Additionally, it could be also

possible that other factors like some nutritional deficiencies such as vitamin-B12 or folate deficiency might be also involved.[153,154]

Thus, we concluded that tumor-bearing Trp53^{flox}WapCre mice display Epo resistant anemia, even when mice were treated with 1000 U/kg of Epo. The medullar erythroid precursors response to Epo is impaired in our anemic Trp53^{flox}WapCre mammary cancer mouse model.

6.2 Anemic tumor-bearing Trp53^{flox}WapCre mice show severe inflammation and immune response

Immune system is strongly stimulated in tumor-bearing Trp53^{flox}WapCre mice with a marked increase of leukocyte numbers in peripheral blood, especially neutrophils and monocytes as of as extensive presence of suppurative inflammation in the tumor tissue. Proinflammatory cytokines are the main responsible factors in AC, and IL-6 has a capital role in the AC pathogenesis in murine models[155] but also in humans.[156] It might contribute to the anemia by several mechanisms such as decreasing plasma iron availably by promoting iron storage inside the cells and reducing intestinal iron absorption,[23] or impairing the Epo production in kidney and EpoR function in the erythroid precursors.[25] Additionally, IL-6 is also involved in some metabolic and nutritional disorders as weight loss and cachexia.[76] We found increased IL-6 expression and plasma levels in our tumor-bearing mice suggesting that IL-6 might contribute to the anemia onset in our model. In addition, we also observed higher IL-1β mRNA expression in tumor tissue than in healthy mammary tissue. IL-1β might impair erythropoiesis by inhibiting Epo production and suppressing proliferation and differentiation of erythroid cells.[23] Furthermore, it might also contribute to the hypoferremia by promoting iron storage inside macrophages.[23] TNFα can suppress erythropoiesis by suppressing autophagy in erythroid progenitors, but we observed lower mRNA levels in tumor tissue than in healthy mammary tissue. It is important to note that in cancer patients cytokines are not consistently increased in plasma[157] due to the fact that many cytokines act at paracrine level in different tissues.[2] Even though, measuring cytokines in plasma might give an indication about which cytokines contribute to the anemia pathogenesis in our model and it will be measured in our lab. To determine how much the T-cells are involved in the pathogenesis of AC, we transplanted tumors of Trp53^{flox}WapCre mice to immunocompromised T-cell negative Foxn1^{nu} mice. 3 out of 5 animals were prematurely euthanized because of tumor ulceration. However, we observed that

the tumors in these immunocompromised mice slightly decreased hemoglobin, hematocrit and serum iron. These data indicate, that T-cells – at least in our model – might not contribute to the anemic phenotype, although they have been shown to play an important role in anemia.[23] However, an experiment with a larger number of mice is required to test this assumption.

We conclude that immune system is strongly activated in tumor-bearing Trp53^{flox}WapCre mice. The immune response in tumor-bearing animals is basically characterized by increased levels of neutrophils and macrophages which contribute to the production of cytokines like IL-6 and IL-1β with likely participate to the anemia onset in our model.

6.3 Hypoferremia in anemic tumor-bearing Trp53^{flox}WapCre

Reduced iron availability for erythropoiesis as a result of proinflammatory cytokines action, specially IL-6, [158] is one of the main etiologic factors in AC.[159] Plasma and tissue iron concentration were reduced in anemic tumor-bearing Trp53^{flox}WapCre mice, however it has to be noted that in liver and spleen total amount of iron stored was higher because the size and weight of both organs was increased in tumor-bearing mice. Additionally, also kidney and bone marrow showed decreased tissue iron, suggesting an iron-imbalance in tumor-bearing mice. We did not observe any special pattern of iron accumulation in tumor tissue, indicating that tumor cells or inflammatory cells present on the tumor environment are not entrapping iron. Iron deficiency was further suggested by low levels of plasma ferritin, which is an indicator for low iron levels in tissue,[160] although inflammation usually even increases plasma ferritin.[161]

The main mechanism how inflammation-induced IL-6 causes iron deficiency is the upregulation of hepcidin,[32] that represents the major hormone controlling iron homeostasis.[162] Interestingly, our anemic mice had high levels of IL-6 and low levels of hepcidin, which contradicts most animal studies on anemia of inflammation.[148] Because we observed no peak in hepcidin expression but a progressing decrease from early to late stages of tumor development, we concluded that hypoferremia in our model might be caused by hepcidin-independent mechanisms[163] such as hypoferremia due to the induction of Toll-like receptors 2 and 6.[41] However, as hepcidin induction occurs very acutely after the inflammatory insult[148,139] but inflammation in our model is chronic, it might be possible that at the time we analyzed hepcidin expression, hepcidin production was already suppressed because low plasma iron levels, hypoxia and increased erythropoiesis,[164] that might have overwritten the stimulatory effect of IL-6. It should be also noted that the iron content in commercial rodent diets is very

high (250 mg/kg in our particular diet) and amply exceed iron requirements of mice.[165] This might cause sustained high hepcidin levels blunting the hepcidin peak that we would expect to see as consequence of inflammation.[32] However, even after feeding mice with an iron sufficient (50 mg/kg iron) diet, hepcidin expression did not increase after tumor onset but decreased, indicating that dietary excess of iron is not the cause of the suppression of the expected but undetectable hepcidin peak. Bone morphogenic protein-6 (BMP-6) acts as a sensor of iron stores and induces hepcidin expression when iron tissue levels are high.[33] We observed reduced *BMP-6* expression in our anemic tumor-bearing mice, suggesting that the progressively reducing iron concentration in tissue might contribute to the reduced hepcidin production. Hepcidin gene expression is suppressed by erythroferrone (Erfe), which is synthetized by erythroid precursors in the bone marrow in response to increased Epo plasma levels.[166] In fact, we also observed increased *Erfe* mRNA expression in the bone marrow (but not in the spleen) of anemic tumor mice, suggesting that Erfe might contribute to the low hepcidin values.

Surprisingly, tumor free Trp53^{flox}WapCre mice had higher iron concentration in spleen and liver than mice of previous studies, [167,168,169] with the exception of one study were C57BL/6 also showed elevated iron tissue concentration.[139] Trp53^{flox}WapCre mice are on a clean, genetic FVB mouse strain background. We compared FVB wild type mice and tumor free Trp53^{flox}WapCre mice to verify that the elevated iron levels were not a result of the genetic modification in our model. **(Fig. S7).** Interestingly, wild type FVB mice have equally high tissue iron levels than Trp53^{flox}WapCre, but they are 6-8-fold higher than in C58BL/6. Despite the high iron content, no iron-induced cytotoxicity was observed. Additionally, our Trp53^{flox}WapCre and wildtype FVB mice were around 30 weeks but C57Bl/6 mice only 16 weeks and ageing causes iron accumulation in tissues. However, age alone is not able to explain the difference in the tissue iron concentration between FVB and C57BL/6 mice. We concluded that mice on FVB genetic background have an altered iron metabolism that leads to higher iron levels and more iron accumulation, which potentially affects hepcidin homeostasis.

To further characterize hypoferremia in Trp53^{flox}WapCre mice, we analyzed the expression of additional genes involved in iron metabolism in the liver. Liver mRNA levels of ferroportin *(Fpn),* the unique known iron exporter, did not change. However, ferroportin is posttranscriptionally and posttranslationally modified,[170] and mRNA expression levels might not reflect the ferroportin protein amount in the cell membranes. The liver mRNA expression of heavy ferritin chain (*Fth1)* decreased in anemic tumor-bearing mice. Ferritin is the main iron storage protein and its expression is regulated at different levels by plasma and labile cellular

iron concentration as well as inflammation.[171] The reduced ferritin plasma levels confirmed the reduced mRNA expression in the liver and it is well described that they are reduced when tissue iron concentration decrease.[160] In contrast, transferrin (*Trf*) mRNA expression in liver increases in anemic tumor-bearing mice. Transferrin is the main iron transporter in plasma and its expression is mainly regulated by inflammatory cytokines,[172] and iron levels.[173] Although transferrin is frequently reported to be down regulated during inflammation,[146] it was increased at both liver mRNA and plasma protein level in our anemic tumor-bearing mice. The induction was indirectly measured by estimating the plasma total iron binding capacity (TIBC), that was increased during anemia potentially because decreased serum iron levels were overwriting the inflammation-induced suppression of gene expression.[173]

In addition to the gene expression in the liver, we analyzed gene expression also in the bone marrow of anemic tumor mice. Transferrin receptor 1 (*TfR1)* mRNA but not transferrin receptor-2 (*TfR2)* mRNA was increased in erythroid cells of bone marrow and spleen. TfR1 takes up transferrin-bound iron[174] and its expression is induced by increased heme levels and EpoR downstream signaling.[175] This suggests that the erythropoietic cells might try to maximize the iron uptake for erythropoiesis.

We concluded that reduced circulating iron levels in our model was due to the entrapment of iron inside spleen and liver. Despite iron concentration is decreased in both organs, the total amount of iron stored increases due to the increasing size of both organs throughout the disease. Whether this iron entrapment is attributed to hepcidin dependent or independent mechanism could not be clearly answered but our data suggest that hepcidin played a minor role in our model. However, we did not analyze iron absorption from the diet, which could also be blocked in tumor-bearing mice and therefore account for the anemia.[176] Additionally, the increased iron demand for the aforementioned extramedullary erythropoiesis in the spleen might cause the reduced iron plasma levels because iron is required for erythropoiesis.[176] Thus, hypoferremia in anemic tumor-bearing Trp53^{flox}WapCre mice might be multifactorial.

6.4 Iron supplementation does not mitigate AC in Trp53^{flox}WapCre mice

Trp53^{flox}WapCre develop hypoferremia during the tumor progression and we analyzed if by supplementing with iron the anemia could be mitigated in tumor-bearing mice. We

intravenously injected anemic tumor-bearing mice with ferric carboxymaltose, that is proven to be safe and effective in humans and mice to treat several kind of anemias and replenish iron stores.[177,178] A single i.v. injection of 13.28 mg/kg of ferric carboxymaltose directly after tumor onset did not increase hemoglobin or hematocrit. Additionally, no increase of iron levels in serum or in organs was observed. However, the iron injection did also not increase tumor progression, which is currently a matter of debate if iron supplementation in anemic cancer patients promotes tumor growth or induces adverse events.[122] To exclude the possibility that i) we used an insufficient dosage of the iron or ii) supplemented iron was used up when tissues were harvested, we injected mice with a higher iron dose (20 mg/kg) on the day of tumor onset and harvested all tissues 15 days after the treatment. We observed a small increase in plasma iron levels but neither hematocrit nor hemoglobin levels increased. Although we cannot exclude that a different application strategy might restore normal blood values, our data suggest that iron deficiency was not the major reason for AC in our mouse model. To verify this conclusion, we injected iron intravenously into anemic tumor mice and analyzed medullar and splenic hematopoiesis 48 h post injection. A slightly increased proportion of late erythroid precursors in the spleen suggests that stress erythropoiesis is taking place and can be even boosted by the supplemented iron. However, iron supplementation has no effect on medullar hematopoiesis. This was further supported by the analyses of bone marrow smears that showed no morphological modifications which could suggest iron restricted erythropoiesis.[179] Additionally we did not observe microcytic and hypochromic circulating RBC, that are frequently observed during anemia caused by iron deficiency.[180] Finally, considering the aforementioned high baseline levels of iron in FVB mice, further supports our conclusion that iron is not the limiting factor in our model.

In conclusion, hypoferremia in our model seems to play a secondary role on the AC in our mouse model and therefore iron supplementation was not able to mitigate the anemia.

6.5 Impaired medullary hematopoiesis in Trp53^{flox}WapCre mice is partially compensated by induced stress erythropoiesis in the spleen

Because iron was not the limiting factor that causes AC in our model, we further characterized erythropoiesis in anemic tumor-bearing Trp53^{flox}WapCre mice. In the study of the bone marrow

smears, we observed that erythroid progenitors were decreased and the proportion of myeloid precursors increased in anemic tumor mice. Because the cellularity of the bone marrow did not change, these results suggest that erythropoiesis is inhibited in bone marrow whereas myelopoiesis is boosted. This fact correlates with other studies of anemia of inflamation.[181,139,182] Despite the difference in the proportion, the precursor morphology of any of the erythropoietic lineages was not changed.

As the late stages of the medullar erythroid maturation are reported to be impaired in mice with anemia of chronic inflamation[139] we studied if the blockade of the late erythropoiesis could contribute to the anemia in our model. The proportion of $Ter119^+$ cells, i.e. late erythroid precursors, was reduced in bone marrow whereas the proportion of $CD45/GR1^+$, i.e. leukocyte progenitors, was increased. The relative proportion of the different stages of late erythroid maturation, i.e. from proerythroblasts to mature blood cells, in bone marrow did not differ between tumor free and tumor-bearing mice, suggesting that late medullar erythropoiesis is not blocked in tumor-bearing $Trp53^{flox}$WapCre mice (**Fig. 26**). In contrast to the bone marrow the spleen responded differently: We observed an increased cellularity and a prominent splenomegaly together with no changes in the proportion of late erythroid precursors ($Ter119^+$) or leukocyte precursors ($CD45/GR1^+$) (**Fig. 26**), indicating that both, myelopoiesis as well as erythropoiesis are increased in the spleen to a similar extent. However, the relative cell proportion within the erythroid linage was increased at all stages of erythroid maturation from proerythroblasts to reticulocytes but not at the mature red blood cell stage (**Fig. 26**). These data suggest that anemic tumor mice responded with splenic stress hematopoiesis, which is a fact frequently observed in murines when hematopoiesis is accelerated under pathologic conditions,[183,184] and it has been also reported in other mouse models of AC.[185,128]

These results suggest that in bone marrow late erythropoiesis is not impaired but a reduced number of late erythroid precursors is present, whereas in the spleen the late erythropoiesis is boosted due to stress erythropoiesis.

Figure 26

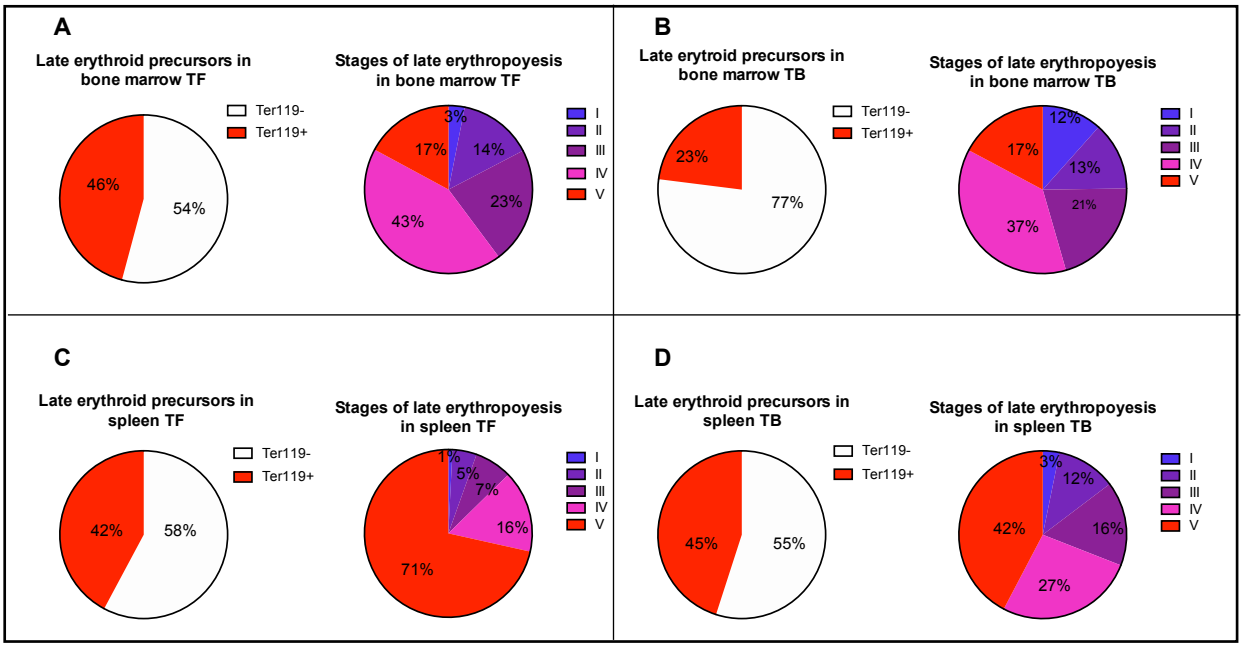

Fig. 26. Representation of the erythropoiesis in bone marrow and spleen of Trp53^{flox}WapCre mice
Shown are Ter119+(red) and Ter119- (white) cells as well as the five stages (I: proerythroblasts, II: basophilic erythroblasts, III: polychromatic erythroblasts, IV: orthochromatic erythroblasts and reticulocytes and V: mature RBC) of late erythroid maturation in (A) bone marrow of tumor free mice, (B) bone marrow of tumor-bearing mice as well as (C) spleen of tumor free mice and (D) spleen of tumor-bearing mice. The scheme visualizes the that the ratio between Ter119 positive and negative cells changes in the bone marrow but not in the spleen of anemic tumor-bearing mice. In contrast, the proportion of the five erythrocyte maturation stages does not change in in the bone marrow but in the spleen of anemic tumor-bearing mice.

In order to investigate why the number of late erythroid precursors in bone marrow was reduced, we analyzed the early stages of the erythropoiesis. The frequency of early hematopoietic precursors, namely hematopoietic stem cells (HSC) or in the multipotent progenitors (MPP) did not differ between tumor free and anemic tumor-bearing mice, suggesting that the stem cell compartment was not impaired **(Fig. 27).** The increased proportion of pre-granulocyte-monocyte lineage cells (pre-GM) and the decreased proportion of pre-megakaryocyte-erythrocyte progenitors (Pre MgE) **(Fig. 27)** suggest that hematopoietic cells are more committed to the generation of granulocytic cells at expenses of the erythropoietic precursors production. The reduced proportion of colony forming units erythrocyte (CFUe) **(Fig. 27)**, which are hematopoietic precursors restricted to the red blood cell production, further supported these findings.

Figure 27

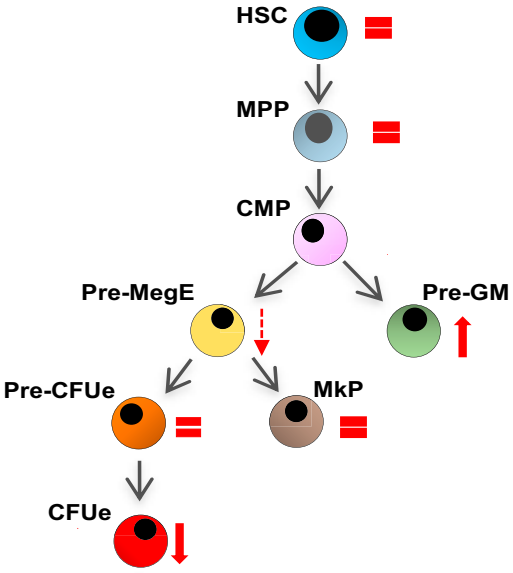

Fig. 27. Schematic representations of alteration in the hematopoietic tree in anemic tumor mice.
Shown is the hematopoietic tree with symbols indicating the changes in tumor-bearing anemic mice: no change visualized by equal symbol, increased proportion visualized by red ascending arrow, decreased proportion visualized by red descending arrow or a decreasing trend visualized by red, dotted descending arrow. Proportion of both pre-megakaryocyte-erythrocyte (Pre MgE) and colony forming units erythrocyte (CFU) are decreased, proportion of pre-granulocyte-monocyte progenitors (Pre-GM), which give rise to granulocytes are increased. Hematopoietic stem cells (HSC), multipotent progenitor (MPP), pre-colony forming units erythrocyte (Pre-CFUe), megakaryocyte progenitors (Mkp).

In summary, we found evidence that the reduced number of bone marrow born erythroid cells is a consequence of a shift during early hematopoiesis, where the fate of precursors shifts from erythroid to myeloid (granulocytes) fate. The decreased erythrocyte production in bone marrow of anemic Trp53^{flox}WapCre mice is partially compensated by a prominent extramedullary hematopoiesis in the spleen, that, however, is not sufficient to fully compensate the impaired RBC production**.** In contrast, myelopoiesis boosted in both hematopoietic organs, causing the increase of the granulocytic cells output.

6.6 Secretion of cytokines by the tumor might stimulate the myelopoiesis in bone marrow and prevent erythropoiesis in Trp53^{flox}WapCre mice

Induced granulocytosis in anemic Trp53^{flox}WapCre mice is also frequently observed in humans patients with different types of cancer[186,187,188,189] (including breast carcinomas[190,182]) and associates with a poor prognosis.[191] Similarly also tumor mouse models respond with induced

myeloid response.[192,193,145,194] This myeloid response produce the increase of tumor-associated myeloid cells (TAMC), including myeloid-derived suppressor cells (MDSCs), neutrophils, and macrophages which promote cancer progression[195,196] through different mechanisms: modulate adaptive immune responses against tumors[197,198], enhance cancer cell stemness,[199] and support angiogenesis, invasion, and metastasis.[200,197,201]

The concentration of some cytokines produced by the tumor or inflammatory cells correlates with the severity of the anemia in chronic disease states[202,203] as well as with the induced myeloid expansion. For example, in murine 4T1 breast tumor-bearing mice, it has been shown that some colony-stimulating factors (G-CSF, GM-CSF, M-CSF) produced by the tumor, caused a leukemoid reaction, i.e. a very severe stimulation of the leukocyte production, in bone marrow and spleen and thus blocking medullar erythropoiesis.[128,182] We analyzed the gene expression of granulocyte-macrophage colony stimulating factor (GM-CSF) and granulocyte-colony stimulating factor (G-CSF) and indeed we found mRNA of both factors was detected in tumor tissue of anemic tumor-bearing Trp53^{flox}WapCre mice but not in heathy mammary gland tissue. G-CSF is the primary extracellular regulator of the granulopoiesis,[204] and GM-CSF has been reported to synergistically act with G-CSF to enhance the granulopoyesis.[205] Additionally, it has been shown that G-CSF can mobilize HSC from the bone marrow which accumulate in the spleen, serving as the precursors for the extramedullary hematopoiesis.[206]

The expression of the stem cell factor (SCF), which is an essential regulator of the erythropoiesis which acts coordinately with Epo to maintain and stimulate erythropoiesis,[207] was reduced in the bone marrow, whereas in the spleen was not modified. Its expression is downregulated by proinflammatory cytokines like IL-6 and IL-1β.

Some cytokines produce its inhibitory effect on the erythropoiesis through the suppressor of cytokine signaling-3 (SOCS-3),[25] which mediates inhibition of Epo-R signaling[62] and also SCF expression.[25] SOCS-3 mRNA expression was also higher in bone marrow of anemic tumor-bearing mice than in tumor free mice. In contrast, SOCS-3 mRNA was not increased in the spleen, another possible explanation why spleen was able increase production of RBC and bone marrow not.

Therefore, we assume that cytokines and not iron deficiency causes the inhibition of the medullar erythropoiesis due to the inhibition of Epo downstream signaling, the suppression of SCF expression and the shift on the hematopoietic progenitors towards a granulocytic fate **(Fig. 28).**

Figure 28

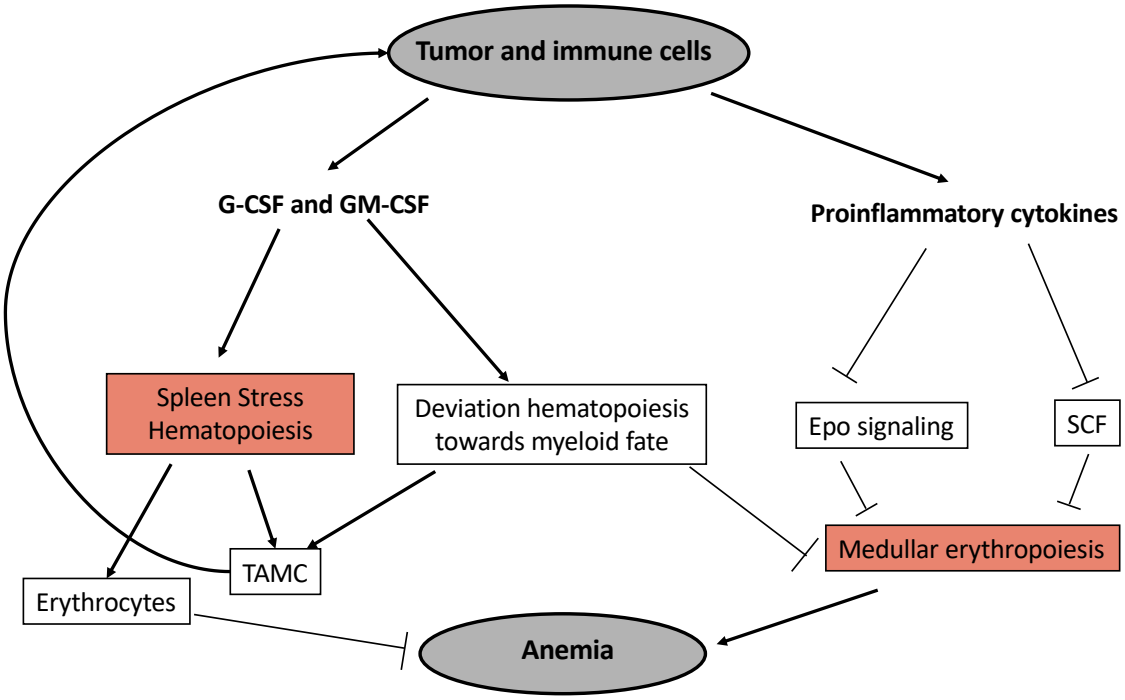

Fig. 28: Pathogenesis of AC in Trp53^{flox}WapCre mice
Tumor cells and immune cells of the tumor microenvironment secrete cytokines which inhibit erythropoiesis through the inhibition of Epo signaling and the downregulation of stem cell factor (SCF) expression. Additionally, tumor and inflammatory cells produce granulocyte-colony stimulating factor (G-CSF) and granulocyte-macrophage colony stimulating factor (GM-CSF) which promote stress hematopoiesis in the spleen, which in one hand partially palliates the anemia but also contribute to the production of tumor associated myeloid cells (TAMC). Additionally, G-CSF and GM-CSF act on the bone marrow promoting the shift of the hematopoiesis towards the production of TAMC at expenses of the erythropoiesis. TAMC contribute to the cancer progression and to the disease perpetuation.

7. Conclusion and outlook

In conclusion, we showed that tumor-bearing Trp53^{flox}WapCre mice develop anemia, which could neither be corrected by Epo treatment nor by iron supplementation as monotherapy (although mice developed hypoferremia). Hypoferremia might be caused by cytokines like IL-6 or IL-1β but because iron might not be limiting erythropoiesis, hypoferremia has only a secondary role in AC in our mouse model. Thus, we conclude that inflammation and cytokines suppress erythropoiesis independently of iron in tumor-bearing Trp53^{flox}WapCre mice. We found evidence for two potential pathways of cytokine mediated suppression of medullar erythropoiesis: i) proinflammatory cytokines such IL-6 and IL-1β seem to inhibit EpoR downstream signaling and SCF expression, e.g. by increasing the mRNA expression of EpoR signaling suppressor SOCS-3. ii) Proinflammatory cytokines such G-CSF and GM-CSF seem to change the differentiation of hematopoietic progenitors by shifting cell differentiation from erythroid linage to a granulocyte fate. Both pathways can explain why anemic tumor-bearing mice do not respond to Epo treatment, even when very high dosages were used.

To our knowledge, the Trp53^{flox}WapCre mouse model is the first one that mimics Epo non-responsiveness similar to human cancer patients and thus, could be a good candidate to analyze this particular type of AC with regard to cellular and molecular differences within the erythroid linage and potential anti-inflammatory treatment options.

Future experiments may involve the complete the characterization of this mouse model of AC. To have a more accurate picture of the inflammatory status of our tumor-bearing mice, the plasmatic concentration of some cytokines that might be involved in the medullar erythropoiesis inhibition need to be analyzed. Additionally, the lifespan of the circulating erythrocytes in our tumor mice should be measured, since it has been reported that inflammation might increase erythrocyte turnover,[148] and therefore, it may be a contributing factor to the AC pathogenesis in our model. Finally, recent studies about the role of splenic stress erythropoiesis on the shift of hematopoietic progenitors fate towards a myeloid fate have been published[128,195] and our mouse model might be a good candidate to study the crosstalk between spleen and bone marrow in AC.

8. References

1. Ludwig, H. *et al.* The European Cancer Anaemia Survey (ECAS): A large, multinational, prospective survey defining the prevalence, incidence, and treatment of anaemia in cancer patients. *Eur. J. Cancer* **40**, 2293–2306 (2004).
2. Tas, F. *et al.* Anemia in oncology practice: relation to diseases and their therapies. *Am. J. Clin. Oncol.* **25**, 371–9 (2002).
3. Knight, K., Wade, S. & Balducci, L. Prevalence and outcomes of anemia in cancer: a systematic review of the literature. *Am. J. Med.* **116**, 11–26 (2004).
4. Birgegård, G. *et al.* Cancer-Related Anemia: Pathogenesis, Prevalence and Treatment. *Oncology* **68**, 3–11 (2005).
5. Dunn, A., Carter, J. & Carter, H. Anemia at the end of life: prevalence, significance, and causes in patients receiving palliative care. *J. Pain Symptom Manage.* **26**, 1132–9 (2003).
6. Schwartz, R. N. Anemia in patients with cancer: Incidence, causes, impact, management, and use of treatment guidelines and protocols. *Am. J. Heal. Pharm.* **64**, S5–S13 (2007).
7. Caro, J. J., Salas, M., Ward, A. & Goss, G. Anemia as an independent prognostic factor for survival in patients with cancer: a systemic, quantitative review. *Cancer* **91**, 2214–21 (2001).
8. Miller, A. H., Ancoli-Israel, S., Bower, J. E., Capuron, L. & Irwin, M. R. Neuroendocrine-immune mechanisms of behavioral comorbidities in patients with cancer. *J. Clin. Oncol.* **26**, 971–82 (2008).
9. Woodson, R. D. & Auerbach, S. Effect of increased oxygen affinity and anemia on cardiac output and its distribution. *J. Appl. Physiol.* **53**, 1299–1306 (2017).
10. Stasi, R., Abriani, L., Beccaglia, P., Terzoli, E. & Amadori, S. Cancer-related fatigue. *Cancer* **98**, 1786–1801 (2003).
11. Blackwell, K., Gascón, P., Sigounas, G. & Jolliffe, L. rHuEPO and improved treatment outcomes: potential modes of action. *Oncologist* **9 Suppl 5**, 41–7 (2004).
12. Glaser, C. M. *et al.* Impact of hemoglobin level and use of recombinant erythropoietin on efficacy of preoperative chemoradiation therapy for squamous cell carcinoma of the oral cavity and oropharynx. *Int. J. Radiat. Oncol. Biol. Phys.* **50**, 705–15 (2001).
13. Fuso, L. *et al.* Pretreatment serum hemoglobin level as a predictive factor of response to neoadjuvant chemotherapy in patients with locally advanced squamous cervical carcinoma: A preliminary report. *Gynecol. Oncol.* **99**, S187–S191 (2005).
14. Gaspar, B. L., Sharma, P. & Das, R. Anemia in malignancies: Pathogenetic and diagnostic considerations. *Hematology* **20**, 18–25 (2015).
15. Zhu, W. & Xu, B. Association of Pretreatment Anemia with Pathological Response and Survival of Breast Cancer Patients Treated with Neoadjuvant Chemotherapy: A Population-Based Study. *PLoS One* **10**, e0136268 (2015).
16. Hattangadi, S. M., Wong, P., Zhang, L., Flygare, J. & Lodish, H. F. From stem cell to red cell: regulation of erythropoiesis at multiple levels by multiple proteins, RNAs, and chromatin modifications. *Blood* **118**, 6258–68 (2011).
17. Zhang, Y. *et al.* Impact of preoperative anemia on relapse and survival in breast cancer patients. *BMC Cancer* **14**, 844 (2014).
18. Höckel, M. & Vaupel, P. Biological consequences of tumor hypoxia. *Semin. Oncol.* **28**, 36–41 (2001).
19. Busti, F., Marchi, G., Ugolini, S., Castagna, A. & Girelli, D. Anemia and Iron Deficiency in Cancer Patients: Role of Iron Replacement Therapy. *Pharmaceuticals (Basel).* **11**, (2018).
20. Goodnough, L. T. Risks of Blood Transfusion. *Anesthesiol. Clin. North America* **23**, 241–252 (2005).
21. Yasuda, Y. *et al.* Erythropoietin regulates tumour growth of human malignancies. *Carcinogenesis* **24**, 1021–1029 (2003).
22. Adamson, J. W. The Anemia of Inflammation/Malignancy: Mechanisms and Management. *Hematology* **2008**, 159–165 (2008).
23. Weiss, G. & Goodnough, L. T. Anemia of Chronic Disease. *N. Engl. J. Med.* **352**, 1011–1023 (2005).

24. Madeddu, C. *et al.* Pathogenesis and Treatment Options of Cancer Related Anemia: Perspective for a Targeted Mechanism-Based Approach. *Front. Physiol.* **9**, 1294 (2018).
25. Spivak, J. L. The anaemia of cancer: Death by a thousand cuts. *Nat. Rev. Cancer* **5**, 543–555 (2005).
26. Reiner, A. P. & Spivak, J. L. Hematophagic histiocytosis. A report of 23 new patients and a review of the literature. *Medicine (Baltimore).* **67**, 369–88 (1988).
27. Gozzelino, R. & Arosio, P. The importance of iron in pathophysiologic conditions. *Front. Pharmacol.* **6**, 26 (2015).
28. Zhang, C. Essential functions of iron-requiring proteins in DNA replication, repair and cell cycle control. *Protein Cell* **5**, 750–760 (2014).
29. Andrews, N. C. & Schmidt, P. J. Iron Homeostasis. *Annu. Rev. Physiol.* **69**, 69–85 (2007).
30. Nemeth, E. & Ganz, T. The Role of Hepcidin in Iron Metabolism. *Acta Haematol.* **122**, 78 (2009).
31. Weiss, G. Iron metabolism in the anemia of chronic disease. *Biochimica et Biophysica Acta - General Subjects* (2009). doi:10.1016/j.bbagen.2008.08.006
32. Nemeth, E. *et al.* IL-6 mediates hypoferremia of inflammation by inducing the synthesis of the iron regulatory hormone hepcidin. *J. Clin. Invest.* **113**, 1271–1276 (2004).
33. Muckenthaler, M. U. *et al.* A Red Carpet for Iron Metabolism. **168**, 344–361 (2017).
34. Nemeth, E. *et al.* Hepcidin Regulates Cellular Iron Efflux by Binding to Ferroportin and Inducing Its Internalization. *Science (80-.).* **306**, 2090–2093 (2004).
35. Ganz, T. & Nemeth, E. Hepcidin and iron homeostasis. *Biochim. Biophys. Acta - Mol. Cell Res.* **1823**, 1434–43 (2012).
36. Kautz, L., Jung, G., Nemeth, E. & Ganz, T. Erythroferrone contributes to recovery from anemia of inflammation. *Blood* **124**, 2569–74 (2014).
37. Theurl, I. *et al.* Dysregulated monocyte iron homeostasis and erythropoietin formation in patients with anemia of chronic disease. *Blood* **107**, 4142–4148 (2006).
38. Atkinson, S. H. *et al.* Tumor necrosis factor SNP haplotypes are associated with iron deficiency anemia in West African children. *Blood* **112**, 4276–4283 (2008).
39. Nairz, M., Theurl, I., Swirski, F. K. & Weiss, G. *"Pumping iron"—how macrophages handle iron at the systemic, microenvironmental, and cellular levels*. **469**, 397–418 (Springer Berlin Heidelberg, 2017).
40. Ludwiczek, S., Aigner, E., Theurl, I. & Weiss, G. Cytokine-mediated regulation of iron transport in human monocytic cells. *Blood* **101**, 4148–4154 (2003).
41. Guida, C. *et al.* A novel inflammatory pathway mediating rapid hepcidin-independent hypoferremia. *Blood* **125**, 2265–2276 (2018).
42. Weiss, G., Ganz, T. & Goodnough, L. T. *Anemia of inflammation*. *Blood* **133**, (American Society of Hematology, 2019).
43. Zivot, A., Lipton, J. M., Narla, A. & Blanc, L. Erythropoiesis: insights into pathophysiology and treatments in 2017. *Molecular medicine (Cambridge, Mass.)* **24**, 11 (2018).
44. Orkin, S. H. Diversification of haematopoietic stem cells to specific lineages. *Nat. Rev. Genet.* **1**, 57–64 (2000).
45. Dzierzak, E. & Philipsen, S. Erythropoiesis: development and differentiation. *Cold Spring Harb. Perspect. Med.* **3**, 1–16 (2013).
46. Gregory, C. & Eaves, A. Human marrow cells capable of erythropoietic differentiation in vitro: definition of three erythroid colony responses. *Blood* **49**, (1977).
47. Granick, S. & Levere, R. D. Heme synthesis in erythroid cells. *Prog. Hematol.* **4**, 1–47 (1964).
48. Kondo, M., Weissman, I. L. & Akashi, K. Identification of clonogenic common lymphoid progenitors in mouse bone marrow. *Cell* **91**, 661–72 (1997).
49. Akashi, K., Traver, D., Miyamoto, T. & Weissman, I. L. A clonogenic common myeloid progenitor that gives rise to all myeloid lineages. *Nature* **404**, 193–197 (2000).
50. Manz, M. G., Miyamoto, T., Akashi, K. & Weissman, I. L. Prospective isolation of human clonogenic common myeloid progenitors. *Proc. Natl. Acad. Sci.* **99**, 11872–11877 (2002).
51. Adolfsson, J. *et al.* Identification of Flt3+ lympho-myeloid stem cells lacking erythro-megakaryocytic potential a revised road map for adult blood lineage commitment. *Cell* **121**, 295–306 (2005).

52. Metcalf, D. Hematopoietic regulators: redundancy or subtlety? *Blood* **82**, (1993).
53. Cazzola, M. *et al.* Defective iron supply for erythropoiesis and adequate endogenous erythropoietin production in the anemia associated with systemic-onset juvenile chronic arthritis. *Blood* **87**, 4824–30 (1996).
54. Koury, S. T., Bondurant, M. C., Koury, M. J. & Semenza, G. L. Localization of cells producing erythropoietin in murine liver by in situ hybridization. *Blood* **77**, 2497–503 (1991).
55. NAETS, J. P. The role of the kidney in erythropoiesis. *J. Clin. Invest.* **39**, 102–10 (1960).
56. Witthuhn, B. A. *et al.* JAK2 associates with the erythropoietin receptor and is tyrosine phosphorylated and activated following stimulation with erythropoietin. *Cell* **74**, 227–36 (1993).
57. Bianchi, R. *et al.* Erythropoietin both protects from and reverses experimental diabetic neuropathy. *Proc. Natl. Acad. Sci.* **101**, 823–828 (2004).
58. Calvillo, L. *et al.* Recombinant human erythropoietin protects the myocardium from ischemia-reperfusion injury and promotes beneficial remodeling. *Proc. Natl. Acad. Sci.* **100**, 4802–4806 (2003).
59. Jelkmann, W. Regulation of erythropoietin production. *J. Physiol.* **589**, 1251–1258 (2011).
60. La Ferla, K., Reinmann, C., Jelkmann, W. J. & Hellwig-Bürgel, T. Inhibition of erythropoietin gene expression signaling involves the transcription factors GATA-2 and NF-κB. *FASEB J.* **16**, 1811–1813 (2002).
61. Okonko, D. O., Marley, S. B., Anker, S. D., Poole-Wilson, P. A. & Gordon, M. Y. Erythropoietin resistance contributes to anaemia in chronic heart failure and relates to aberrant JAK–STAT signal transduction. *Int. J. Cardiol.* **164**, 359–364 (2013).
62. Carow, B., Rottenberg, M. E., Mattei, F. & Pucillo, C. SOCS3, a major regulator of infection and inflammation. (2014). doi:10.3389/fimmu.2014.00058
63. Buck, I., Morceau, F., Grigorakaki, C., Dicato, M. & Diederich, M. Linking anemia to inflammation and cancer: The crucial role of TNFα. *Biochem. Pharmacol.* **77**, 1572–1579 (2009).
64. Libregts, S. F. *et al.* Chronic IFN-γ production in mice induces anemia by reducing erythrocyte life span and inhibiting erythropoiesis through an IRF-1/PU.1 axis. *Blood* **118**, 2578–2588 (2011).
65. Pietras, E. M. *et al.* Chronic interleukin-1 drives haematopoietic stem cells towards precocious myeloid differentiation at the expense of self-renewal HHS Public Access. *Nat Cell Biol* **18**, 607–618 (2016).
66. Broudy, V. C. Re. nice. pd. Stem cell factor and hematopoiesis. *Blood* **90**, 1345–1364 (1997).
67. Linenberger, M. L. *et al.* Stem cell factor production by human marrow stromal fibroblasts. *Exp. Hematol.* **23**, 1104–14 (1995).
68. Williams, D. E. *et al.* Identification of a ligand for the c-kit proto-oncogene. *Cell* **63**, 167–74 (1990).
69. Flanagan, J. G. & Leder, P. The kit ligand: a cell surface molecule altered in steel mutant fibroblasts. *Cell* **63**, 185–94 (1990).
70. Broudy, V. C., Lin, N. L., Priestley, G. V, Nocka, K. & Wolf, N. S. Interaction of stem cell factor and its receptor c-kit mediates lodgment and acute expansion of hematopoietic cells in the murine spleen. *Blood* **88**, 75–81 (1996).
71. Tsiftsoglou, A. S., Vizirianakis, I. S. & Strouboulis, J. Erythropoiesis: Model systems, molecular regulators, and developmental programs. *IUBMB Life* **61**, 800–830 (2009).
72. Dos Santos, C. O. *et al.* An iron responsive element-like stem-loop regulates α-hemoglobin-stabilizing protein mRNA. *J. Biol. Chem.* **283**, 26956–26964 (2008).
73. Macciò, A. *et al.* High Serum Levels of Soluble IL-2 Receptor, Cytokines, and C Reactive Protein Correlate with Impairment of T Cell Response in Patients with Advanced Epithelial Ovarian Cancer. *Gynecol. Oncol.* **69**, 248–252 (1998).
74. Ladányi, A. *et al.* T-cell activation marker expression on tumor-infiltrating lymphocytes as prognostic factor in cutaneous malignant melanoma. *Clin. Cancer Res.* **10**, 521–30 (2004).
75. Seymour, J. F., Talpaz, M., Cabanillas, F., Wetzler, M. & Kurzrock, R. Serum interleukin-6 levels correlate with prognosis in diffuse large-cell lymphoma. *J. Clin. Oncol.* **13**, 575–582 (1995).

76. Kurzrock, R. The role of cytokines in cancer-related fatigue. *Cancer* **92**, 1684–1688 (2001).
77. Petruzzelli, M. & Wagner, E. F. Mechanisms of metabolic dysfunction in cancer-associated cachexia. *Genes Dev.* **30**, 489–501 (2016).
78. Rodgers, G. M. *et al. NCCN Guidelines Version 2.2018 Panel Members Cancer-and Chemotherapy-Induced Anemia*. (2018).
79. Chaturvedi, S. & Savona, M. R. *Cancer-related anemia. Hospital Physician Hematology Board Review Manual* **10**, (2014).
80. Toy, P. *et al.* Transfusion-related acute lung injury: definition and review. *Crit. Care Med.* **33**, 721–6 (2005).
81. Vincent, J. L. *et al.* Anemia and blood transfusion in critically ill patients. *JAMA* **288**, 1499–507 (2002).
82. Vamvakas, E. C. Deleterious clinical effects of transfusion-associated immunomodulation: fact or fiction? *Blood* **97**, 1180–1195 (2002).
83. Tonia, T. *et al.* Erythropoietin or darbepoetin for patients with cancer. *Cochrane Database Syst. Rev.* **12**, CD003407 (2012).
84. Seidenfeld, J. *et al.* Epoetin treatment of anemia associated with cancer therapy: a systematic review and meta-analysis of controlled clinical trials. *J. Natl. Cancer Inst.* **93**, 1204–14 (2001).
85. Bohlius, J. *et al.* Erythropoietin for patients with malignant disease. in *The Cochrane Database of Systematic Reviews* (ed. Bohlius, J.) CD003407 (John Wiley & Sons, Ltd, 2004). doi:10.1002/14651858.CD003407.pub2
86. Auerbach, M. *et al.* Intravenous Iron Optimizes the Response to Recombinant Human Erythropoietin in Cancer Patients With Chemotherapy-Related Anemia: A Multicenter, Open-Label, Randomized Trial. *J. Clin. Oncol.* **22**, 1301–1307 (2004).
87. Pedrazzoli, P. *et al.* Randomized Trial of Intravenous Iron Supplementation in Patients With Chemotherapy-Related Anemia Without Iron Deficiency Treated With Darbepoetin Alfa. *J. Clin. Oncol.* **26**, 1619–1625 (2008).
88. Rodgers, G. M. A perspective on the evolution of management of cancer- and chemotherapy-induced anemia. *J. Natl. Compr. Canc. Netw.* **10**, 434–7 (2012).
89. Rizzo, J. D. *et al.* American Society of Clinical Oncology/American Society of Hematology Clinical Practice Guideline Update on the Use of Epoetin and Darbepoetin in Adult Patients With Cancer. *J. Oncol. Pract.* **6**, 317–320 (2010).
90. Nekoui, A. & Blaise, G. Erythropoietin and Nonhematopoietic Effects. *Am. J. Med. Sci.* **353**, 76–81 (2017).
91. Bohlius, J., Weingart, O., Trelle, S. & Engert, A. Cancer-related anemia and recombinant human erythropoietin—an updated overview. *Nat. Clin. Pract. Oncol.* **3**, 152–164 (2006).
92. Storring, P. L. *et al.* Epoetin alfa and beta differ in their erythropoietin isoform compositions and biological properties. *Br. J. Haematol.* **100**, 79–89 (1998).
93. Newland, A. M. & Black, C. D. Tumor Progression Associated with Erythropoiesis-Stimulating Agents. *Ann. Pharmacother.* **42**, 1865–1870 (2008).
94. Pfeffer, M. A. *et al.* A Trial of Darbepoetin Alfa in Type 2 Diabetes and Chronic Kidney Disease. *N. Engl. J. Med.* **361**, 2019–2032 (2009).
95. Bohlius, J. *et al.* Erythropoietin or Darbepoetin for patients with cancer - meta-analysis based on individual patient data. *Cochrane Database Syst. Rev.* CD007303 (2009). doi:10.1002/14651858.CD007303.pub2
96. Wright, J. R. *et al.* Randomized, Double-Blind, Placebo-Controlled Trial of Erythropoietin in Non–Small-Cell Lung Cancer With Disease-Related Anemia. *J. Clin. Oncol.* **25**, 1027–1032 (2007).
97. Bennett, C. L. *et al.* Venous Thromboembolism and Mortality Associated With Recombinant Erythropoietin and Darbepoetin Administration for the Treatment of Cancer-Associated Anemia. *JAMA* **299**, 914 (2008).
98. Smith, R. E. *et al.* Darbepoetin Alfa for the Treatment of Anemia in Patients With Active Cancer Not Receiving Chemotherapy or Radiotherapy: Results of a Phase III, Multicenter, Randomized, Double-Blind, Placebo-Controlled Study. *J. Clin. Oncol.* **26**, 1040–1050 (2008).
99. Aapro, M., Osterwalder, B., Scherhag, A. & Burger, H. U. Epoetin-β treatment in patients with cancer chemotherapy-induced anaemia: the impact of initial haemoglobin and target

haemoglobin levels on survival, tumour progression and thromboembolic events. *Br. J. Cancer* **101**, 1961–1971 (2009).
100. Spivak, J. L., Gascon, P. & Ludwig, H. Anemia Management in Oncology and Hematology. *Oncologist* **14**, 43–56 (2009).
101. Henke, M. *et al.* Erythropoietin to treat head and neck cancer patients with anaemia undergoing radiotherapy: randomised, double-blind, placebo-controlled trial. *Lancet* **362**, 1255–1260 (2003).
102. Juneja, V. *et al.* Continuing Reassessment of the Risks of Erythropoiesis-Stimulating Agents in Patients with Cancer. *Clin. Cancer Res.* **14**, 3242–3247 (2008).
103. Arcasoy, M. O. *et al.* Functional significance of erythropoietin receptor expression in breast cancer. *Lab. Invest.* **82**, 911–8 (2002).
104. Acs, G. *et al.* Hypoxia-inducible erythropoietin signaling in squamous dysplasia and squamous cell carcinoma of the uterine cervix and its potential role in cervical carcinogenesis and tumor progression. *Am. J. Pathol.* **162**, 1789–806 (2003).
105. Brown, W. M. *et al.* Erythropoietin Receptor Expression in Non-Small Cell Lung Carcinoma: A Question of Antibody Specificity. *Stem Cells* **25**, 718–722 (2006).
106. Henke, M. *et al.* Do Erythropoietin Receptors on Cancer Cells Explain Unexpected Clinical Findings? *J. Clin. Oncol.* **24**, 4708–4713 (2006).
107. Feldman, L. *et al.* Erythropoietin stimulates growth and STAT5 phosphorylation in human prostate epithelial and prostate cancer cells. *Prostate* **66**, 135–145 (2006).
108. Dunlop, E. A., Percy, M. J., Boland, M. P., Maxwell, A. P. & Lappin, T. R. Induction of Signalling in Non-Erythroid Cells by Pharmacological Levels of Erythropoietin. *Neurodegener. Dis.* **3**, 94–100 (2006).
109. Lester, R. D., Jo, M., Campana, W. M. & Gonias, S. L. Erythropoietin Promotes MCF-7 Breast Cancer Cell Migration by an ERK/Mitogen-activated Protein Kinase-dependent Pathway and Is Primarily Responsible for the Increase in Migration Observed in Hypoxia. *J. Biol. Chem.* **280**, 39273–39277 (2005).
110. Leyland-Jones, B. & BEST Investigators and Study Group. Breast cancer trial with erythropoietin terminated unexpectedly. *Lancet. Oncol.* **4**, 459–60 (2003).
111. Heeschen, C. *et al.* Erythropoietin is a potent physiologic stimulus for endothelial progenitor cell mobilization. *Blood* **102**, 1340–1346 (2003).
112. Aapro, M., Jelkmann, W., Constantinescu, S. N. & Leyland-Jones, B. Effects of erythropoietin receptors and erythropoiesis-stimulating agents on disease progression in cancer. *Br. J. Cancer* **106**, 1249–1258 (2012).
113. Gilreath, J. A., Stenehjem, D. D. & Rodgers, G. M. Diagnosis and treatment of cancer-related anemia. *Am. J. Hematol.* **89**, 203–212 (2014).
114. Rodgers, G. M. *et al.* Cancer- and chemotherapy-induced anemia. *J. Natl. Compr. Canc. Netw.* **10**, 628–53 (2012).
115. Auerbach, M. *et al.* Darbepoetin alfa 300 or 500 µg once every 3 weeks with or without intravenous Iron in patients with chemotherapy-induced anemia. *Am. J. Hematol.* **85**, 655–663 (2010).
116. Bastit, L. *et al.* Randomized, Multicenter, Controlled Trial Comparing the Efficacy and Safety of Darbepoetin Alfa Administered Every 3 Weeks With or Without Intravenous Iron in Patients With Chemotherapy-Induced Anemia. *J. Clin. Oncol.* **26**, 1611–1618 (2008).
117. Hedenus, M. *et al.* Addition of intravenous iron to epoetin beta increases hemoglobin response and decreases epoetin dose requirement in anemic patients with lymphoproliferative malignancies: a randomized multicenter study. *Leukemia* **21**, 627–632 (2007).
118. Steinmetz, T. *et al.* Clinical experience with ferric carboxymaltose in the treatment of cancer- and chemotherapy-associated anaemia. *Ann. Oncol.* **24**, 475–482 (2013).
119. Steensma, D. P. *et al.* Phase III, Randomized Study of the Effects of Parenteral Iron, Oral Iron, or No Iron Supplementation on the Erythropoietic Response to Darbepoetin Alfa for Patients With Chemotherapy-Associated Anemia. *J. Clin. Oncol.* **29**, 97–105 (2011).
120. Silverstein, S. B. & Rodgers, G. M. Parenteral iron therapy options. *Am. J. Hematol.* **76**, 74–78 (2004).
121. Litton, E., Xiao, J. & Ho, K. M. Safety and efficacy of intravenous iron therapy in reducing

requirement for allogeneic blood transfusion: systematic review and meta-analysis of randomised clinical trials. *BMJ* **347**, f4822–f4822 (2013).
122. Torti, S. V & Torti, F. M. Iron and cancer: more ore to be mined. doi:10.1038/nrc3495
123. Weinberg, E. D. The role of iron in cancer. *Eur. J. Cancer Prev.* **5**, 19–36 (1996).
124. Glaspy, J. *et al.* Impact of therapy with epoetin alfa on clinical outcomes in patients with nonmyeloid malignancies during cancer chemotherapy in community oncology practice. Procrit Study Group. *J. Clin. Oncol.* **15**, 1218–1234 (1997).
125. Kim, A. *et al.* Mouse Models of Anemia of Cancer. *PLoS One* **9**, e93283 (2014).
126. Noguchi-Sasaki, M., Sasaki, Y., Shimonaka, Y., Mori, K. & Fujimoto-Ouchi, K. Treatment with anti-IL-6 receptor antibody prevented increase in serum hepcidin levels and improved anemia in mice inoculated with IL-6–producing lung carcinoma cells. *BMC Cancer* **16**, 270 (2016).
127. Mori, K. *et al.* Novel models of cancer-related anemia in mice inoculated with IL-6-producing tumor cells. *Biomed. Res.* **30**, 47–51 (2009).
128. Liu, M. *et al.* Macrophages support splenic erythropoiesis in 4T1 tumor-bearing mice. *PLoS One* **10**, 1–16 (2015).
129. Derksen, P. W. B. *et al.* Mammary-specific inactivation of E-cadherin and p53 impairs functional gland development and leads to pleomorphic invasive lobular carcinoma in mice. *Dis. Model. Mech.* **4**, 347–358 (2011).
130. Coles, C. *et al.* p53 mutations in breast cancer. *Cancer Res.* **52**, 5291–8 (1992).
131. Zhang, Y. *et al.* Establishment of a murine breast tumor model by subcutaneous or orthotopic implantation. *Oncol. Lett.* **15**, 6233–6240 (2018).
132. Ganzoni, A. M. [Intravenous iron-dextran: therapeutic and experimental possibilities]. *Schweiz. Med. Wochenschr.* **100**, 301–3 (1970).
133. Rozen, S. & Skaletsky, H. Primer3 on the WWW for general users and for biologist programmers. *Methods Mol. Biol.* **132**, 365–86 (2000).
134. Livak, K. J. & Schmittgen, T. D. Analysis of Relative Gene Expression Data Using Real-Time Quantitative PCR and the 2−ΔΔCT Method. *Methods* **25**, 402–408 (2001).
135. Torrence JD, B. T. Tissue iron stores. in *Ed. Methods in Hematology.* (ed. Cook, J.) 104-109. (Churchill Livingston Press, 1980).
136. Reagan, W. J. *et al.* Best Practices for Evaluation of Bone Marrow in Nonclinical Toxicity Studies. doi:10.1177/0192623310396907
137. Chen, K. *et al.* Resolving the distinct stages in erythroid differentiation based on dynamic changes in membrane protein expression during erythropoiesis. *Proc. Natl. Acad. Sci. U. S. A.* **106**, 17413–8 (2009).
138. Chen, K. *et al.* Resolving the distinct stages in erythroid differentiation based on dynamic changes in membrane protein expression during erythropoiesis.
139. Prince, O. D. *et al.* Late stage erythroid precursor production is impaired in mice with chronic inflammation. *Haematologica* **97**, 1648–56 (2012).
140. Pronk, C. J. H. *et al.* Elucidation of the Phenotypic, Functional, and Molecular Topography of a Myeloerythroid Progenitor Cell Hierarchy. *Cell Stem Cell* **1**, 428–442 (2007).
141. *GraphPad Statistics Guide*. (1995).
142. What is the meaning of * or ** or *** in reports of statistical significance from Prism or InStat? - FAQ 978 - GraphPad. Available at: https://www.graphpad.com/support/faq/what-is-the-meaning-of--or--or--in-reports-of-statistical-significance-from-prism-or-instat/. (Accessed: 14th March 2019)
143. Andersson, L. C., von Willebrand, E., Jokinen, M., Karhi, K. K. & Gahmberg, C. G. Glycophorin A as an Erythroid Marker in Normal and Malignant Hematopoiesis. in 338–342 (Springer, Berlin, Heidelberg, 1981). doi:10.1007/978-3-642-67984-1_60
144. Singh, R. P. *et al.* HIF prolyl hydroxylase 2 (PHD2) is a critical regulator of hematopoietic stem cell maintenance during steady-state and stress. (2013). doi:10.1182/blood-2012-12-471185
145. Mac Manus, M. P., Elder, G. E., Abram, W. P. & Bridges, J. M. Effect of recombinant human erythropoietin on anemia caused by a murine mammary carcinoma. *Exp. Hematol.* **18**, 848–52 (1990).

146. Jain, S., Gautam, V. & Naseem, S. Acute-phase proteins: As diagnostic tool. *J. Pharm. Bioallied Sci.* **3**, 118–27 (2011).
147. Babitt, J. L. & Lin, H. Y. Mechanisms of anemia in CKD. *J. Am. Soc. Nephrol.* **23**, 1631–4 (2012).
148. Kim, A. *et al.* A mouse model of anemia of inflammation: complex pathogenesis with partial dependence on hepcidin. *Blood* **123**, 1129–36 (2014).
149. Cooper, A. C., Mikhail, A., Lethbridge, M. W., Kemeny, D. M. & Macdougall, I. C. Increased expression of erythropoiesis inhibiting cytokines (IFN-gamma, TNF-alpha, IL-10, and IL-13) by T cells in patients exhibiting a poor response to erythropoietin therapy. *J. Am. Soc. Nephrol.* **14**, 1776–84 (2003).
150. Ludwig, H. *et al.* Prediction of response to erythropoietin treatment in chronic anemia of cancer. *Blood* **84**, 1056–1063 (1994).
151. Goodnough, L. T., Skikne, B. & Brugnara, C. Review article Erythropoietin , iron , and erythropoiesis. *Hematology* **96**, 823–833 (2000).
152. Wallerstein, R. O. Laboratory evaluation of anemia. *West. J. Med.* **146**, 443–51 (1987).
153. Nagao, T. & Hirokawa, M. Diagnosis and treatment of macrocytic anemias in adults. *J. Gen. Fam. Med.* **18**, 200–204 (2017).
154. Green, R. & Dwyre, D. M. Evaluation of Macrocytic Anemias. *Semin. Hematol.* **52**, 279–286 (2015).
155. Langdon, J. M. *et al.* Hepcidin-dependent and hepcidin-independent regulation of erythropoiesis in a mouse model of anemia of chronic inflammation. *Am. J. Hematol* **89**, 470–479 (2014).
156. Maccio, A. *et al.* Hemoglobin levels correlate with interleukin-6 levels in patients with advanced untreated epithelial ovarian cancer : role of inflammation in cancer-related anemia. **106**, 362–368 (2018).
157. Pisa, P., Stenke, L., Bernell, P., Hansson, M. & Hast, R. Tumor necrosis factor-alpha and interferon-gamma in serum of multiple myeloma patients. *Anticancer Res.* **10**, 817–20
158. Wrighting, D. M. & Andrews, N. C. Interleukin-6 induces hepcidin expression through STAT3. *Blood* **108**, 3204–3209 (2006).
159. Poggiali, E., Migone De Amicis, M. & Motta, I. Anemia of chronic disease: A unique defect of iron recycling for many different chronic diseases. *European Journal of Internal Medicine* (2014). doi:10.1016/j.ejim.2013.07.011
160. Wang, W., Knovich, M. A., Coffman, L. G., Torti, F. M. & Torti, S. V. Serum ferritin: Past, present and future. *Biochim. Biophys. Acta* **1800**, 760–9 (2010).
161. Ludwig, U. H. Iron metabolism and iron supplementation in cancer patients. doi:10.1007/s00508-015-0842-3
162. Gassmann, M. & Muckenthaler, M. U. Adaptation of iron requirement to hypoxic conditions at high altitude. **119**, 1432–1440 (2015).
163. Willemetz, A. *et al.* Iron- and Hepcidin-Independent Downregulation of the Iron Exporter Ferroportin in Macrophages during Salmonella Infection. *Front. Immunol.* **8**, 498 (2017).
164. Ganz, T. Hepcidin and iron regulation , 10 years later. **117**, 4425–4433 (2018).
165. Nutrition, N. R. C. (US) S. on L. A. *Nutrient Requirements of Laboratory Animals*. *Nutrient Requirements of Laboratory Animals: Fourth Revised Edition, 1995* (National Academies Press (US), 1995). doi:10.17226/4758
166. Ganz, T. Erythropoietic regulators of iron metabolism. *Free Radic. Biol. Med.* (2018). doi:10.1016/J.FREERADBIOMED.2018.07.003
167. Foot, N. J., Gembus, K. M., Mackenzie, K. & Kumar, S. Ndfip2 is a potential regulator of the iron transporter DMT1 in the liver. *Sci. Rep.* **6**, 24045 (2016).
168. Fleming, R. E. *et al.* Mouse strain differences determine severity of iron accumulation in Hfe knockout model of hereditary hemochromatosis. *Proc. Natl. Acad. Sci. U. S. A.* **98**, 2707–11 (2001).
169. Spasic, M. V. *et al.* Physiologic systemic iron metabolism in mice deficient for duodenal Hfe. **109**, 4511–4517 (2007).
170. Ward, D. & Kaplan, J. Ferroportin-mediated iron transport : expression and regulation. **1823**, 1426–1433 (2013).

171. Torti, F. M. & Torti, S. V. *Regulation of ferritin genes and protein*. (2002).
172. Nemeth, E. & Ganz, T. Anemia of inflammation. *Hematology/Oncology Clinics of North America* (2014). doi:10.1016/j.hoc.2014.04.005
173. Mcknight, G. S., Lee, D. C., Hemmaplardh, D., Finch, C. A. & Palmiter$, R. D. *Transferrin Gene Expression EFFECTS OF NUTRITIONAL IRON DEFICIENCY*. THE JOURNAL OF BIOLOGICAL CHEMISTRY* **255**, (1980).
174. Rishi, G. & Subramaniam, V. N. The relationship between systemic iron homeostasis and erythropoiesis. *Biosci. Rep.* **37**, (2017).
175. Cotner, T., Gupta, A. D., Papayannopoulou, T. & Stamatoyannopoulos, G. Characterization of a novel form of transferrin receptor preferentially expressed on normal erythroid progenitors and precursors. *Blood* **73**, 214–21 (1989).
176. Finch, C. Regulators of iron balance in humans. *Blood* **84**, 1697–702 (1994).
177. Keating, G. M. Ferric Carboxymaltose: A Review of Its Use in Iron Deficiency. *Drugs* **75**, 101–127 (2015).
178. Lofruthe, N. *et al.* Intravenous Iron Carboxymaltose as a Potential Therapeutic in Anemia of Inflammation. *PLoS One* **11**, e0158599 (2016).
179. Greer, J. P. *Wintrobe's clinical hematology*.
180. Buttarello, M. Laboratory diagnosis of anemia: are the old and new red cell parameters useful in classification and treatment, how? *Int. J. Lab. Hematol.* **38**, 123–132 (2016).
181. Reissmann, K. R. & Udupa, K. B. Effect of inflammation on erythroid precursors (BFU-E and CFU-E) in bone marrow and spleen of mice. *J. Lab. Clin. Med.* **92**, 22–9 (1978).
182. Sally, A. & Jr, K. W. H. Murine mammary carcinoma 4T1 induces a leukemoid reaction with splenomegaly : Association with tumor-derived growth factors. **82**, 12–24 (2007).
183. Millot, S. *et al.* Erythropoietin stimulates spleen BMP4-dependent stress erythropoiesis and partially corrects anemia in a Mouse model of generalized inflammation. *Blood* **116**, 6072–6081 (2010).
184. Lenox, L. E., Perry, J. M. & Paulson, R. F. BMP4 and Madh5 regulate the erythroid response to acute anemia. *Blood* **105**, 2741–2748 (2005).
185. Sio, A. *et al.* Dysregulated Hematopoiesis Caused by Mammary Cancer Is Associated with Epigenetic Changes and Hox Gene Expression in Hematopoietic Cells. *Cancer Res.* **73**, 5892–5904 (2013).
186. Melhem, M. F. *et al.* Cytokines in inflammatory malignant fibrous histiocytoma presenting with leukemoid reaction. *Blood* **82**, 2038–44 (1993).
187. Matsumoto, M., Yazawa, Y. & Kanzaki, M. An autopsy case of liposarcoma with granulocytic leukemoid reaction. *Acta Pathol. Jpn.* **26**, 399–408 (1976).
188. Zhou, W., He, H., Zhang, Z. & Ge, J. Leukemoid reaction associated with transitional cell carcinoma: A case report and literature review. *Niger. J. Clin. Pract.* **17**, 391 (2014).
189. Schniewind, B. *et al.* Paraneoplastic leukemoid reaction and rapid progression in a patient with malignant melanoma: establishment of KT293, a novel G-CSF-secreting melanoma cell line. *Cancer Biol. Ther.* **4**, 23–7 (2005).
190. Tabuchi, T., Ubukata, H., Saniabadi, A. R. & Soma, T. Granulocyte apheresis as a possible new approach in cancer therapy: A pilot study involving two cases. *Cancer Detect. Prev.* **23**, 417–21 (1999).
191. Kasuga, I. *et al.* Tumor-related leukocytosis is linked with poor prognosis in patients with lung carcinoma. *Cancer* **92**, 2399–405 (2001).
192. Boggs, D. R., Malloy, E., Boggs, S. S., Chervenick, P. A. & Lee, R. E. Kinetic studies of a tumor-induced leukemoid reaction in mice. *J. Lab. Clin. Med.* **89**, 80–92 (1977).
193. Lan, S., Rettura, G., Levenson, S. M. & Seifter, E. Granulopoiesis associated with the C3HBA tumor in mice. *J. Natl. Cancer Inst.* **67**, 1135–8 (1981).
194. Thomas, E., Smith, D. C., Lee, M. Y. & Rosse, C. Induction of granulocytic hyperplasia, thymic atrophy, and hypercalcemia by a selected subpopulation of a murine mammary adenocarcinoma. *Cancer Res.* **45**, 5840–4 (1985).
195. Wu, C. *et al.* Spleen mediates a distinct hematopoietic progenitor response supporting tumor-promoting myelopoiesis. *J. Clin. Invest.* **128**, 3425–3438 (2018).
196. McAllister, S. S. & Weinberg, R. A. The tumour-induced systemic environment as a critical

regulator of cancer progression and metastasis. *Nat. Cell Biol.* **16**, 717–727 (2014).
197. Noy, R. & Pollard, J. W. Tumor-Associated Macrophages: From Mechanisms to Therapy. *Immunity* **41**, 49–61 (2014).
198. Kumar, V., Patel, S., Tcyganov, E. & Gabrilovich, D. I. The Nature of Myeloid-Derived Suppressor Cells in the Tumor Microenvironment. *Trends Immunol.* **37**, 208–220 (2016).
199. Cui, T. X. *et al.* Myeloid-Derived Suppressor Cells Enhance Stemness of Cancer Cells by Inducing MicroRNA101 and Suppressing the Corepressor CtBP2. *Immunity* **39**, 611–621 (2013).
200. Kitamura, T., Qian, B.-Z. & Pollard, J. W. Immune cell promotion of metastasis. *Nat. Rev. Immunol.* **15**, 73–86 (2015).
201. Kitamura, T. *et al.* CCL2-induced chemokine cascade promotes breast cancer metastasis by enhancing retention of metastasis-associated macrophages. *J. Exp. Med.* **212**, 1043–1059 (2015).
202. Maury, C. P., Andersson, L. C., Teppo, A. M., Partanen, S. & Juvonen, E. Mechanism of anaemia in rheumatoid arthritis: demonstration of raised interleukin 1 beta concentrations in anaemic patients and of interleukin 1 mediated suppression of normal erythropoiesis and proliferation of human erythroleukaemia (HEL) cells in vitro. *Ann. Rheum. Dis.* **47**, 972–8 (1988).
203. Nikolaisen, C., Figenschau, Y. & Nossent, J. C. Anemia in early rheumatoid arthritis is associated with interleukin 6-mediated bone marrow suppression, but has no effect on disease course or mortality. *J. Rheumatol.* **35**, 380–6 (2008).
204. Lieschke, G. J. *et al.* Mice lacking granulocyte colony-stimulating factor have chronic neutropenia, granulocyte and macrophage progenitor cell deficiency, and impaired neutrophil mobilization. *Blood* **84**, 1737–46 (1994).
205. Metcalf, D. & Nicola, N. A. Proliferative effects of purified granulocyte colony-stimulating factor (G-CSF) on normal mouse hemopoietic cells. *J. Cell. Physiol.* **116**, 198–206 (1983).
206. Tesio, M. *et al.* Pten loss in the bone marrow leads to G-CSF-mediated HSC mobilization. *J. Exp. Med.* **210**, 2337–49 (2013).
207. Munugalavadla, V. & Kapur, R. Role of c-Kit and erythropoietin receptor in erythropoiesis. *Crit. Rev. Oncol. Hematol.* **54**, 63–75 (2005).

9. Supplemental

Figure S1

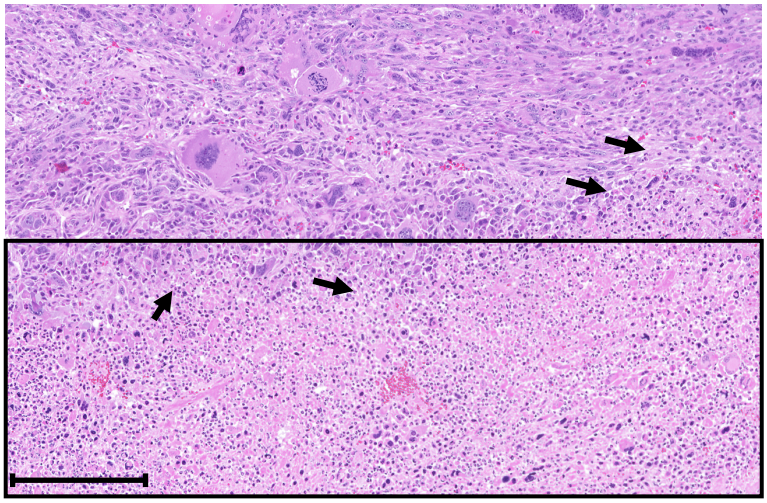

Fig. S1. Tumor tissue of tumor-bearing Trp53^{flox}WapCre
Shown is a representative H&E stained tissue section of tumor tissue of a Trp53^{flox}WapCre when the mouse reached experimental termination criteria by maximum permitted tumor size (end stage). Upper part of the picture: mammary carcinoma cells with diffuse neutrophilic inflammation (black arrows). Lower part (black rectangle): extensive necrotic area with degraded neutrophilic infiltrated (black arrows). Scale bar 250 µm.

Figure S2

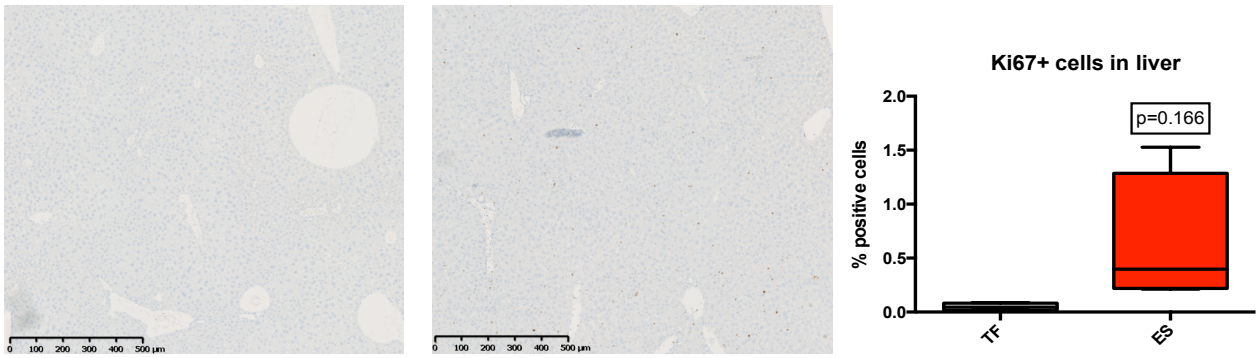

Fig. S2. Ki67 immunostaining on liver of Trp53^{flox}WapCre
Shown are representative ki-67 immunostained tissue sections of liver of **(A)** tumor free and **(B)** tumor-bearing at end stage Trp53^{flox}WapCre mice. **Panel C** shows the percentage of Ki-67+ cells in liver of tumor free (TF, white boxes) and tumor-bearing mice at end stage (ES, red boxes). End stage was considered when the mouse reached experimental termination criteria by maximum permitted tumor size. An Unpaired Student's t-test (panel C) was performed. (n=4). Scale bar 500 µm.

Figure S3

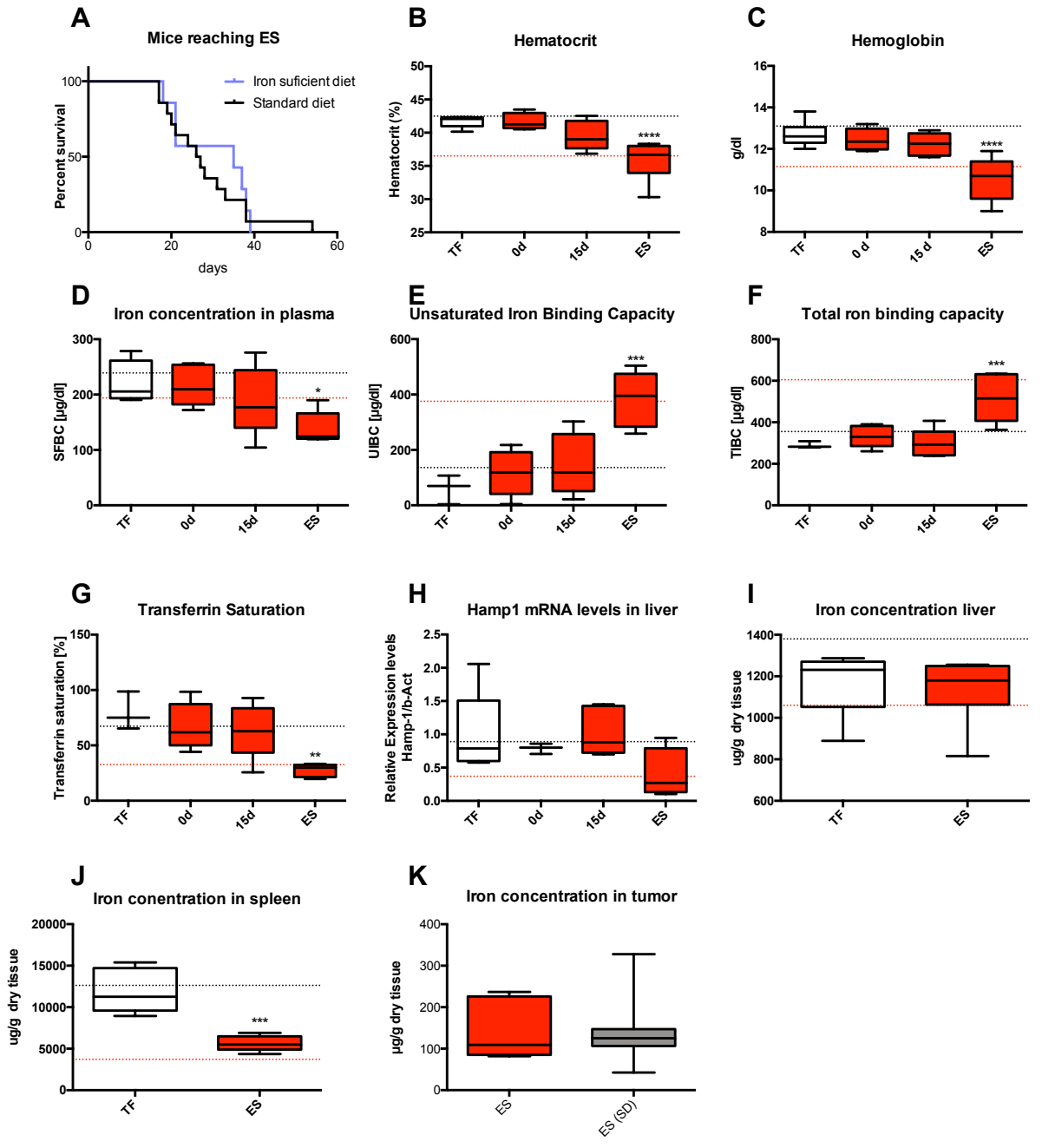

Fig. S3: Tumor progression, hematology and iron parameters in tumor-bearing Trp53^{flox}WapCre mice fed with an iron sufficient diet (50 mg/kg) from 18 weeks of age

Shown is **(A)** Kaplan-Meier survival curve, **(B)** hematocrit, **(C)** hemoglobin, **(D)** plasma iron concentration, **(E)** unsaturated iron binding capacity, **(F)** total iron binding capacity **(G)** transferrin saturation, **(H)** relative mRNA hepcidin-1 expression, **(I)** iron concentration in liver, **(J)** iron concentration in spleen and **(K)** iron concentration in tumor of free mice (TF, white boxes) and tumor-bearing (red boxes) Trp53^{flox}WapCre mice at different stages of tumor progression: immediately after tumor diagnosis (0d), 7 days after tumor diagnosis (7d) and at end stage (ES, when maximal permitted tumor size was reached). Animals were fed with an iron sufficient diet (50 mg/kg). Black dotted line indicates the median of tumor free mice fed with a standard diet (250 mg/kg iron) and red dotted line indicates the median of tumor-bearing Trp53^{flox}WapCre mice at end stage fed with the standard diet (250 mg/kg iron). Data are shown as (panel A) Kaplan-Meier Survival curve (n=3-7) and (panel B-K) as box plot with min to max whiskers. One-way ANOVA with Dunnett's Multiple Comparison post hoc test (panel B-H), a Mann Whitney test (panel I, K) or an Unpaired Student's t-test (panel J) was performed. (n=5-11). ****p<0.000, *p<0.05, ***p<0.001, **p<0.01.

Figure S4

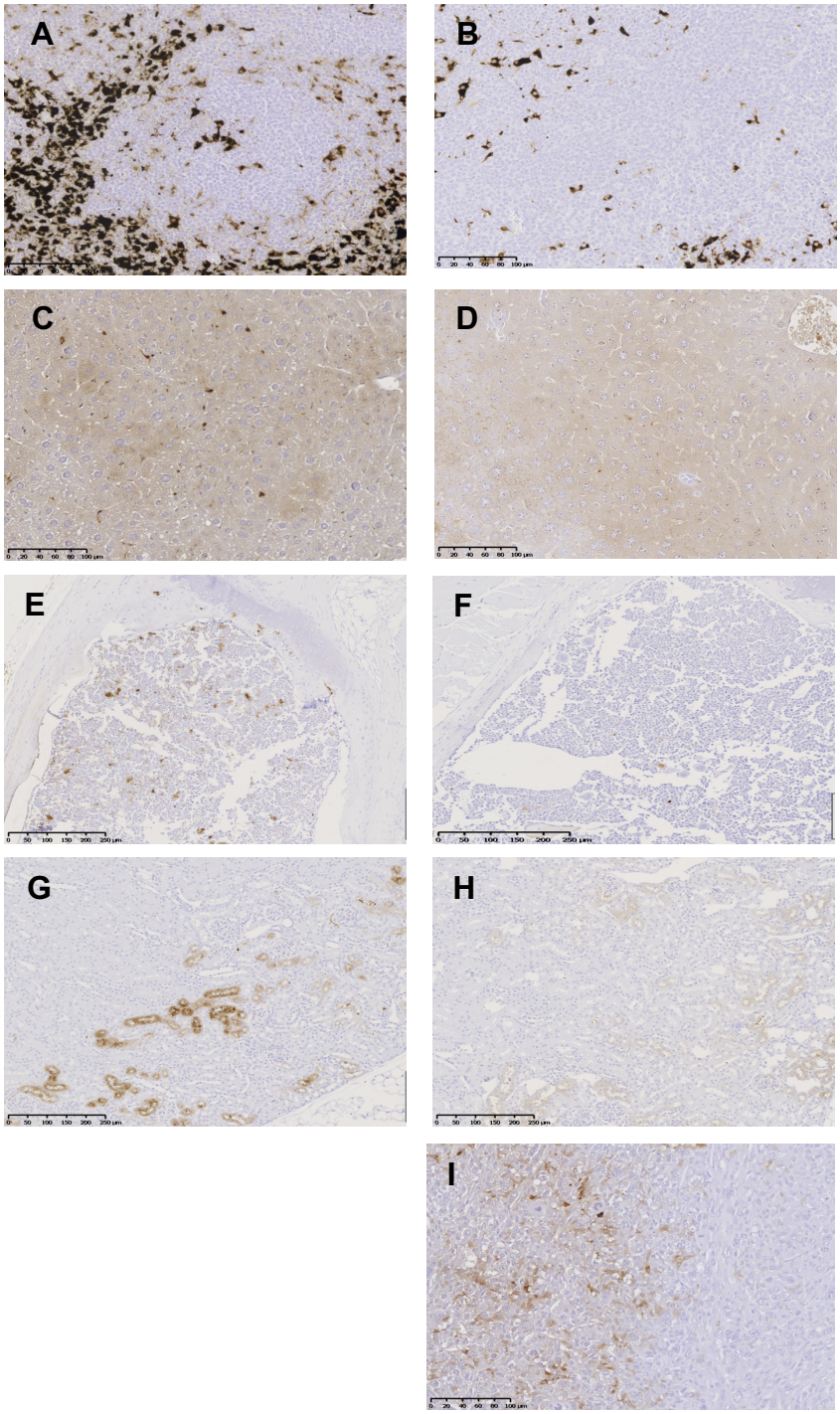

Fig. S4. Iron accumulation and distribution in spleen, liver, bone marrow, kidney and tumor of Trp53^{flox}WapCre mice fed with an iron sufficient diet (50 mg/kg) from 18 weeks of age.
Tissue sections were stained with Perls' DAB-enhanced to stain (**A, B)** spleen, **(C, D)** liver**, (E, F)** bone marrow, **(G, H)** kidney and **(I)** tumor tissue. Shown are representative images of tumor free mice (left panels) and tumor-bearing mice at end stage, i.e. when they reached maximal permitted tumor size (right panels) Trp^{53}floxWapCre mice fed with an iron sufficient diet (50 mg/kg Fe) from 18 weeks of age. Scale bar 100 or 250 µm.

Figure S5

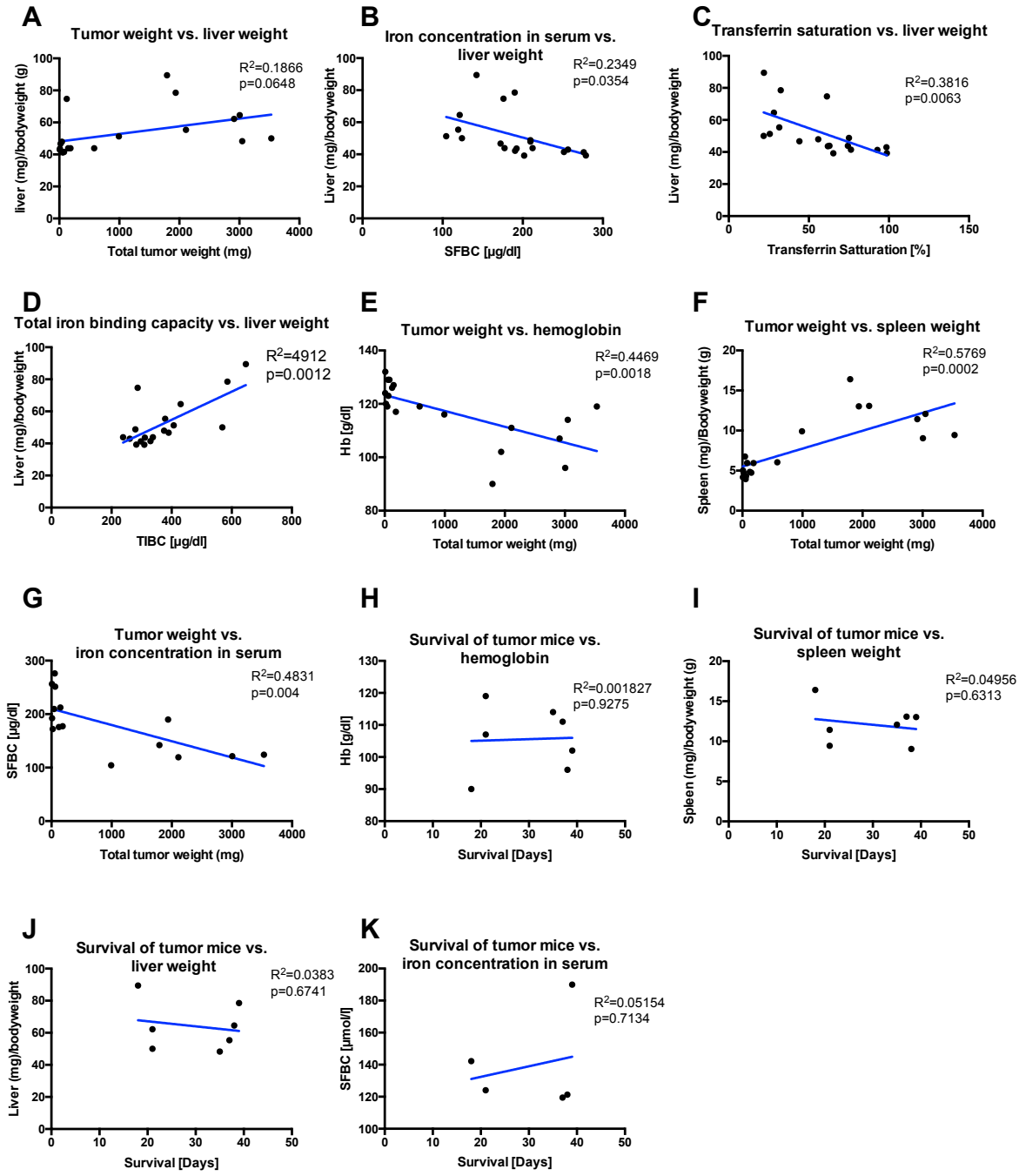

Fig. S5. Correlation between different parameters related to anemia in cancer in Trp53^{flox}WapCre mice fed with an iron sufficient diet (50 mg/kg) from 18 weeks of age.

Shown is the linear correlation analysis of liver weight normalized to the body weight (y-axis) vs. (A) tumor weight, (B) iron concentration in serum, (C) transferrin saturation, and (D) total binding capacity. Hemoglobin (E), spleen weight (F) and iron concentration in serum (G) versus tumor weight. Hemoglobin (H), spleen weight (I), liver weight normalized to body weight (J) and iron concentration in serum (K) vs. the survival (days) of tumor-bearing Trp53^{flox}WapCre mice fed with an iron sufficient diet (50 mg/kg) from 18 weeks of age at different stages of the disease. Data shown as individual mouse data with regression lines. Linear regression analyses were performed. R^2 is the coefficient of determination and p the p-value. (n=5-19)

Figure S6

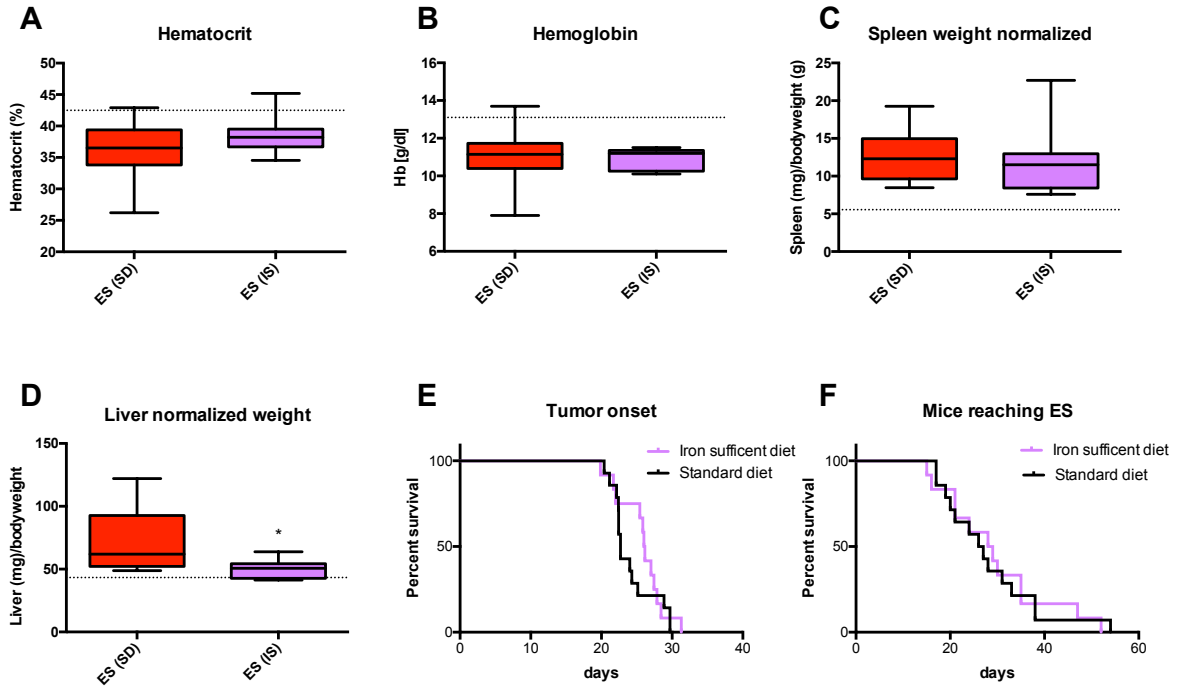

Fig. S6: Hematology, organ weight, tumor onset and survival of tumor-bearing Trp53^{flox}WapCre mice fed with an iron sufficient diet (50 mg/kg) from birth.

Shown is **(A)** hematocrit, **(B)** hemoglobin, **(C)** spleen weight and **(D)** liver weight normalized to the body weight**. (E)** Kaplan-Meier survival curve of the tumor onset and **(F)** Kaplan-Meier survival curve of the tumor-bearing mice reaching end stage (ES, when maximal permitted tumor size was reached). Animals were fed with a standard diet containing 250 mg/kg iron [ES (SD), red boxes] or with an iron sufficient diet (50 mg/kg) [ES (IS), purple boxes]. Data are shown as (panel A-D) box plot with min to max whiskers and (panel E, F) Kaplan-Meier Survival curve. An Unpaired Student's t-test (A, C) or a Mann Whitney test (B, D) was performed (n=8-37). *p<0.05.

Figure S7

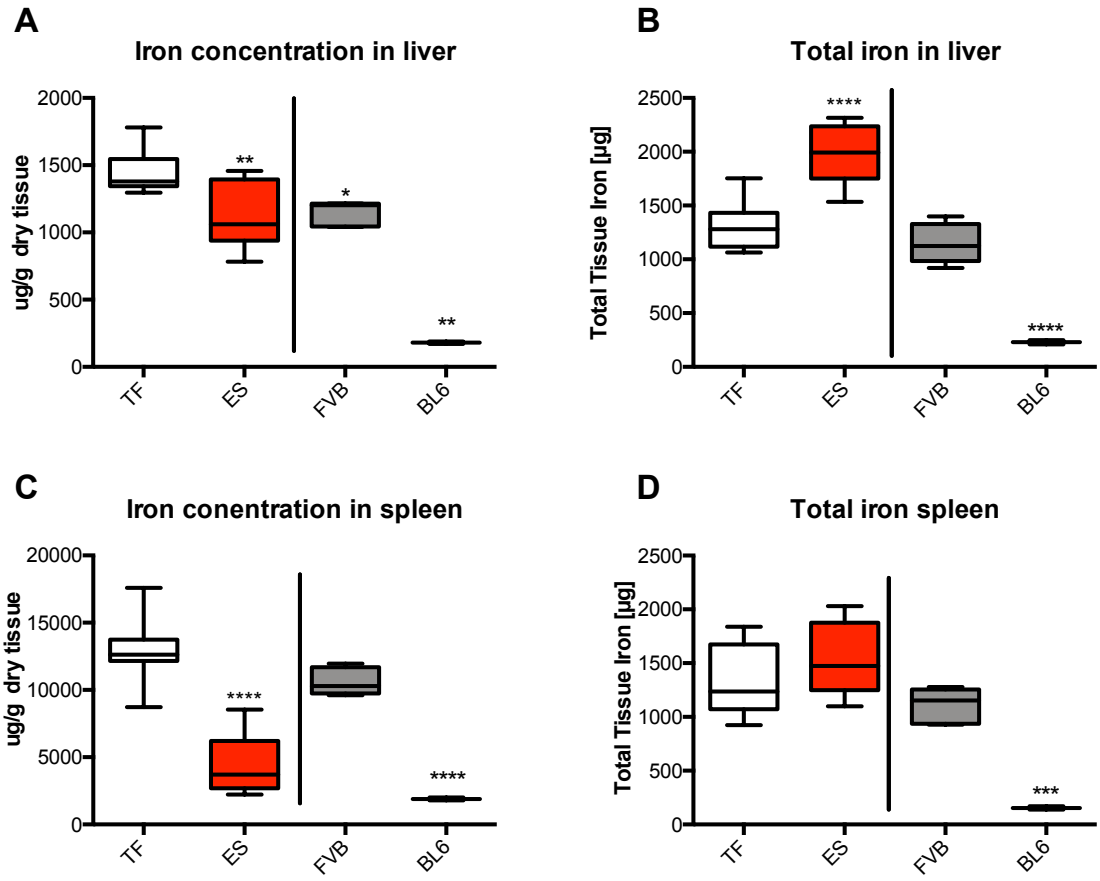

Fig. S7: Comparation of tissue iron in Trp53^{flox}WapCre mice with FVB wildtype and BL6 wildtype mice
Shown is **(A)** iron concentration in liver, **(B)** total iron content in liver **(C)** iron concentration in spleen **(D)** and total iron content in spleen **(E)** of tumor-bearing Trp53^{flox}WapCre mice at end stage, i.e. reaching maximal permitted tumor size (ES, red boxes), tumor-free Trp53^{flox}WapCre mice (TF, white boxes), FVB wild type mice (FVB, grey boxes) and C57BL/6 wild type mice (BL6). Data are shown as box plot with min to max whiskers. One-way ANOVA with a Dunn's Multiple Comparison post hoc test was performed (n=2-9). *p<0.05; **p<0.01; ***p<0.001; ****p<0.0001.

10. Acknowledgement

First of all, I would like to give a special thanks to Dr. Markus Thiersch for giving me the opportunity to learn and work in such fascinating field of research and for always being supportive and comprehensive during these two years at the Institute. I really enjoyed that time and I am sure it will have a great impact in my life. I would also like to tank Prof. Dr. med vet. Max Gassmann for giving me the opportunity to work in the Institute of Veterinary Physiology and specially for the opportunity to participate in the organization of the 5th International Atacama Symposium in Chile. It was undoubtedly an enriching and unforgettable experience. Also, I thank Ben Wielockx for being my external co-supervisor.

I would also like to thank my lab and office collages from the Institute of Veterinary Physiology for the nice working atmosphere and being always open to help me at the lab and especially to Mostafa Aboouf, Julia Armbuster, Hyrije Ademi, Fraser Simpson, Tri Le, Glenda Cosi and Aurelia Leimbacher for their help on my animal experiments. I would also specially thank Nadine Jänicke for introducing me at the lab and transferring me very efficiently highly valuable knowledge and tips for the work at the lab, since most of the techniques were completely new to me.

Furthermore, I would like to thank Josep Monné Rodriguez from the Institute of Veterinary Pathology for collaborating with the histologic analysis and always being so helpful and open to discuss the results. Also, to Martina Stirn for performing the bone marrow smears analysis, to Florian Sparber and Catherine Eichwald for their help with the flow cytometer, to Ben Wielockx and Rashim pal Singh for the flow cytometry analysis of the early erythropoiesis, to Maja Ruetten for her collaboration in the pathology analyses, and to Felix Funk and Susanna Burckhardt from Vifor Pharma for believing in this project and for their always helpful scientific input.

I want to thank Vifor Pharma for their financial support. This project would not have been possible without it.

Last but not least, I would like to thank my family and specially my husband for the encouragement throughout my life, his unconditional support, his love and for always believing in me.

11. Curriculum Vitae

Núria Fàbregas Bregolat

3rd of May of 1985

Barcelona

Spanish

September/1990	–	June/1997	**School education.** Escola Ronçana, Santa Eulàlia de Ronçana, Spain
15th June 2003			**Bachillerat científic.** Institut la Vall del Tenes, Santa Eulàlia de Ronçana, Spain
October /2003	–	September/2008	**Degree in Veterinary Medicine.** Universitat Autònoma de Barcelona, Bellaterra, Spain
September / 2010			**Master's in veterinary research.** Universitat Autònoma de Barcelona, Bellaterra, Spain
March/2017	–	June/2019	**Preparation of the thesis** under the direction of Prof. Dr. med. vet. Max Gassmann at the Institute of Veterinary Physiology of the Vetsuisse Faculty, University of Zurich Prof. Dr. med. vet. Max Gassmann
January/2009	–	May/2009	Professional training in Kedrah Stud farm. Cahir, Ireland
June/2009	–	September/2009	Disease Control Support, Tragsa-Tragsega. Barcelona, Spain
September/2009	–	June/2011	Externship in the Equine Reproduction Service of the Veterinary faculty of the Universitat Autònoma de Barcelona. Bellaterra, Spain
April/2011	–	June/2016	Full time Veterinary Surgeon. Grup Veterinària, Santa Eulàlia de Ronçana, Spain